On Using Graphical Calculi: Centers, Zeroth Hochschild Homology and Possible Compositions of Induction and Restriction Functors in Various Diagrammatical Algebras

Joelle Brichard

Submitted in partial fulfillment of the
requirements for the degree of
Doctor of Philosophy
in the Graduate School of Arts and Sciences

COLUMBIA UNIVERSITY

2011

ABSTRACT

On Using Graphical Calculi: Centers, Zeroth Hochschild Homology and Possible Compositions of Induction and Restriction Functors in Various Diagrammatical Algebras

Joelle Brichard

This thesis is divided into three chapters, each using certain graphical calculus in a slightly different way. In the first chapter, we compute the dimension of the center of the 0-Hecke algebra $\mathcal{H}_n$ and of the Nilcoxeter algebra $\mathcal{NC}_n$ using a calculus of diagrams on the Moebius band. In the case of the Nilcoxeter algebra, this calculus is shown to produce a basis for $Z(\mathcal{NC}_n)$ and the table of multiplication in this basis is shown to be trivial. We conjecture that a basis for $Z(\mathcal{H}_n)$ can also be obtained in a specific way from this topological calculus. In the second chapter, we also use a calculus of diagrams on the annulus and the Moebius band to determine the zeroth Hochschild Homology of Kuperberg's webs for rank two Lie algebras. We use results from Sikora and Westbury to prove the linear independence of these webs on these surfaces. In the third chapter, we use other diagrams to attempt to find explicitely the possible compositions of the induction and restriction functors in the cyclotomic quotients of the NilHecke algebra. We use a computer program to obtain partial results.

Contents

List of Figures

Acknowledgements and Dedication

It is my pleasure to thank my advisor Mikhail Khovanov for introducing me to the topics of this thesis and for his help, patience and guidance throughout the research and writing phases that have lead to the completion of this document. I am also deeply grateful for everybody in the mathematics department at Columbia from whom I have learned a lot, especially Aaron Lauda, Benjamin Elias and Adam Levine. Finally, I want to thank my parents for their encouragment, my husband Paul Elliott for his unwavering support and my two children Claire and Vincent for bringing so much joy to my life. To them I dedicate this thesis.

Chapter 1

Introduction

This thesis focuses on algebras that can be represented in a diagramatical way and on properties which are more easily analysed using these diagrams.

The goal of Chapter 2 is to learn about the centers of two generic algebras; the Nilcoxeter algebra $\mathcal{NC}_n$ and the 0-Hecke algebra $\mathcal{H}_n$. These algebras have appeared in the context of categorification of superalgebras and rings of quasi-symmetric functions. Both of these algebras are Frobenius, although they are not symmetric. Section 2.2 introduces an isomorphism between the center of a symmetric Frobenius algebras and the dual of the quotient space $A/[A, A]$ of the algebra by its commutator subspace. In the case of non-symmetric Frobenius algebras, we need to use the Nakayama automorphism to define a twisted commutator subspace. The center of a non-symmetric Frobenius algebra is then shown to be isomorphic to the dual of the quotient space $A/[A, A]_t$ of the algebra by its twisted commutator subspace.

In Section 2.3, we remark that for $A = \mathcal{NC}_n$ or $A = \mathcal{H}_n$, $A/[A, A]$ corresponds to the space of diagrams on the annulus and $A/[A, A]_t$ to the space of diagrams on the Moebius band. Section 2.4 then classifies diagrams from $\mathcal{NC}_n$ on the Moebius band, starting with diagrams of a single connected component called prime diagrams. We show that there is a unique prime diagram going around the Moebius band n times. We then list all the ways these connected components can be combined to create more complex diagrams. This allows us to find the dimension of the center of $\mathcal{NC}_n$ in Section 2.5.1. Using the isomorphism of Section 2.2, we find a concrete diagrammatical basis for the center of $\mathcal{NC}_n$ in Section 2.5.2 and then show in Section 2.5.3 that the product structure of the center, in that basis, is trivial.

In Section 2.6, we use the previous results and apply them to $\mathcal{H}_n$. We show that $\mathcal{H}_n$ has the same irreducible and independent diagrams on the Moebius band as $\mathcal{NC}_n$ and that, therefore, the dimension of its center is the same as the dimension of $\mathcal{NC}_n$. However, we are unable to find, in general, a

diagrammatical basis for the center of $\mathcal{H}_n$ and its product structure. The added difficulty comes from the fact that, as far as we know, there is no grading on $\mathcal{H}_n$.

Chapter 3 looks at algebras coming from Kuperberg's spiders. These spiders come from the representation theories of rank 2 Lie algebras and their quantum deformation. Here again we study the diagrams corresponding to each algebra on the annulus and on the Moebius band. Unfortunately, these algebras are not Frobenius, so the spaces of diagrams on the annulus and Moebius band do not correspond to the centers. Nevertheless, they do correspond to the zeroth Hochschild homology of the algebra as a bimodule over itself, with a twisted action in the case of diagrams on the Moebius band.

In Section 3.2, we classify the irreducible diagrams for the rank 2 webs on the annulus and on the Moebius band. In most cases, the only irreducible diagrams are non-trivial loops. However, it is not obvious that these irreducible diagrams are linearly independent, and indeed, some are not. In Section 3.3, we use results from [21] to either show that the reduction rules we have from Kuperberg's definition are both terminal and confluent and that the irreducible diagrams in fact form a basis or that these rules are not terminal and confluent. In the second case, new rules are introduced that make the new set terminal and confluent. In some cases, the new rules change the set of irreducible diagrams found in Section 3.2. These results allow us to find the dimension of the zeroth Hochschild homology of these algebras.

Finally Chapter 4 is an attempt at finding concrete realizations of the natural transformations between the compositions of the induction and restriction functors in the cyclotomic quotient of the NilHecke algebra. Most of what we know about these quotients now come from their relation with the cohomology of Grassmanians as described in [16]. After finding a diagramatical basis of monomials for these quotients in Section 4.4, we describe, in Section 4.5, a computer program that we used to derive constraints as linear equations on certain of the bimodule maps we were looking for. The partial results are shown in Section 4.6. We were able to find the maps associated with the crossings, dots, counter-clockwise cup and clockwise cap in all generality. The clockwise cup and counter-clockwise cap were the difficult ones and we were only able to find them explicitely for $m \leq 3$ and all possible levels N. It is conjectured that a different basis, perhaps one not made of monomials, is needed to generalize these results.

Chapter 2

The Centers of the Nilcoxeter and 0-Hecke Algebras

2.1 Generic Algebras

Given a Coxeter system (W, S) and an associative unital commutative algebra $\mathcal{A}$, we start by defining the generic algebra $\mathcal{E}_{\mathcal{A}}(a_s, b_s)$. This approach is taken from [7]. Generic algebras depend on parameters $\{a_s, b_s \in \mathcal{A}\}_{s \in S}$ subject to the condition that $a_s = a_t$ and $b_s = b_t$ whenever s and t are conjugates in W. $\mathcal{E}_{\mathcal{A}}(a_s, b_s)$ are generated by elements T_w for $w \in W$ with relations

1. $T_s T_w = T_{sw}$ if $l(sw) > l(w)$,
2. $T_s T_w = a_s T_w + b_s T_{sw}$ if $l(sw) < l(w)$.

The two algebras of concern in this Chapter are both examples of this type of generic algebras with Coxeter group $\mathcal{S}_n$. Other important examples include the group algebra $\mathcal{A}[W]$ which is obtained by setting all $a_s = 0$ and $b_s = 1$. Hecke algebras are also examples of this construction for $\mathcal{A} = \mathbb{Z}[q, q^{-1}]$ and with $a_s = q - 1$ and $b_s = q$ for all $s \in S$. For more on Coxeter groups and Hecke algebras see [8] and [7].

There is another set of relations equivalent to the ones above:

1. $T_s T_w = T_{sw}$ if $l(sw) > l(w)$,
2. $T_s^2 = a_s T_s + b_s T_e$,

with T_e the identity element. $\mathcal{E}$ is generated as an algebra by the T_s, $s \in S$ and $1 = T_e$.

Any generic algebra with Coxeter group $\mathcal{S}_n$, is given by the following three types of relations:

1. $T_iT_{i+1}T_i = T_{i+1}T_iT_{i+1}$

2. $T_iT_j = T_jT_i$ for $|i-j| > 1$

3. $T_i^2 = a_iT_i + b_iT_e$,

for $1 \leq i \leq n-1$.

2.1.1 The Nilcoxeter Algebra

The Nilcoxeter algebra, which we denote $\mathcal{NC}_n$, is an example of a generic algebra associated to $\mathcal{S}_n$ where we set $a_s = b_s = 0$ for all $s \in S$. This algebra first appeared in [1] in relation to the cohomology of flag varieties. It was also studied by Lascoux and Schützenberger [15], Macdonald [18], Fomin and Stanley [5] and others. Khovanov has shown in [9] that it categorifies the polynomial representation of the Weyl algebra and work by Khovanov and Lauda showed its relevance to the categorification of quantum groups [12]. In terms of the generators T_i, where $T_i = T_{s_i}$, for $s_i \in \mathcal{S}_n$ the transposition $(i \;\; i+1)$, the Nilcoxeter algebra is defined by:

1. $T_iT_{i+1}T_i = T_{i+1}T_iT_{i+1}$

2. $T_iT_j = T_jT_i$ for $|i-j| > 1$

3. $T_i^2 = 0$.

We therefore also have

$$T_iT_w = \begin{cases} T_{s_iw} & if\ l(s_iw) > l(w) \\ 0 & if\ l(s_iw) < l(w) \end{cases}.$$

2.1.2 The 0-Hecke Algebra

The 0-Hecke algebra, here denoted $\mathcal{H}_n$, is the Hecke algebra associated to $\mathcal{S}_n$ with $q = 0$. Equivalently, it is the generic algebra where we have set $a_s = 1$ and $b_s = 0$ for all $s \in S$. That is, the third relation on the T_i now becomes

$$T_i^2 = T_i.$$

This implies that

$$T_iT_w = \begin{cases} T_{s_iw} & if\ l(s_iw) > l(w) \\ T_w & if\ l(s_iw) < l(w) \end{cases}$$

Norton studied the Hecke algebra of a Coxeter group at $q = 0$ for all types in [20]; she classified the irreducible modules, described the decomposition of the algebra into left ideals as well as the Cartan invariants. In [3], Carter gave decomposition numbers for $\mathcal{H}_n$ in the type A case. Krob and Thibon gave a representation-theoretic interpretation of non-commutative algebras [13] and works by Duchamp, Hivert and Thibon [4] showed that the representations of $\mathcal{H}_n$ in type A categorify the ring of quasi-symmetric functions.

2.2 The Centers of Frobenius Algebras

A finite dimensional, unital, associative algebra $\mathcal{A}$ defined over a field k is said to be a Frobenius algebra if $\mathcal{A}$ is equipped with a non-degenerate trace map $\epsilon : \mathcal{A} \to k$. We now derive some general facts about the centers of Frobenius algebras and then introduce a trace map which makes both $\mathcal{NC}_n$ and $\mathcal{H}_n$ into Frobenius algebras. The facts derived here are crucial to our approach to describing the centers of $\mathcal{NC}_n$ and $\mathcal{H}_n$.

2.2.1 Symmetric Frobenius Algebras

To investigate the centers of Frobenius algebras, it is sometimes convenient to use a duality relation between the center $Z(\mathcal{A})$ of $\mathcal{A}$ and a quotient of $\mathcal{A}$ by certain subspaces. In the case of symmetric Frobenius algebras, this subspace is simply the commutator subspace generated by all elements of the form $ab - ba$ for $a, b \in \mathcal{A}$.

To see this, let $\mathcal{A}$ be a Frobenius algebra over a field k, $\epsilon : \mathcal{A} \to k$ its trace map and assume that $\mathcal{A}$ is a symmetric algebra, meaning that $\epsilon(ab) = \epsilon(ba)$ for all a, b. Denote by $\mathcal{A}^* = \mathrm{Hom}_k(\mathcal{A}, k)$, the dual of $\mathcal{A}$. Then ϵ extends to an isomorphism of $\mathcal{A}$-bimodules:

$$\begin{aligned} \phi : \mathcal{A} &\to \mathcal{A}^* \\ 1 &\mapsto \epsilon \\ a &\mapsto \epsilon(\ *a). \end{aligned}$$

Let $[\mathcal{A}, \mathcal{A}]$ denote the commutator subspace of $\mathcal{A}$: the space spanned by elements of the form $ab - ba$ for $a, b \in \mathcal{A}$.

Proposition: *If $\mathcal{A}$ is a symmetric Frobenius algebra, then*

$$(\mathcal{A}/[\mathcal{A},\mathcal{A}])^* \simeq Z(\mathcal{A}),$$

as vector spaces.

Let

$$\begin{aligned} \Psi : Z(\mathcal{A}) &\rightarrow (\mathcal{A}/[\mathcal{A},\mathcal{A}])^* \\ z &\mapsto z\epsilon : \mathcal{A} \rightarrow k; z\epsilon(a) = \epsilon(za) = \epsilon(az). \end{aligned}$$

Ψ is well-defined:

$$z\epsilon([a,b]) = z\epsilon(ab-ba) = \epsilon(zab-zba) = \epsilon(bza) - \epsilon(zba) = \epsilon(zba) - \epsilon(zba) = 0$$

since z is a central element and $\mathcal{A}$ is symmetric.
Ψ is injective: since the map $\mathcal{A} \rightarrow \mathcal{A}^*$ is an isomorphism and the map $Z(\mathcal{A}) \rightarrow \mathcal{A}$ is an inclusion, the composition $Z(\mathcal{A}) \rightarrow \mathcal{A} \rightarrow \mathcal{A}^*$ is injective. Moreover, we have seen that the map $Z(\mathcal{A}) \rightarrow \mathcal{A}^*$ factors through $Z(\mathcal{A}) \rightarrow (\mathcal{A}/[\mathcal{A},\mathcal{A}])^*$, which means that $\Psi : Z(\mathcal{A}) \rightarrow (\mathcal{A}/[\mathcal{A},\mathcal{A}])^*$ is injective as well.
Ψ is surjective: let $\alpha \in (\mathcal{A}/[\mathcal{A},\mathcal{A}])^*$. Because

$$\pi : \mathcal{A} \rightarrow \mathcal{A}/[\mathcal{A},\mathcal{A}]$$

is surjective, its dual

$$\pi^*(\mathcal{A}/[\mathcal{A},\mathcal{A}])^* \rightarrow \mathcal{A}^*$$

must be injective. We know from the isomorphism $\phi : \mathcal{A} \rightarrow \mathcal{A}^*$ that $\pi^*(\alpha) = z\epsilon$ for some $z \in \mathcal{A}$. We must check that $z \in Z(\mathcal{A})$. Now, since $\alpha \in (\mathcal{A}/[\mathcal{A},\mathcal{A}])^*$, $z\epsilon([a,b]) = 0$ for all $a, b \in \mathcal{A}$. Hence

$$\epsilon(z[a,b]) = \epsilon(zab) - \epsilon(zba) = \epsilon(zab) - \epsilon(azb) = \epsilon([z,a]b) = 0.$$

Since the trace ϵ is non-degenerate, this cannot be true for all $b \in \mathcal{A}$ unless $[z,a] = 0$. This is true for all $a \in \mathcal{A}$ as well, so we conclude that $z \in Z(\mathcal{A})$, with $\Psi(z) = \alpha$.

2.2.2 Non-Symmetric Frobenius Algebras

We now look at the case when $\mathcal{A}$ is not a symmetric Frobenius algebra. Since

$$\epsilon : \mathcal{A} \to k$$

is non-degenerate, one can define an automorphism $f : \mathcal{A} \to \mathcal{A}$ called a Nakayama automorphism such that $\epsilon(ab) = \epsilon(bf(a))$. Note that we then have $f(ab) = f(a)f(b)$. Using this automorphism, one can state a duality very similar to the one we have derived in the case of the symmetric Frobenius algebras.

Given the automorphism f on $\mathcal{A}$, let us denote the "twisted" commutator of a and b by $[a, b]_t = ab - f(b)a$. Similarly, let $[\mathcal{A}, \mathcal{A}]_t$ be the subalgebra of $\mathcal{A}$ spanned by elements $ab - bf(a)$. We also define the twisted center of $\mathcal{A}$ as follows:

$$TZ(\mathcal{A}) = \{b \in \mathcal{A} | ab - f(b)a = 0 \text{ for all } a \in \mathcal{A}\}.$$

Proposition: *Using the above notation,*

$$Z(\mathcal{A}) \backsimeq (\mathcal{A}/[\mathcal{A}, \mathcal{A}]_t)^* \tag{2.1}$$

$$TZ(\mathcal{A}) \backsimeq (\mathcal{A}/[\mathcal{A}, \mathcal{A}])^*. \tag{2.2}$$

(1) The proof closely resembles the one for $\mathcal{A}$ symmetric. Let

$$\begin{aligned} \Psi : Z(\mathcal{A}) &\to (\mathcal{A}/[\mathcal{A}, \mathcal{A}]_t)^* \\ z &\mapsto z\epsilon : \mathcal{A} \to k; z\epsilon(a) = \epsilon(za). \end{aligned}$$

Ψ is well-defined:

$$z\epsilon([a, b]_t) = z\epsilon(ab - f(b)a) = \epsilon(zab - zf(b)a) = \epsilon(a(zb)) - \epsilon(f(b)za) = 0$$

since z is central and $\epsilon(ab) = \epsilon(bf(a))$.

Ψ is injective: The proof is exactly as for $\mathcal{A}$ symmetric.

Ψ is surjective: Let $\alpha \in (\mathcal{A}/[\mathcal{A}, \mathcal{A}]_t)^*$ and $\pi^* : (\mathcal{A}/[\mathcal{A}, \mathcal{A}]_t)^* \to \mathcal{A}^*$. Then $\pi^*(\alpha) = z\epsilon$ for some $z \in \mathcal{A}$ and $z\epsilon([a, b]_t) = 0$ for all $a, b \in \mathcal{A}$. We must verify that z is in the center $Z(\mathcal{A})$.

$$0 = z\epsilon([a,b]_t) = \epsilon(zab) - \epsilon(zf(b)a) = \epsilon(f(b)za) - \epsilon(zf(b)a) = \epsilon([f(b),z]a).$$

Since this is true for all $a \in \mathcal{A}$ and since ϵ is non-degenerate, then $[f(b), z]$ must vanish for all $b \in \mathcal{A}$, which means that z is central.

(2) Let

$$\begin{aligned} \Psi : TZ(\mathcal{A}) &\rightarrow (\mathcal{A}/[\mathcal{A},\mathcal{A}])^* \\ c \mapsto c\epsilon : \mathcal{A} &\rightarrow k; c\epsilon(a) = \epsilon(ca). \end{aligned}$$

Ψ is well-defined:

$$c\epsilon([a,b]) = \epsilon(cab) - \epsilon(cba) = \epsilon(cab) - \epsilon(f(a)cb) = \epsilon((ca - f(a)c)b) = \epsilon(0) = 0.$$

Ψ is injective: The proof is as before.

Ψ is surjective: We have as before $c\epsilon = \pi^*(\alpha)$ and we need to check that $c \in TZ(\mathcal{A})$.

$$0 = c\epsilon([a,b]_t) = \epsilon(cab) - \epsilon(cba) = \epsilon(cab) - \epsilon(f(a)cb) = \epsilon([c,a]_t b)$$

so that $[c,a]_t = 0$ and $c \in TZ(\mathcal{A})$.

Note that $\mathcal{A}/[\mathcal{A},\mathcal{A}]$ and $\mathcal{A}/[\mathcal{A},\mathcal{A}]_t$ are no longer algebras, but vector spaces, both for $\mathcal{A} = \mathcal{NC}_n$ and $\mathcal{A} = \mathcal{H}_n$.

2.2.3 The Nilcoxeter and 0-Hecke Algebras as Non-Symmetric Frobenius Algebras

We can endow the 0-Hecke and Nilcoxeter algebras with trace mapϵ, making them Frobenius algebras. Some of our constructions and arguments will be similar for both $\mathcal{NC}_n$ and $\mathcal{H}_n$. In these cases we denote either of them by $\mathcal{A}_n$, where $\mathcal{A}_n$ is generated by $T_1, T_2, \ldots, T_{n-1}$ or simply by $\mathcal{A}$. Then $\epsilon : \mathcal{A} \rightarrow k$ is defined as $\epsilon(T_\sigma) = 1$ if $l(\sigma)$ is maximal (the maximal permutation has length $n(n-1)/2$ for the algebra on n strands) and $\epsilon(T_\sigma) = 0$ otherwise. With a slight abuse of notation, we now refer to σ or even T_σ as maximal when $l(\sigma)$ is maximal. The maximal T_σ is called max_n.

We would like to show that ϵ is a non-degenerate trace map and makes $\mathcal{NC}_n$ and $\mathcal{H}_n$ into Frobenius algebras.

ϵ being non-degenerate follows from that for any $\sigma \in S_n$, there exist $\gamma, \gamma' \in S_n$ such that $T_\sigma T_\gamma = T_{\gamma'} T_\sigma = max_n$. The properties of the length function on $\mathcal{S}_n$ and the multiplication rules derived in 2.1.1 and 2.1.2 imply that this is indeed the case.

The 0-Hecke and Nilcoxeter algebras are not symmetric. However, one can define an involution f on $\mathcal{A}$ for both $\mathcal{A} = \mathcal{NC}_n$ and $\mathcal{A} = \mathcal{H}_n$:

$$\begin{aligned} f(T_i) &= T_{n-i}, 1 \leq i \leq n-1 \\ f(ab) &= f(a)f(b). \end{aligned}$$

It is clear that $\forall \sigma,\ f(T_\sigma) = T_\gamma$ for some γ, and that $l(\sigma) = l(\gamma)$. It immediately follows that σ is maximal if and only if γ is maximal, so that $\epsilon(T_\sigma) = 0$ if and only if $\epsilon(T_\gamma) = 0$. Hence, $\epsilon(a) = \epsilon(f(a))$ for all $a \in A$.

2.3 Topological Calculi of Diagrams

In order to determine the dimension of the center of our Frobenius algebra $\mathcal{A} = \mathcal{NC}_n$ or $\mathcal{A} = \mathcal{H}_n$, we make use of the relation

$$Z(\mathcal{A}) \backsimeq (\mathcal{A}/[\mathcal{A}, \mathcal{A}]_t)^*$$

and determine the dimension of $\mathcal{A}/[\mathcal{A}, \mathcal{A}]_t$. A basis element of $\mathcal{A}$ can be represented as a monotonic immersion of n unit intervals $[0, 1]$ in $\mathbb{R} \times [0, 1]$, subject to some relations. We can see this element as n strings each going from a top position $1 \leq i \leq n$ at 1 to a bottom position $1 \leq j \leq n$ at 0. A generator T_i of $\mathcal{A}$ is represented by the crossing of the i and $i+1$ strings. The braid relations of $\mathcal{A}$ allow us to change this diagram of strings using the third Reidemeister move ($T_i T_{i+1} T_i = T_{i+1} T_i T_{i+1}$) and to move far away crossings up and down with respect to each other ($T_i T_j = T_j T_i$ for $|i - j| > 1$). We read diagrams from top to bottom.

2.3.1 Diagrams on a Flat Band

A diagram like the one described above, a monotonic immersion of n unit intervals $[0, 1]$ in $\mathbb{R} \times [0, 1]$, can be used to represent a basis element of the symmetric group ring $\mathbb{C}[\mathcal{S}_n]$ if we impose the usual Reidemeister moves as relations. By changing the relations appropriately, it can also represent a basis

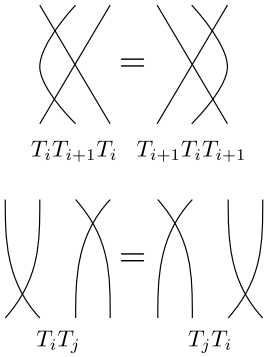

Figure 2.1: These diagrams show the graphical relations common to $\mathbb{C}[\mathcal{S}_n]$, $\mathcal{NC}_n$ and $\mathcal{H}_n$. The relation used to simplify T_i^2 is what distinguishes these algebras.

element of $\mathcal{NC}_n$ or $\mathcal{H}_n$. To $s_i \in \mathcal{S}_n$ or $T_i \in \mathcal{A}$ we assign a crossing of the i and $i+1$ strands, to a product s_is_j or T_iT_j we assign a crossing of the i and $i+1$ strands followed by a crossing of the j and $j+1$ strands and to a linear combination of basis elements we assign a formal sum of diagrams. The relations imposed are:

for a basis element of $\mathbb{C}[\mathcal{S}_n]$:

1. $s_is_{i+1}s_i = s_{i+1}s_is_{i+1}$
2. $s_is_j = s_js_i$ for $|i-j| > 1$
3. $s_i^2 = 1$

for a basis element of $\mathcal{NC}_n$:

1. $T_iT_{i+1}T_i = T_{i+1}T_iT_{i+1}$
2. $T_iT_j = T_jT_i$ for $|i-j| > 1$
3. $T_i^2 = 0$

and for a basis element of $\mathcal{H}_n$:

1. $T_iT_{i+1}T_i = T_{i+1}T_iT_{i+1}$
2. $T_iT_j = T_jT_i$ for $|i-j| > 1$
3. $T_i^2 = T_i$.

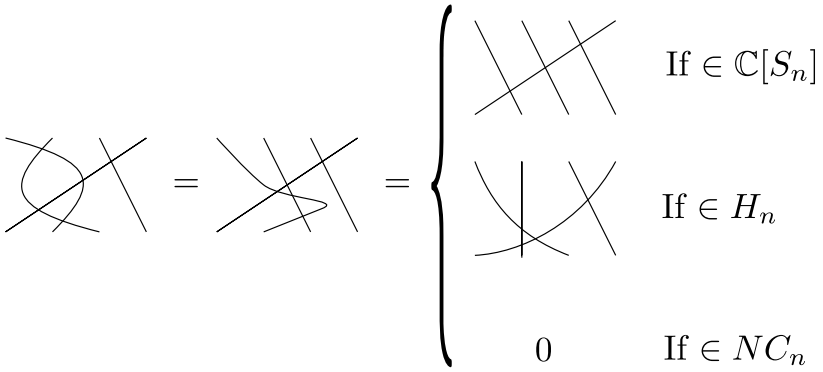

Figure 2.2: This first diagram is equivalent to three distinct diagrams in $\mathbb{C}[\mathcal{S}_n]$, $\mathcal{H}_n$ and $\mathcal{NC}_n$ respectively.

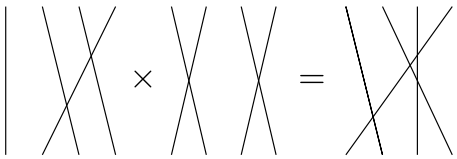

Figure 2.3: Multiplication of basis elements corresponds to concatenation of diagrams.

Right multiplication of two basis elements b_1, b_2 then becomes the juxtaposition of the diagram for b_2 under the diagram for b_1, then rescaled to be in $\mathbb{R} \times [0, 1]$ as shown in Figure 2.3.

To each word $w = s_{i_1} \dots s_{i_k}$ in $\mathcal{S}_n$ there is assigned an element $T_w = T_{i_1} \dots T_{i_k}$ of $\mathcal{A}$ and a diagram D. In the Nilcoxeter algebra case, if w is not reduced, then, $T_w = 0$ and $D = 0$. In the 0-Hecke algebra case, $T_w = T_{w'}$ for some reduced word w' and likewise, $D = D'$ for some reduced diagram D'. Note that in general w and w' are not equivalent words in $\mathcal{S}_n$. Moreover, because a reduced word in $\mathcal{S}_n$ can be related to any other equivalent reduced word through the braid relations alone, diagrams in $\mathcal{NC}_n$ or $\mathcal{H}_n$ corresponding to reduced words equivalent in $\mathcal{S}_n$ are also equivalent in $\mathcal{NC}_n$ or $\mathcal{H}_n$. Conversely, if two reduced diagrams are equivalent, then the reduced words to which they correspond are also equivalent in $\mathcal{S}_n$.

2.3.2 Diagrams on a Cylinder: The Quotients of the Nilcoxeter and 0-Hecke Algebras by Their Commutator Subgroups

Looking at diagrams on $\mathbb{R} \times S^1$ instead of $\mathbb{R} \times [0, 1]$ imposes the new relation $ab = ba$ on $\mathcal{A}$ as shown in Figure 2.4. This is equivalent to working in $\mathcal{A}/[\mathcal{A}, \mathcal{A}]$.

Figure 2.5 examplifies some of the consequences of this new relation for $\mathcal{A} = \mathcal{NC}_n$. Recall that $\mathcal{A}/[\mathcal{A}, \mathcal{A}]$ is no longer an algebra but a vector space, both in the case $\mathcal{A} = \mathcal{NC}_n$ and $\mathcal{A} = \mathcal{H}_n$, since

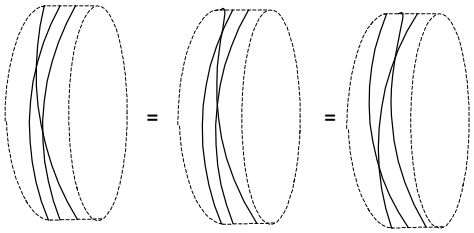

Figure 2.4: Being on a cylinder imposes the relation $ab = ba$ since the top crossing can be carried around the cylinder to become the bottom crossing.

Figure 2.5: These first two diagrams represent basis elements equivalent in $\mathcal{A}/[\mathcal{A},\mathcal{A}]$ but not in $\mathcal{A}$ for $\mathcal{A} = \mathcal{NC}_n$. The third one represent the zero element in $\mathcal{A}/[\mathcal{A},\mathcal{A}]$ for $\mathcal{A} = \mathcal{NC}_n$. This is because of the new relation $ab = ba$ which is imposed by working on a cylinder instead of a flat band.

multiplication is no longer well-defined.

2.3.3 Diagrams on the Moebius band : The Quotients of the Nilcoxeter and 0-Hecke Algebras by Their Twisted Commutator Subgroups

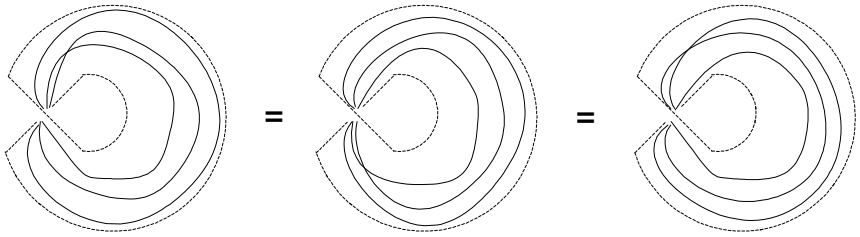

Figure 2.6: Being on the Moebius band imposes the new relation $ab = bf(a)$ with $f(T_i) = T_{n-i}$ since a crossing T_i can be dragged along the Moebius band to become T_{n-i}.

A basis element of $\mathcal{A}/[\mathcal{A},\mathcal{A}]_t$ can be represented as a diagram of n strings living on a Moebius band. On the Moebius band, a crossing T_i, if last in the diagram, can be pushed around the band to become a crossing T_{n-i} first in the diagram. Figure 2.6 shows how this can be done. Thus, $TT_i = T_{n-i}T$ as desired in $\mathcal{A}/[\mathcal{A},\mathcal{A}]_t$. Indeed, on the Moebius band, this new relation corresponds exactly to the involution used to define the relation on $\mathcal{A}/[\mathcal{A},\mathcal{A}]_t$. We typically represent these diagrams on a flat band, but one should mentally identify the top and bottom of the band in opposite directions so as to form a Moebius band.

Figure 2.7 gives an example of Nilcoxeter diagrams which are equivalent on the Moebius band but not on a flat band or on a cylinder. The elements they represent are therefore identified in $\mathcal{A}/[\mathcal{A},\mathcal{A}]_t$.

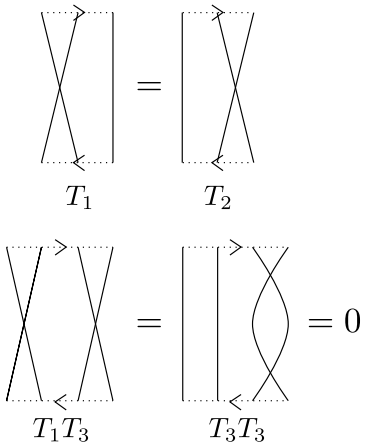

Figure 2.7: The first two diagrams of this Figure are representations of the same element in $\mathcal{A}/[\mathcal{A},\mathcal{A}]_t$. On the Moebius band, if the left crossing is pushed once around, it becomes the right crossing. This corresponds to the identification of diagrams in $\mathcal{A}$ under the involution $f(T_i) = T_{n-i}$. The second diagram is 0 in $\mathcal{A}/[\mathcal{A},\mathcal{A}]_t$ for $\mathcal{A}= \mathcal{NC}_n$.

With the goal of understanding the center of $\mathcal{A}$, we classify these diagrams on the Moebius band. The cases $\mathcal{A} = \mathcal{NC}_n$ and $\mathcal{A} = \mathcal{H}_n$ are very similar. We therefore carry out this classification in detail for $\mathcal{A} = \mathcal{NC}_n$ and later give a summary of the corresponding results for $\mathcal{A} = \mathcal{H}_n$.

2.4 Nilcoxeter Diagrams on the Moebius band

To begin our study of diagrams on the Moebius band, we fix some notation. First note that on the Moebius band, as well as on the cylinder, these n strings could actually be any number $c \leq n$ of immersed circles. Each circle is called a component of the diagram and the number of times a single immersed circle goes around the Moebius band, i.e. the degree of that immersion, is called the thickness of that component. The sum of the individual thicknesses of the components of a diagram is n, the thickness of the diagram. Figure 2.8 shows four diagrams of thickness four that decompose into components of different thicknesses. In general, one can see that a diagram on Moebius band of thickness $2k$ with no crossing must consist of k components each of thickness 2; one of the components having both top and bottom positions 1 and n, another positions 2 and $n-1$, etc. The diagram corresponding to the image of max_n in $\mathcal{A}/[\mathcal{A},\mathcal{A}]_t$, the diagram with the maximum number of crossings, must consist of n components each of thickness 1; one component having top position 1 and bottom position n, another top position 2 and bottom position

$n-1$, etc.

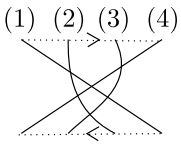

(a) Four components of thickness one

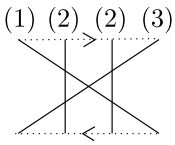

(b) Three components of thickness one, two and one

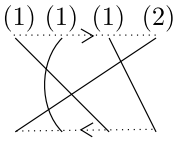

(c) Two components of thickness three and one

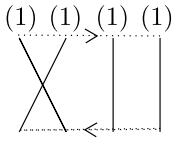

(d) One component of thickness four

Figure 2.8: These four non-zero diagrams are all of total thickness four but decompose into different prime components.

We now want to introduce the notion of a path p. A path is defined in a specific component C of a diagram D. If C has thickness m and D has thickness n, we define p as a sequence $(p(0), p(1), \ldots, p(m-1))$ where $1 \leq p(i) \leq n$, $p(i) \in \{\text{top position of a strand which belongs to } C\}$ is the top position of the strand of C after going around the Moebius band i times starting at $p(0)$. We always consider this sequence $mod(n)$ and all statements made about it should be understood as such. Figure 2.9 gives an example of a path for the central component of thickness four of this composite diagram of total thickness six. The starting position of this path is $p(0) = 3$.

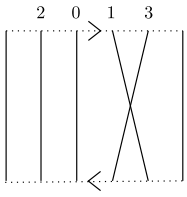

Figure 2.9: The central component of thickness four of this diagram was here marked with the path $(p(0), p(1), p(2), p(3)) = (3, 4, 2, 5)$. The other component has thickness two.

For each component C, this sequence is determined by D once $p(0)$ is chosen. Hence, two paths p, p' in the same component can only differ by an integer $l \leq m$, the lag of one path behind the other such that $p(i) = p'(i + l)$.

2.4.1 Prime Diagrams

A prime diagram is a diagram consisting of a single component. We will see that there is a unique prime diagram of thickness n for each n.

The Minimum Number of Crossings of a Prime Diagram

First, let us look at the minimal number of crossings such a diagram must have. If, instead of being on the Moebius band, we were on a simple cylinder $S^1 \times [1, n]$, the minimal condition for the n strands to be connected, to be part of the same component, would be clear: the diagram would have to correspond to an n-cycle in $\mathcal{S}_n$, in particular, it would need to have at least the $n-1$ possible crossings $T_1, \ldots, T_{n-1}$. In fact, it needs to have exactly each possible crossing once since on the cylinder, two strings are part of the same component if and only if they cross exactly once. Similarly, since, on Moebius band, the string with top position i and the one with bottom position $n-i+1$ are already part of the same component, one can quickly see that on the Moebius band, a diagram of thickness n needs at least one of T_i or T_{n-i} for each $1 \leq i \leq \lfloor (n-1)/2 \rfloor$ to be connected. Thus, we know:

Lemma: *The minimum number of crossings required for a diagram of $\mathcal{NC}_n$ with n strand to be a prime diagram is $\lfloor (n-1)/2 \rfloor$.*

The Exact Number of Crossings of a Prime Diagram of $\mathcal{NC}_n$

We need the following result to determine the maximum number of crossings that a non-zero prime diagram can have.

Lemma: *A diagram D on the Moebius band is zero if and only if there is more than one crossing between two fixed paths.*

The first implication is clear: if there are two consecutive crossings T_i for some i in D, then these two crossings must occur between the same two paths. Conversely, given two paths p and p', one can see them as being both "on top" of the other strands of D for each i. One can then slide a crossing occuring between these two paths around the Moebius band to the next or previous i. The only obstacle to doing this is if there is already a crossing between these paths at this i, in which case we have two consecutive crossings and $D = 0$. If there are two crossings between these two paths occuring at different i, one can then move one of them around the Moebius band until they are consecutive and annihilate the diagram. Figure 2.10 shows how this is done for a specific example.

We have already shown that in order for D to be prime, it must have at least $\lfloor (n-1)/2 \rfloor$ crossings. We now check that this is actually the maximum number of crossings a prime diagram of thickness n can

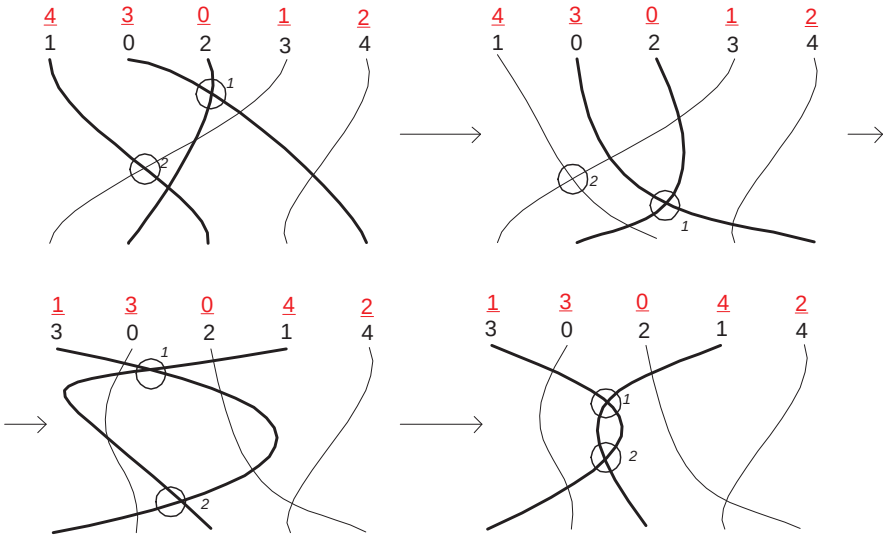

Figure 2.10: Two paths and two crossings have been marked on this Figure. Crossing 1 occurs at $i = 0$ and crossing 2 at $i = 1$. The bold strands are considered to be "on top" of the others, allowing us to see easily how to move crossings between them. One can first slide crossing 1 down the diagram. Then it can be pushed around the Moebius band to $i = 1$ so that the two crossings now both occur at $i = 1$. They become consecutive and D is seen to be zero. Note that these two paths actually cross a third time originally at $i = 3$.

have if it is to be non-zero.

We want to prove the following:

Proposition: *A prime diagram of thickness n has exactly $\lfloor (n-1)/2 \rfloor$ crossings.*

Let us for a moment fix a component C of thickness m. We want to look at (unordered) pairs of paths in C, but some pairs are redundant. For instance, in Figure 2.9, we would like the two pairs of paths $(p = (3, 4, 2, 5), p' = (2, 5, 3, 4))$ and $(q = (4, 2, 5, 3), q' = (5, 3, 2, 4))$ to be equivalent. We therefore consider pairs of paths modulo relative starting points, that is we impose the relation

$$(p, p') \equiv (q, q') \Leftrightarrow (p(i), p'(i)) = (q(i + c), q'(i + c))$$

for some integer c (remember that we are working $mod(m)$). Note that if p' lags on p by l, then p lags on p' by $m - l$. Since we are looking at unordered pairs and since any two pairs with the same lag are equivalent by the above relation, any pair of paths (p, p') such that $p(i) = p'(i + l)$ is equivalent to any pair (q, q') such that $q(i) = q'(i + n - l)$ since then $q'(i) = q(i + l)$. The pairs of paths modulo relative starting points are therefore indexed by an integer $1 \leq l \leq \lfloor m/2 \rfloor$. In our example of Figure 2.9, we thus have a total of 2 classes of pairs of paths, those which have a lag of 1 or equivalently of 3 such as

$(p = (1, 3, 4, 2), p' = (2, 4, 1, 3))$, and those which have a lag of 2 such as $(q = (1, 3, 4, 2), q' = (3, 1, 2, 4))$. Remember that when the same pair of paths intersects twice, the diagram is zero. Moreover, a crossing belongs to a pair of paths if and only if it also belongs to all equivalent pairs. Thus, there can be only one crossing per equivalence class of pairs of paths for the component to be non-zero. Since there are $\lfloor m/2 \rfloor$ equivalence classes of pairs of paths, there can be a maximum of $\lfloor m/2 \rfloor$ crossings within a component of thickness m for the diagram D to be non-zero.

In this section, we are concerned with prime diagrams, so now let D=C. For a prime diagram of odd thickness n, the maximum number of crossings we have just derived $\lfloor n/2 \rfloor = \lfloor (n-1)/2 \rfloor$, the minimum number of crossings previously derived, and the claim is proved. For D of even thickness n, we will show that D cannot actually realize this maximum of $\lfloor n/2 \rfloor$ crossings; it has either no more than $n/2 - 1 = \lfloor (n-1)/2 \rfloor$ crossings or is zero, which completes the proof of our claim for all prime diagrams. In fact, we show that a non-zero even prime diagram cannot have a middle crossing $T_{n/2}$. First, note that the paths p and p', $p(0) < p'(0)$ never intersect iff

$$p(2k) < p'(2k)$$

and

$$p(2k+1) > p'(2k+1)$$

for all k (again, we consider both 2k and 2k+1 as integers $mod(n)$).

First, let us look at diagrams D that contain no middle crossing $T_{n/2}$ and consider the paths (p, p'); $p(0) = n/2$, $p'(0) = n/2 + 1$. Since no strand ever crosses the middle point of the diagram, we have

$$p(2k) \leq n/2,\ p'(2k) \geq n/2 + 1$$

and

$$p(2k+1) \geq n/2 + 1,\ p'(2k+1) \leq n/2$$

such that $p(2k) < p'(2k)$ and $p(2k+1) > p'(2k+1)$ and p, p' do not intersect. Having at least one class of pairs of paths which do not intersect, such a diagram D has a maximum of $n/2 - 1 = \lfloor (n-1)/2 \rfloor$ crossings. Assume then that D does contain a middle crossing $T_{n/2}$. Without loss of generality, assume that $T_{n/2}$ is the top crossing of the diagram and consider the same paths $(p, p'); p(0) = n/2, p'(0) = n/2 + 1$. Now, since these paths cross immediately, $p(1) \leq n/2 < n/2 + 1 \leq p'(1)$. Suppose that these paths do not

intersect again, then

$$p(2k) > p'(2k)$$

and

$$p(2k-1) < p'(2k-1)$$

for $k > 0$. But we know that

$$n/2 = p(0) = p(n) = p(2(n/2)) < p'(2(n/2)) = p'(n) = p'(0) = n/2 + 1,$$

which is a contradiction. Therefore, (p,p') must intersect more than once and D is zero.

The Crossings of a Prime Diagram

We have now shown that a prime diagram of thickness n must have exactly $\lfloor (n-1)/2 \rfloor$ crossings. Moreover, we know that these crossings are exactly T_i or T_{n-i} for each $1 \leq i \leq \lfloor (n-1)/2 \rfloor$. In any case, each T_i appears at most once, which allows us to push all of the crossings to the left side of the diagram and thus assume that the $\lfloor n/2 \rfloor$ crossings are exactly the T_i for $1 \leq i \leq \lfloor (n-1)/2 \rfloor$. Indeed, to see this first assume inductively that all T_j, for $j > n-i$, have already been pushed to the left side. We can do this since there is at most one T_{n-2} crossing that could prevent T_{n-1} from being moved. If there is a T_{n-2} crossing above or below T_{n-1}, the latter is free to be pushed in the other direction and if there is no T_{n-2} then the T_{n-1} crossing can be pushed either up or down the Moebius band to become T_1. Consider now what could block T_{n-i}. Everything to its right has already been pushed, so only T_{n-i-1} above or below it can block it. It is therefore free to be pushed in the other direction. Therefore, from now on when we think of a prime diagram, we always represent it with its crossings being $T_1, T_2, \ldots, T_{\lfloor (n-1)/2 \rfloor}$ in some order. It remains to show that these $\lfloor (n-1)/2 \rfloor !$ diagrams are in fact all equal in $\mathcal{A}/[\mathcal{A}, \mathcal{A}]_t$.

Uniqueness of Prime Diagrams

Proposition: $T_1 T_2 \ldots T_{\lfloor (n-1)/2 \rfloor} = T_{\sigma(1)} T_{\sigma(2)} \ldots T_{\sigma(\lfloor (n-1)/2 \rfloor)} \in \mathcal{A}/[\mathcal{A}, \mathcal{A}]_t$ *for all* $\sigma \in S_{\lfloor (n-1)/2 \rfloor}$. First, let us look at the case when σ is a cyclic permutation. Fix $m = \lfloor (n-1)/2 \rfloor$. Now,

$$T_1(T_2 \ldots T_m) = (T_2 \ldots T_m) T_{n-1} = T_{n-1}(T_2 \ldots T_m) = (T_2 \ldots T_m) T_{n-(n-1)=1}$$

since $|(n-1) - i| > 1$ for $2 \leq i \leq m$. More generally, if we have any diagram $D = T_{\sigma'(1)} T_{\sigma'(2)} \ldots T_{\sigma'(m)}$ for $\sigma' \in S_m$, then

$$T_{\sigma'(1)}(T_{\sigma'(2)}\dots T_{\sigma'(m)}) =(T_{\sigma'(2)}\dots T_{\sigma'(m)})T_{n-\sigma'(1)} =$$
$$T_{n-\sigma'(1)}(T_{\sigma'(2)}\dots T_{\sigma'(m)}) = (T_{\sigma'(2)}\dots T_{\sigma'(m)})T_{\sigma'(1)} \quad (*)$$

because in fact $n-\sigma'(1) > m+1$ so that $|(n-\sigma'(1))-i| > 1$ for $1 \leq i \leq m$ unless n is odd and $\sigma'(1) = m$. Then $n-\sigma'(1) = m+1$, but we still have that $|(m+1)-\sigma'(j)| > 1$ for $2 \leq j \leq m$ since $\sigma'(j) \neq m$ for $j \neq 1$ so that (*) still holds. Diagramatically, we have taken the top crossing and pushed it onto the right side of the diagram, where it is free to be pushed to the top again. We can then push it back to the bottom left side of the diagram. Hence the Lemma holds for σ a cyclic permutation. Figure 2.11 shows how this is done for a simple example.

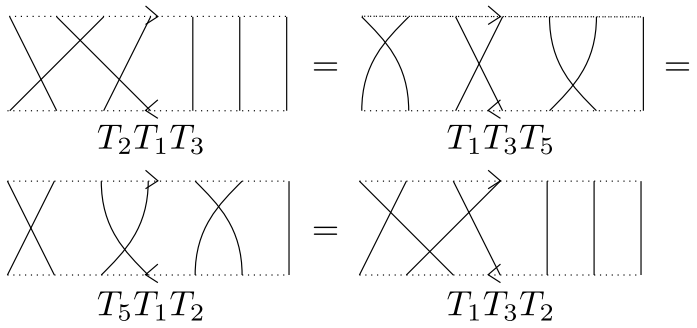

Figure 2.11: This Figure shows how one can cyclically permute the crossings of a non-zero prime diagram.

Now let us compose a permutation σ' with a transposition $(i \;\; i+1)$. Since we already know that this diagram is invariant under cyclic permutations of its crossings, we can actually assume that $i = 1$. If $\sigma'(2) \neq \sigma'(1) \pm 1$, $\sigma'(1)$ and $\sigma'(2)$ commute and we are done. Without loss of generality, assume therefore

that $\sigma'(2) = \sigma'(1) + 1$. Let k be such that $\sigma'(k) = \sigma'(2) + 1$. So

$$\begin{aligned}
\mathbf{T}_{\sigma'(\mathbf{2})}\mathbf{T}_{\sigma'(\mathbf{1})}(\dots T_{\sigma'(k)} \dots T_{\sigma'(m)}) = \\
(T_{n-\sigma'(k)} \dots T_{n-\sigma'(m)})(\mathbf{T}_{\sigma'(\mathbf{2})}\mathbf{T}_{\sigma'(\mathbf{1})})(\dots T_{\sigma'(k-1)}) = \\
\mathbf{T}_{\sigma'(\mathbf{2})}(T_{n-\sigma'(k)} \dots T_{n-\sigma'(m)}\mathbf{T}_{\sigma'(\mathbf{1})} \dots T_{\sigma'(k-1)}) = \\
(T_{n-\sigma'(k)} \dots T_{n-\sigma'(m)}\mathbf{T}_{\sigma'(\mathbf{1})} \dots T_{\sigma'(k-1)})\mathbf{T}_{\sigma'(\mathbf{2})} = \\
(T_{n-\sigma'(k)} \dots T_{n-\sigma'(m)})\mathbf{T}_{\sigma'(\mathbf{1})}\mathbf{T}_{\sigma'(\mathbf{2})}(\dots T_{\sigma'(k-1)}) = \\
\mathbf{T}_{\sigma'(\mathbf{1})}\mathbf{T}_{\sigma'(\mathbf{2})}(\dots T_{\sigma'(k)} \dots T_{\sigma'(m)})
\end{aligned}$$

using the fact that it is invariant under cyclic permutations. Thus this diagram is in fact invariant under all permutations $\sigma \in S_{\lfloor (n-1)/2 \rfloor}$.

This Lemma now allows us to conclude that there is exactly one prime diagram of thickness n for each n. This diagram can be represented as $D = T_1 T_2 \dots T_{\lfloor (n-1)/2 \rfloor)}$.

2.4.2 Composite Diagrams

We now need to see how prime diagrams can be combined into non-zero composite diagrams. At first glance, there seems to be a number of ways to combine diagrams. However, results from **??** imply that, given isotopic diagrams D and D', if D has more crossings than D', then $D = 0$.

Thus all non-zero diagrams in $\mathcal{A}/[\mathcal{A}, \mathcal{A}]_t$ with the same prime components $C_1, \dots, C_k$ have the same number of crossings and that number is the minimum of the isotopy class. Note that such a minimum must exist and that the corresponding diagram, having no two paths crossing more than once since it is minimal, is non-zero.

Note also that the relations on these diagrams being local, any relation on a prime component continues to hold when the component is combined in a composite diagram.

Combining Even Prime Diagrams

Consider a diagram D with even prime components C_1, C_2 of respective thicknesses $2k_1, 2k_2$. Since even prime diagrams have no middle crossings, we can combine C_1 and C_2 by either nesting C_2 inside C_1, which means having C_1 at positions $1, 2 \dots, k_1, k_1 + 2k_2 + 1, k_1 + 2k_2 + 2 \dots, 2k_1 + 2k_2$ both on top and bottom and C_2 at positions $k_1 + 1, k_1 + 2, \dots k_1 + 2k_2$ or vice versa. Neither of these two arrangements will add crossings between C_1 and C_2: if C_1 has $k_1 - 1$ crossings and C_2 has $k_2 - 1$ crossings and D has

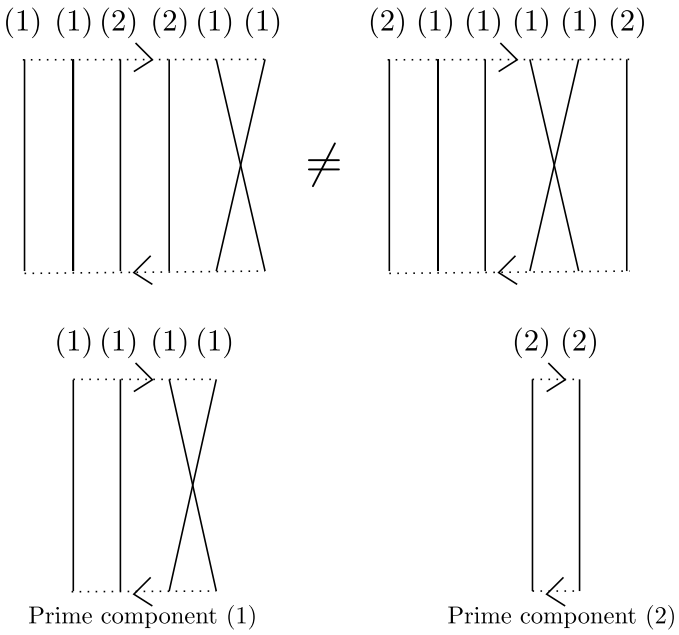

Figure 2.12: These two diagrams are both non-zero since they are minimal and their decomposition into prime components is the same. However, they do not represent the same element of $\mathcal{A}/[\mathcal{A},\mathcal{A}]_t$. This shows that prime component decompositions does not quite determine unique elements in $\mathcal{A}/[\mathcal{A},\mathcal{A}]_t$.

$k_1 + k_2 - 2$ crossings in either arrangement, which are therefore both minimal. Let D be the diagram with C_1 in the center and D' the one with C_2 in the center. Then an isotopy from D to D' requires the second Reidemeister move which creates double crossings and the isotopy therefore goes through zero. Hence, D and D' are distinct non-zero diagrams in $\mathcal{A}/[\mathcal{A},\mathcal{A}]_t$. One can also quickly see that $D \neq D'$ by noticing that the crossings of a particular component always involve only strands of that component, no matter the chosen representation, and so D and D' will always have different representations, unless $C_1 = C_2$.

Combining Odd and Even Components

Next, given a component K (prime or composite) of total odd thickness with k crossings, and even prime components $C_1, \ldots, C_m$, with $n_1, \ldots, n_m$ crossings respectively, the minimal arragements have no intercomponent crossings: they have $k + n_1 + \cdots + n_m$ crossings. These arrangements all involve K in the center, disjoint from the even components, which are split each in the middle around K. If $C_1, \ldots, C_m$ are all distinct, then there are $m!$ arrangements of this type. By the same argument as in the case of two even diagrams, there is no isotopy between these arrangements that does not require the second Reidemeister move, so these $m!$ diagrams are in fact distinct. Figure 2.14 is an example of such a minimal

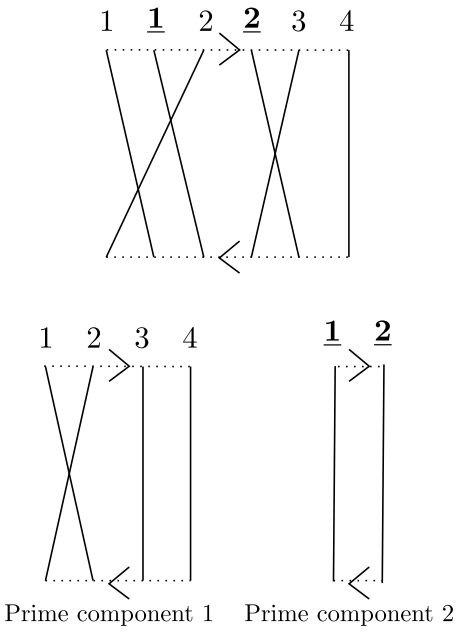

Figure 2.13: This is a non minimal arrangement of two even prime components. The strands are numbered with their positions in their respective prime components to show their assignment functions f_{C_i} more clearly. The inter-component crossings can be avoided by splitting one of the components in two and placing the other in the center. This diagram, not being minimal, is zero.

arrangement. Since K has odd thickness and thus cannot be split in its middle, if it is not in the center, then it is also not disjoint from the even components. The corresponding diagram is then not minimal and is therefore zero.

Combining Odd Prime Diagrams

Let us now see how to combine two odd diagrams C_1, C_2 of thicknesses $2k_1+1, 2k_2+1$ respectively, into a diagram D. To try to find a combination, one can start by numbering $2k_1+1$ of the $2k_1+2k_2+2 := n$ top positions of D with numbers $1, .., 2k_1+1$ in a certain color. These would be the top position for the strands of C_1. First note that once these top positions for C_1 are chosen, the bottom ones are determined. Indeed, if the number i was assigned to the top position j of D, then the number $n-i$ is assigned to the bottom position $n-j+1$. We call this assignment from $\{1, 2, \ldots, 2k_i+1\} \hookrightarrow \{1, 2, \ldots, n\}$, f_{C_i}. There seems to be many ways one can choose the positions of C_1 and C_2 in D, but we will see that there is in fact a unique choice that makes D non-zero.

Lemma: *There is a unique non-zero diagram D with prime components $C_1, \ldots C_m$ of respective thicknesses $2k_1+1, \ldots 2k_m+1$.*

We describe an arrangement and then argue that it is the unique one with the minimum number of

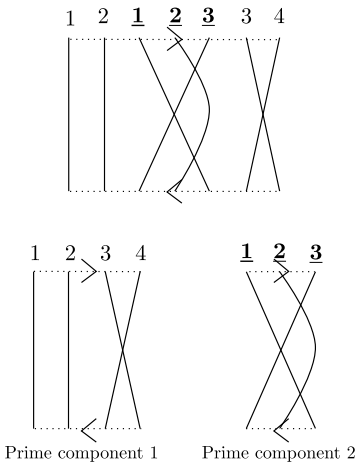

Figure 2.14: This is a minimal diagram with one odd (composite) and one even prime component. The strands are numbered with their positions in their respective prime components to show their assignment functions f_{C_i} more clearly. Minimal arrangements of this kind always involve placing the odd component in the center so as to not create inter-component crossings.

crossings. Without loss of generality, assume that

$$2k_1 + 1 \leq 2k_2 + 1 \leq \cdots \leq 2k_m + 1.$$

Let $n := 2k_1 + 2k_2 + \cdots + 2k_m + m$ be the total thickness of D. We build the diagram component by component. Let D_i be the diagram of thickness $n_i := 2k_1 + 2k_2 + \cdots + 2k_i + i$ with prime components $C_1, \ldots, C_i$ obtained after the i^{th} step of this procedure. The following assignment functions are the ones yielding the unique minimal diagram D_{i+1}:

$$f_{C_{i+1}}(j) = \begin{cases} j & j \leq k_{i+1} \\ j + n_i + k_{i+1} & j > k_{i+1} \end{cases}$$

and

$$f_{D_i}(l) = l + k_{i+1},$$

which means that we keep the previous composite D_i in the center and give C_{i+1} the edge positions.

First, we want to minimize the number of extra crossings of a component with itself. If possible, it is clear that a minimal diagram is one where the placement of each component does not add crossings between strands of the same component. If f is not monotonic, extra crossings might be created, while none are added if f is monotonic. Therefore, we need monotonic assignment functions to create minimal

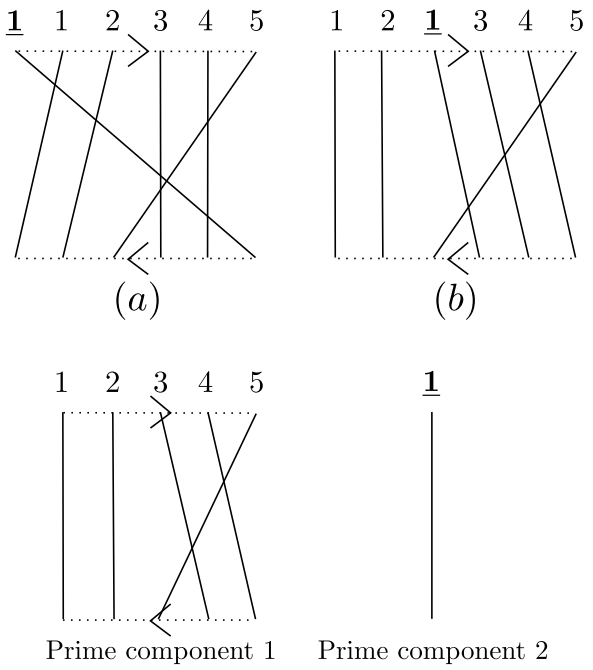

Figure 2.15: The strands of these two diagrams are numbered with their positions in their respective prime components to show their assignment functions f_{C_i} more clearly. Diagram (a) is non-minimal because the thickest odd component was placed in the center of the diagram, creating 1×5 inter-component crossings, while diagram (b), by placing the thickest component on the outside, minimized inter-component crossings to 1×1.

diagrams. Note that for each component of thickness m, if $f' = m + 1 - f$ then f and f' are equivalent on the Moebius band. Indeed, f and f' make for diagrams that are reflections of each oher and those are quickly seen to be the same by rotating the Moebius band. We therefore only consider strictly increasing monotonic assignment functions f. Moreover, all assignment functions f_{C_i} for C_i a prime component which do not increase the number of crossings within C_i itself are equivalent since all diagrams of C_i with the minimal number of crossings are equivalent.

We also want to minimize crossings between D_i and C_{i+1}, which means that we want to avoid alternating positions, ie. situations like

$$f_{D_i}(j) < f_{C_{i+1}}(k) < f_{D_i}(l)$$

which add unnecessary intercomponent crossings. For a component C of thickness m in a diagram of total thickness n, the botttom j position is the same as the top j position whenever

$$f(j) = n + 1 - f(m + 1 - j).$$

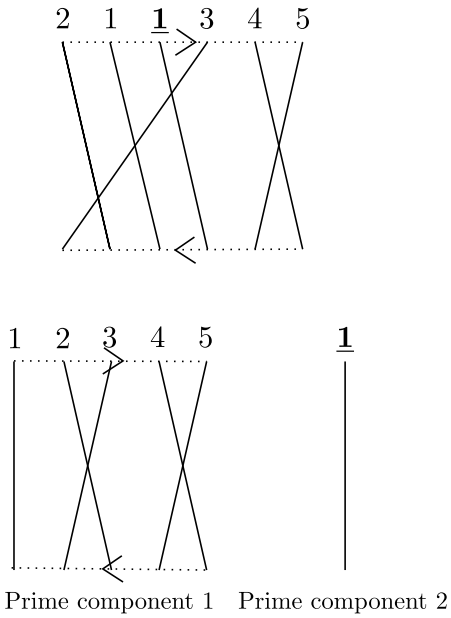

Figure 2.16: The assignment function f_{C_1} shown by the numbered strands is not monotonic and thus does not preserve the number of crossings of that prime component of thickness five. This diagram is therefore zero.

When this is not true, we have additional intercomponent crossings. Therefore, minimizing the crossings means that we want one component in the center and one on the outside of the diagram, each symmetric in their assignment.

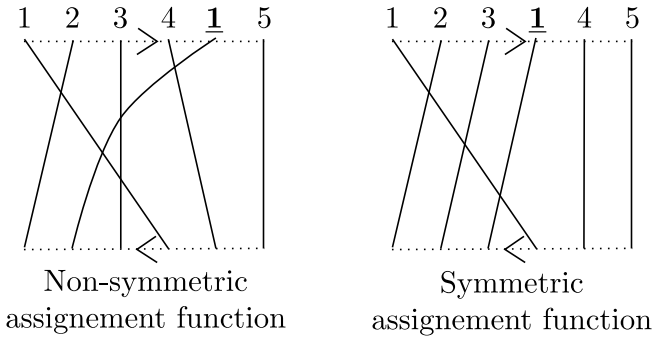

Figure 2.17: The assignment functions f_{C_i} shown by the numbered strands is not symmetric and does not minimize the number of intercomponent crossings. This diagram is therefore zero.

Inductively, we see that in any diagram, there is one strand per odd component crossing the center line of the diagram. Therefore, if D_i is placed as the outside component in D_{i+1}, there are $i \times (2k_{i+1}+1)$ crossings between D_i and C_{i+1}, since D_i is composed of i odd prime components and one strand for each of these prime components will cross the $2k_{i+1}+1$ strands of C_i. Now, an odd component cannot really

be split in two and placed on the outside because of the symmetry requirement. Placing it on the outside therefore implies taking the first and last k position, both top and bottom to minimize crossings. The remaining position has bottom position assignment $n_{i+1}+1-j$ if it has top assignment j. C_{i+1} being an odd prime component, we know that, in the standard representation of this diagram, the strand having top position $k_{i+1}+1$ has bottom position 1 in C_{i+1} and the one having bottom position $k_{i+1}+1$ has top position k_{i+1}. This means that in D_{i+1}, if $f_{Ci+1}(k_{i+1}) = j$, the strand having top position $k_{i+1}+1$ in C_{i+1} will cross D_i $j-k_{i+1}$ times and the one with bottom position $k_{i+1}+1$ in C_{i+1} will cross D_i $n_{i+1}+1-j-(k_{i+1}+1)$ times for a total of

$$j-k_{i+1}+n_{i+1}+1-j-(k_{i+1}+1) = n_{i+1}-(2k_{i+1}+1) = n_i$$

times. Now, $i \times (2k_{i+1}+1) > n_i$ since we have ordered the components such that

$$k_1 \leq k_2 \leq k_3 \leq \ldots.$$

Therefore, placing the (thickest) prime odd component C_{i+1} as the outside component always yields a minimal diagram. It remains to see whether the diagram is invariant under the choice of $f_{Ci+1}(k_{i+1}) = j$, the position in D_{i+1} of the middle position of C_{i+1}. This can be seen by pushing the crossing T_{j-1} around the Moebius band so that it becomes $T_{n_i+1}+1-j-1$. The diagram thus becomes exactly the diagram with $f_{Ci+1}(k_{i+1}) = j-1$. Doing the opposite, we get the diagram with $f_{Ci+1}(k_{i+1}) = j+1$, and so we see that D_{i+1} is invariant under the choice of j. There is therefore a unique diagram D on the Moebius band with prime components $C_1, \ldots, C_m$.

This completes the classification of Nilcoxeter diagrams on the Moebius band. We have learned that there is a unique prime diagram of thickness n for each n, that there is a unique diagram with only odd prime components $C_1, \ldots, C_m$ and that in general, the number of arrangements depends on the number of even prime components of each thickness.

2.5 The Center of the Nilcoxeter Algebra

2.5.1 The Dimension of the Center

We have now enumerated all the possible arrangements of prime components into composite diagrams. Given m even prime components $C_1, \ldots, C_m$, having i_j of them with thickness $2j$, and odd prime com-

ponents $C'_1, \ldots, C'_m$, one can make exactly $\frac{m!}{\Pi_j (i_j!)}$ distinct non-zero diagrams D with this prime decomposition. We can now count the number of non-zero diagrams of thickness n in $\mathcal{A}/[\mathcal{A}, \mathcal{A}]_t$, each of which is a basis element of $\mathcal{A}/[\mathcal{A}, \mathcal{A}]_t$. This number is also the dimension of the center Z of $\mathcal{A}$:

Proposition:

$$dim(Z) = \sum_{\lambda \vdash n} \frac{n_\lambda!}{m_\lambda},$$

where λ runs over all partitions of n, n_λ is the number of even parts in λ and $m_\lambda = \Pi_j (i_j!)$.

For instance, for $n = 3$ we have partitions

$$(1,1,1), (1,2), (3)$$

and the formula gives us

$$dim(Z) = 0!/0! + 1!/1! + 0!/0! = 3.$$

A more interesting case is $n = 6$ where we have partitions

$$(1,1,1,1,1,1), (1,1,1,1,2), (1,1,1,3), (1,1,2,2), (1,1,4), (1,5), (1,2,3), (2,2,2), (2,4), (3,3), (6).$$

The formula then is

$$dim(Z) = 0!/0! + 1!/1! + 0!/0! + 2!/2! = 1!/1! + 0!/0! + 1!/1! + 3!/3! + 2!/1!1! + 0!/0! + 1!/1! = 12.$$

The partition $(2,4)$ gives us two distinct diagrams while all the others give unique diagrams.

2.5.2 A Basis for the Center

We now know the dimension of the center of $\mathcal{NC}_n$, but we would also like to have a basis for this center. Recall that we used the fact that

$$Z(\mathcal{A}) \backsimeq (\mathcal{A}/[\mathcal{A}, \mathcal{A}]_t)^*$$

and that this isomorphism is given by the trace map ϵ. Therefore, we just need to find the dual of the diagrams we counted in the previous section.

Theorem: *The classes of diagrams of thickness n on the Moebius band are in bijection with the basis elements of $Z(\mathcal{NC}_n)$ via the algorithm described below.*

First, given an element $T_\alpha \in \mathcal{A}$, we call T_β complementary to T_α if $\epsilon(T_\alpha T_\beta) = 1$, $\alpha, \beta \in \mathcal{S}_n$. Note that

for $\mathcal{A} = \mathcal{NC}_n$, this is equivalent to $\alpha\beta = max_n$. There is a unique reduced complementary T_β for each T_α up to the relations in $\mathcal{NC}_n$.

Now, we need to find the element of $Z(\mathcal{A})$ corresponding to a basis element of $\mathcal{A}/[\mathcal{A},\mathcal{A}]_t$. Since the distinct diagrams of thickness n formed a basis for the vector space $\mathcal{A}/[\mathcal{A},\mathcal{A}]_t$, their corresponding elements in $Z(\mathcal{A})$ are also linearly independent and therefore form a linear basis for $Z(\mathcal{A})$. The element z of $Z(\mathcal{A})$ corresponding to a given basis element $\overline{b}$ is such that $\epsilon(bz) = 1$ for any $b \in \mathcal{A}$ with $\pi(b) = \overline{b}$, $\pi : \mathcal{A} \to \mathcal{A}/[\mathcal{A},\mathcal{A}]_t$ being the projection map. To find these elements of $Z(\mathcal{A})$, we first need to find the elements of the coset of $\mathcal{A}$ corresponding to a given element of $\mathcal{A}/[\mathcal{A},\mathcal{A}]_t$. The element of $Z(\mathcal{A})$ we want is then the sum of the complementary elements of the elements of that coset.

Let us compute an example for $n = 3$. Take the identity element in $\mathcal{A}/[\mathcal{A},\mathcal{A}]_t$ represented by three non-intersecting strands on the Moebius band. Its coset in $\mathcal{A}$ is just itself: T_e. Its complementary element is T_{max_n}, our first basis element for $Z(\mathcal{A})$. Conversely, the coset of $T_{max_n} \in \mathcal{A}/[\mathcal{A},\mathcal{A}]_t$ is again just $T_{max_n} \in \mathcal{A}$ and its complementary element is the identity $T_e \in Z(\mathcal{A})$, our second basis element. Now let us consider $T_1 \in \mathcal{A}/[\mathcal{A},\mathcal{A}]_t$. Its coset is $\{T_1, T_2\} \subset \mathcal{A}$ since T_1 is equivalent to T_2 in $\mathcal{A}/[\mathcal{A},\mathcal{A}]_t$. Their complementary elements are $T_{s_2s_1} = T_2T_1$ and $T_{s_1s_2} = T_1T_2$ respectively. Our third basis element is therefore $T_2T_1 + T_1T_2$. This ends our computation of the basis of $Z(\mathcal{A})$ for $n = 3$. See Figure 2.18 for the diagrams corresponding to this computation.

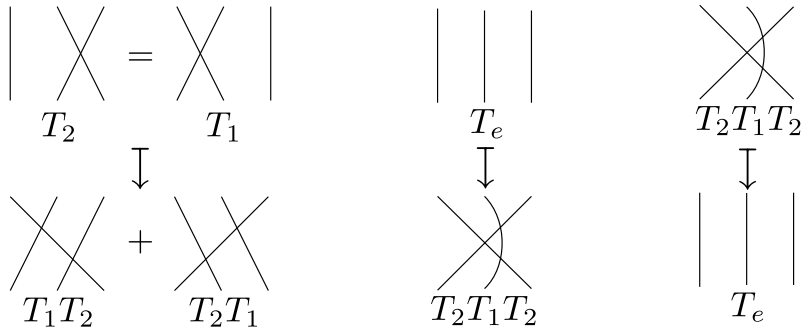

Figure 2.18: This figures shows the cosets corresponding to diagrams on the Moebius band of total thickness three and the basis elements of $Z(\mathcal{NC}_n)$ formed by taking the sum of their complements.

The Nilcoxeter algebra is a graded algebra with the grading given by the length function on $\mathcal{S}_n$. Equivalently, the grading of a basis element is given by the number of crosssings in its corresponding diagram. Note that the process described above to find a basis for $Z(\mathcal{A})$ yields a homogeneous basis since every element of the coset of an element of $\mathcal{A}/[\mathcal{A},\mathcal{A}]_t$ has the same length, or the same number of crossings and so do their complements.

2.5.3 Multiplication in the Center of $\mathcal{NC}_n$

We would now like to know what the multiplication table looks like in the basis we have described in the previous section.

Here is our first claim:

Lemma: *Every diagram corresponding to a basis element of $\mathcal{A}/[\mathcal{A},\mathcal{A}]_t$ other than T_{max_n} has a vertical line as its first or last strand. Equivalently, a basis element of $\mathcal{A}/[\mathcal{A},\mathcal{A}]_t$ other than T_{max_n} cannot have both T_1 and T_{n-1} in its expression.* First, let us look at a non-zero diagram D on the Moebius band corresponding to a partition of n which has at least one even part. Then, we know that one of these even prime diagrams is on the outside of D and disjoint from its other components. We also know that all the elements in the coset of this prime even diagram have at least one such vertical strand as either their first or last strand. Since this even component is disjoint from all the other components of the diagram, this vertical strand clearly remains in all elements of the coset of D. Figure 2.19 shows this for all the diagrams in the coset corresponding to the partition $6 = 4 + 1 + 1$.

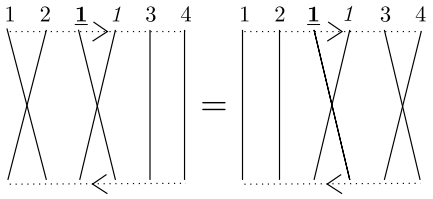

Figure 2.19: These are the diagrams in the coset corresponding to the partition $6 = 4 + 1 + 1$. Note that the even component of thickness four is always disjoint from the odd components of thickness one. Since the prime diagram of thickness four always has a vertical strand either as its first or last strand, so do all these composite diagrams.

We now look at a non-zero diagram D on the Moebius band which is composed solely of odd prime components. Since D is not the diagram for T_{max_n}, one of its prime components has thickness greater than one. Let the thickest prime component C of D have thickness $2k + 1$. Remember from the classification of these diagram that this means that this component C must be the component occupying positions 1 and n both at the top and at the bottom of the diagram. This is true for any diagram equivalent to D. Once again, every diagram of an odd prime component must have a vertical strand at position 1 or $2k + 1$. This is true also of C in D since C occupies positions 1 and n both at the top and bottom of the diagram. Figure 2.20 shows that this is true in the case of the diagrams corresponding to the partition $4 = 3 + 1$.

Our main result for this section:

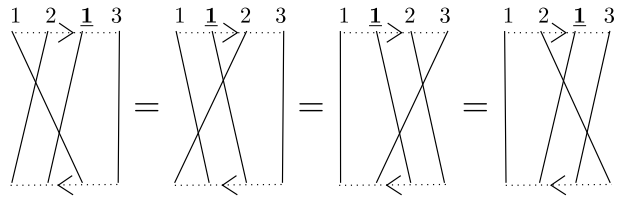

Figure 2.20: These are the diagrams in the coset corresponding to the partition $4 = 3 + 1$. Note that the prime component of thickness three is on the outside of the odd component of thickness one. Since the prime diagram of thickness three always has a vertical strand either as its first or last strand, so do all these composite diagrams.

Theorem: *The multiplication table for the center of $\mathcal{NC}_n$ in the basis described above is trivial.*

This vertical strand in every element of the cosets of our basis elements means that their complement must have either a strand going from top position 1 to bottom position n or from top position n to bottom position 1, depending on whether the vertical strand is at position 1 or n, since T_{max_n} has both of these diagonals. Since every basis element of $Z(\mathcal{A})$ is a sum of such complements, every diagram appearing in any basis element of $Z(\mathcal{A})$ has such a diagonal.

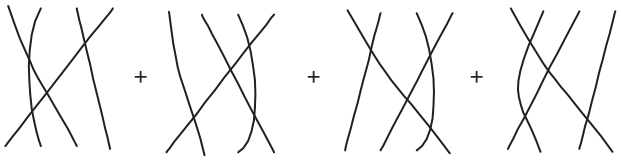

Figure 2.21: This is the basis element of $Z(\mathcal{NC}_n)$ for $n = 4$ corresponding to the partition $4 = 3 + 1$. It is the sum of the complements of the elements in the corresponding coset in $\mathcal{NC}_n$shown in Figure 2.20.

Multiplying two elements with the opposite diagonals obviously yields a non-minimal, and therefore trivial diagram since the strand in the product corresponding to these diagonals crosses every other strand twice.

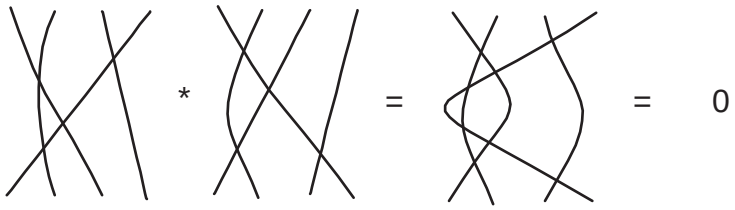

Figure 2.22: This is an example of the multiplication of two elements of $\mathcal{NC}_n$ with opposite full diagonals. Such a product is always zero.

If we multiply two elements with the same diagonal, we also have a trivial diagram. Indeed, remember

that if two strands cross more than once, the diagram is zero. Since this diagonal strand crosses all other strands in the first element and does not remain vertical in the second because of the full diagonal of this second diagram, it must cross at least one strand twice.

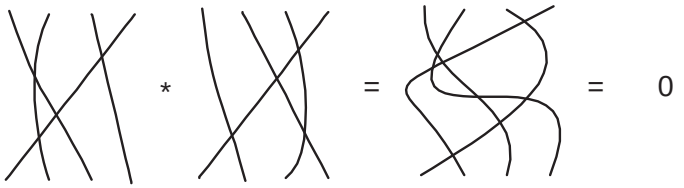

Figure 2.23: This is an example of the multiplication of two elements of $\mathcal{NC}_n$ with the same full diagonal. Such a product is always zero since the strand corresponding to the diagonal in the first element crosses at least one strand twice.

Hence, the product of any basis element by any element other than the identity is zero and the multiplication table of $Z(\mathcal{A})$ is trivial as claimed.

2.6 The Center of the 0-Hecke Algebra

2.6.1 0-Hecke Diagrams on the Moebius band

The classification of $\mathcal{H}_n$ diagrams on the Moebius band band is identical to that of $\mathcal{NC}_n$ diagrams. All of the arguments of Section 2.4 go through for $\mathcal{H}_n$. In $\mathcal{H}_n$, we want to count distinct diagrams on the Moebius band. To do so, we only count minimal diagrams, those with the least number of crossings amongst each class of equivalent diagrams. Remember that in $\mathcal{NC}_n$, non-minimal diagrams were trivial, which is not true in $\mathcal{H}_n$. However, every time a diagram was eliminated for being zero in $\mathcal{NC}_n$, it is eliminated for not being minimal in $\mathcal{H}_n$. Zero diagrams in $\mathcal{NC}_n$ correspond exactly to non-minimal diagrams in $\mathcal{H}_n$. Non-zero diagrams which are equivalent in $\mathcal{NC}_n$ are also equivalent in $\mathcal{H}_n$ and non-minimal diagrams which are equivalent in $\mathcal{H}_n$ are equivalent in $\mathcal{NC}_n$.

This last fact requires more thought, but can be shown using "fake crossings". After verifying that fake crossings can be moved around using Reidemeister moves very much like regular crossings in Figure 2.24, we can argue that any series of moves from one diagram D in $\mathcal{H}_n$ to another diagram D' having no more crossings than D can be made to start by using the relation $T_i^2 = T_i$, thus showing that this first diagram was not irreducible. Let us suppose the a series of moves from $D$to D' starts by doing the reverse of this relation thus doubling a crossing. We call the two resulting crossings a and b. Since D' has no more crossings than D, after a series of Reidemeister 3 moves, we must reduce two crossings c

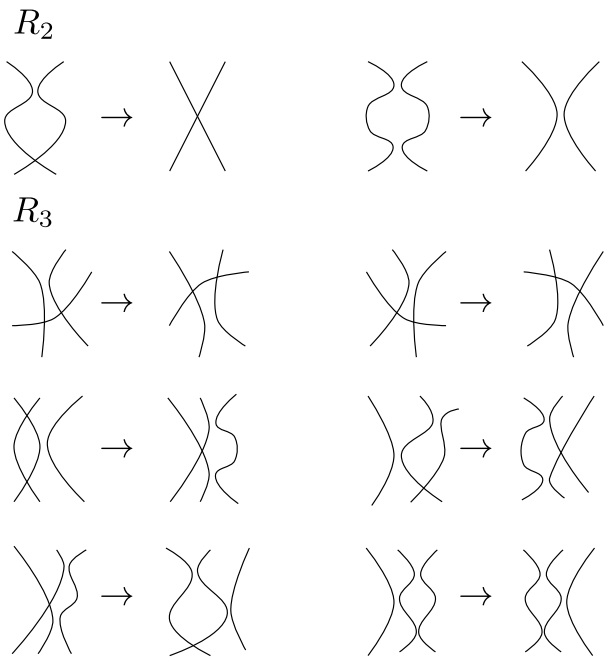

Figure 2.24: This Figure shows that fake crossings can be moved using Reidemeister moves much like regular crossings.

and d to one. If one of a or b becomes one of c or d. Let us say that a becomes c. Then we can create a fake a instead of actually doubling the crossings, do the series of $R3$ moves and then "fakely" reduce what has become a fake c. If, on the other hand, a and b do not become either c or d, we can create a fake a and do the series of $R3$ moves to get to where we would have reduced c and d. Since a is disjoint from c and d, we can still carry out the reduction. We now create a fake c and reverse the $R3$ moves to go back to the beginning, where we double the first crossing to create the real a and b. We then, once more, go through the $R3$ moves to where we would have reduced c and d, but that was already done. We have therefore done exactly the same changes as with the original series of moves, but starting with a reduction.

Hence, the vector spaces $\mathcal{A}/[\mathcal{A},\mathcal{A}]_t$ for $\mathcal{A} = \mathcal{NC}_n$ and $\mathcal{A} = \mathcal{H}_n$ are isomorphic and their bases are represented by the same diagrams on the Moebius band.

Therefore, the dimensions of the centers of $\mathcal{NC}_n$ and $\mathcal{H}_n$ are the same:

Proposition:

$$dim(Z) = \sum_{\lambda \vdash n} \frac{n_\lambda!}{m_\lambda},$$

where λ runs over all partitions of n, n_λ is the number of even parts in λ and $m_\lambda = \Pi_j(i_j!)$.

2.6.2 A Basis for the Center

Finding the basis for the center of $\mathcal{H}_n$ corresponding to our basis for $\mathcal{A}/[\mathcal{A},\mathcal{A}]_t$ is more complex than in the case of the Nilcoxeter algebra. In that previous case, it was easy to see what linear combination of diagrams would complement any diagram representing a given basis element of $\mathcal{A}/[\mathcal{A},\mathcal{A}]_t$. In other words, given a basis element $\overline{b} \in \mathcal{A}/[\mathcal{A},\mathcal{A}]_t$, we needed to find an element $z \in Z(\mathcal{A})$ such that $\epsilon(bz) = 1$ for any $b \in \mathcal{A}$ with $\pi(b) = \overline{b} \in \mathcal{A}/[\mathcal{A},\mathcal{A}]_t$. This z was simply the sum of the complements of all such $b \in \mathcal{A}$.

Because of the relation

$$T_i^2 = T_i,$$

the coset of an element of $\mathcal{A}/[\mathcal{A},\mathcal{A}]_t$ tends to be much bigger for $\mathcal{A} = \mathcal{H}_n$ than for $\mathcal{A} = \mathcal{NC}_n$. To generate all of the elements of this coset, one needs to first generate all diagrams which are equivalent on the Moebius band, just as was done for $\mathcal{NC}_n$. Then, we use the above relation to double each crossing in turn and again generate all equivalent diagrams. Repeat this process until all the new diagrams are redundant. This algorithm generates many redundant diagrams which should be ignored.

Then, an element of $\mathcal{H}_n$ may have more than one complement. However, note that a diagram in $\mathcal{H}_n$ can only have one complement with a given number of crossings. It then becomes clear that a simple sum of complements like the one we had for $\mathcal{NC}_n$ will not do; one needs a more complicated linear combination of them. Figure 2.25 gives the answer for $n = 3$.

We have not, as of yet, been able to explicitly determine the product structure of the center of $\mathcal{H}_n$in the basis corresponding to diagrams on the Moebius band .

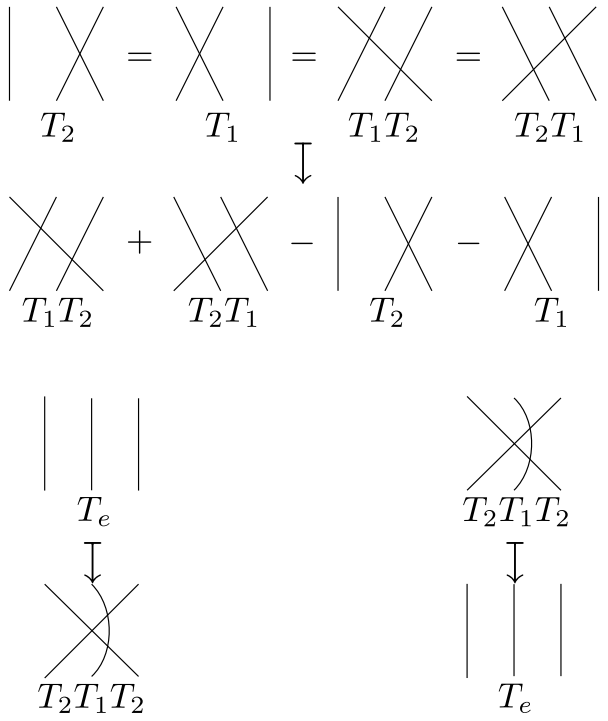

Figure 2.25: This Figure shows the cosets corresponding to diagrams on the Moebius band of total thickness three and the basis elements of $Z(\mathcal{H}_n)$ formed by taking the sum of their complements.

Chapter 3

Kuperberg's Webs on the Annulus and the Moebius band

3.1 Zeroth Hochschild Homology

Let k be a ring, A an associative k-algebra, and M an A-bimodule. We will write $A^{\otimes n}$ for the n-fold tensor product of A over k. The chain complex that gives rise to Hochschild homology is given by

$$C_n(A, M) := M \otimes A^{\otimes n}$$

with boundary operator d_i defined by

$$d_0(m \otimes a_1 \otimes \cdots \otimes a_n) = ma_1 \otimes a_2 \cdots \otimes a_n$$

$$d_i(m \otimes a_1 \otimes \cdots \otimes a_n) = m \otimes a_1 \otimes \cdots \otimes a_i a_{i+1} \otimes \cdots \otimes a_n$$

$$d_n(m \otimes a_1 \otimes \cdots \otimes a_n) = a_n m \otimes a_1 \otimes \cdots \otimes a_{n-1}$$

Here a_i is in A for all $1 \leq i \leq n$ and $m \in M$. If we let

$$b = \sum_{i=0}^{n} (-1)^i d_i,$$

then $bb = 0$, so $(Cn(A, M), b)$ is a chain complex called the Hochschild complex, and its homology is the Hochschild homology of A with coefficients in M. We denote the nth Hochschild homology of A

with coefficients in M by $HH_n(A, M)$. Of particular concern to us here is the zeroth homology of this complex. At the left end, the complex is

$$0 \leftarrow C_0 = M \leftarrow C_1 = M \otimes A \leftarrow \dots,$$

with $b_0 : C_1 \to C_0$ as the boundary map. Note that $b_0 : M \bigotimes A \to M$ is $d_0 - d_1$, and $(d_0 - d_1)(m \otimes a) = ma - am$ so that the image of b_0 is the k-bimodule $[M, A]$ of M generated by all terms $ma - am, m \in M, a \in A$. Therefore, $HH_0(A, M) \cong M/[M, A]$.

Now, if we let M be the A-bimodule A, the zeroth Hochschild homology $HH_0(A, A) \cong A/[A, A]$. When we looked at symmetric Frobenius Algebras in Section 2.2.1, we saw that their center $Z(A)$ was isomorphic to $(A/[A, A])^*$ and therefore also isomorphic to $A/[A, A] \cong HH_0(A, A)$ as vector spaces. When we work on the annulus, we impose the relation $ab = ba$ and we are therefore working in $A/[A, A]$.

Since $\mathcal{NC}_n$ and $\mathcal{H}_n$ are not symmetric Frobenius algebras, we defined an involution f and a twisted commutator subspace $[A, A]_t$ generated by elements of the form $ab - bf(a)$. This gave us an isomorphism between their center $Z(A)$ and $(A/[A, A])^*$. The involution f corresponds in these cases to taking the mirror image of a diagram. Working on the Moebius band, we impose the relation $ab = bf(a)$ and so are working in $A/[A, A]_t$.

In the cases where we do not have a non-degenerate trace map and thus we do not have a Frobenius algebra, we cannot easily relate these spaces to the center of A. However, we can still talk about $HH_0(A, A)$, which corresponds to the space of diagrams on the annulus. This is what we endeavor to do here in the following sections. The space of diagrams on the Moebius band can be seen as the zeroth Hochschild homology of the bimodule A acted upon by A with a twisted action corresponding to reflecting an element before multiplying it. As far as we know, this homology does not correspond to another known characteristic of the algebra, but we may perhaps learn something by looking at it nevertheless.

3.2 Kuperberg's Webs

Spiders and Webs for Rank 2 Lie Algebras

In [14], Greg Kuperberg introduces spiders for rank 2 Lie algebras. The idea arises from the problem of the characterization of the dual vector space of invariant tensors $Inv(V_1 \otimes V_2 \otimes \cdots \otimes V_n)$, where each V_i is a finite-dimensional irreducible representation of a compact group G or simple Lie algebra $\mathfrak{g}$. Of course, nowadays, we also want to consider quantum groups $U_q\mathfrak{g}$. The noncocommutativity of $U_q\mathfrak{g}$ complicates

matters, but, as Kuperberg points out, we still have the following natural operations on the invariant spaces:

Tensor product:

$$Inv(V) \otimes Inv(W) \hookrightarrow Inv(V \otimes W)$$

Cyclic permutation:

$$Inv(V \otimes W) \to Inv(W \otimes V)$$

Contraction:

$$Inv(V \otimes V^* \otimes W) \to Inv(W).$$

A spider is an abstraction of a representation theory that includes these three operations. It is a collection of modules or vector spaces corresponding to invariant spaces along with three operations: join, rotation and stitch, corresponding to tensor product, cyclic permutation and contraction. These operations are described using planar graphs called webs.

In his paper [14], Kuperberg defines spiders for rank two Lie algebras in terms of generators and relations and then proves that they are isomorphic to the representation theories of the rank two Lie algebras and their quantum deformation. These spiders generalize the A_1 case; the Temperley-Lieb algebra, which was already known.

Kuperberg's webs are generally considered in D^2, but we will here consider them on other surfaces: the annulus and the Moebius band primarily. Note that the join operation is then no longer defined and so we do not have spiders anymore, but simply webs.

3.2.1 A_1-Webs

Let F be a surface (oriented or not) and $B \subset \partial F$ be a distinguished set of base points. We will sometimes overload the notation and instead of B talk about m, by which we mean that B is a set of m distinct points. An A_1 web is an unoriented graph where all univalent vertices are points of B and all other vertices are 4-valent. We call those 4-valent vertices crossings. Crossings have an overstrand and an understrand.

Following the notation in [21], we denote the set of all A_1-webs in (F, B) by $\mathcal{W}_{A_1}(F, B)$. If we now let R be a ring with a distinguished invertible element a, we can define the A_1-web space over R as the R-module

$$\mathbb{A}_1(F, B, R) = R\mathcal{W}_{A_1}(F, B)/\mathcal{R}(T_1, T_2),$$

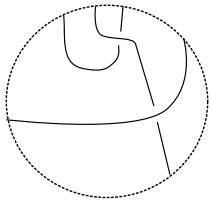

Figure 3.1: This is an example of an A_1-web in D^2 with B consisting of six points. This web has six univalent vertices and two 4-valent vertices or crossings.

where $\mathcal{R}(T_1, T_2)$ is the R-submodule generated by the elements T_1 and T_2 depicted in Figure 3.2.

$$T_1 = \times - q \rangle\langle - q^{-1} \cup$$
$$T_2 = \bigcirc - (q^2 + q^{-2}) \ \emptyset$$

Figure 3.2: The two elements T_1 and T_2 corresponding to the reduction rules in $\mathbb{A}_1(F, B, R)$.

From the elements T_1 and T_2, we get the reductions rules S_1 and S_2 of Figure 3.3, which allow us to reduce all crossings and all trivial loops, respectively.

$$S_1 : \times \to q \rangle\langle + q^{-1} \cup$$
$$S_2 : \bigcirc \to (q^2 + q^{-2}) \ \emptyset$$

Figure 3.3: These are the two reduction rules in $\mathbb{A}_1(F, B, R)$

It is worth mentioning that if B consists of $2n$ points, n of which we depict at the bottom of an interval and n at the top, reduced elements of $\mathbb{A}_1(I \times I, B, R)$ are elements of the Temperley-Lieb algebra TL_n. Because of this close relation, we will sometimes use notation from TL_n to describe elements of $\mathbb{A}_1(I \times I, B, R)$.

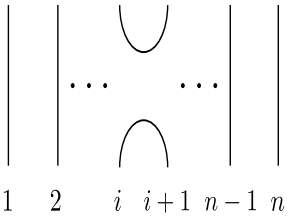

Figure 3.4: The generator u_i of the Temperley-Lieb algebra TL_n.

Figure 3.4 illustrates the generator u_i of TL_n to which we will refer later. Such diagrams are read

from bottom to top so that right multiplication is concatenation of diagrams from the top, as in the examples of Figure 3.5. For more information on the Temperley-Lieb algebra see REF.

Figure 3.5: This is an example of diagramatical multiplication in the Temperly-Lieb algebra TL_n.

A_1-Webs on the Annulus

We look here at the space $\mathbb{A}_1(A, \emptyset, R)$ of A_1-webs embedded in the annlus without boundary points. We will often simplify this notation to $\mathbb{A}_1(A)$. We shall sometimes want to refer to a subspace of $\mathbb{A}_1(A)$ generated by crossingless elements of $\mathbb{A}_1(D^2, 2n, R)$ that do not have trivial loops. These are embedded in the annulus by separating the $2n$ boundary points as n "top" points and n "bottom" points, so that the web looks like an irreducible element of the Tempeley-Lieb algebra TL_n, and then identifying the first top point with the first bottom point etc. This subspace will be denoted by $\mathbb{A}_{1,n}(A)$. As we are looking for irreducible elements of $\mathbb{A}_1(A)$, we can exclude all diagrams with crossings and with trivial loops in D^2 since those can be reduced further by reduction rules S_1 and S_2 before being embedded. We will speak of n as the maximal number of strands.

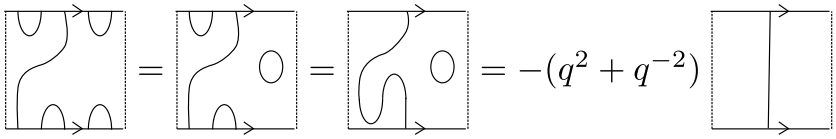

Figure 3.6: The reduction of an element of $\mathbb{A}_{1,5}(A)$

Taking an element of TL_n and embedding it in the annulus in this way, we will be left with trivial and non-trivial loops. After using our reduction rule S_2 to remove all trivial loops, we shall have only non-trivial loops. Furthermore, we assert that the non-trivial loops all have winding number 1. This is clear since for a loop to go twice around the annulus, it would have to cross itself and the web would therefore be reducible via rule S_1.

We can be even more precise and state the following:

Proposition: *The irreducible elements of* $\mathbb{A}_{1,n}(A)$ *are the diagram with* n *non-trivial loops, the diagram with* $n-2$ *non-trivial loops,* $n-4$ *non-trivial loops, etc.*

It is easy to see that we do in fact have at least all of these diagrams: embedding the diagram

corresponding to $e \in TL_n$ will give us the diagram with n loops, embedding the diagram corresponding to $u_i \in TL_n, i \leq n-1$ the diagram with $n-2$ loops, the one corresponding to $u_i u_{i+1} \in TL_n, i \leq n-2$ the diagram with $n-4$ loops and, in general, embedding the diagram corrresponding to $u_i u_{i+1} ... u_{i+l} \in TL_n, i \leq n-(l+1)$ will give us the diagram in A with $n-2(l+1)$ non-trivial loops.

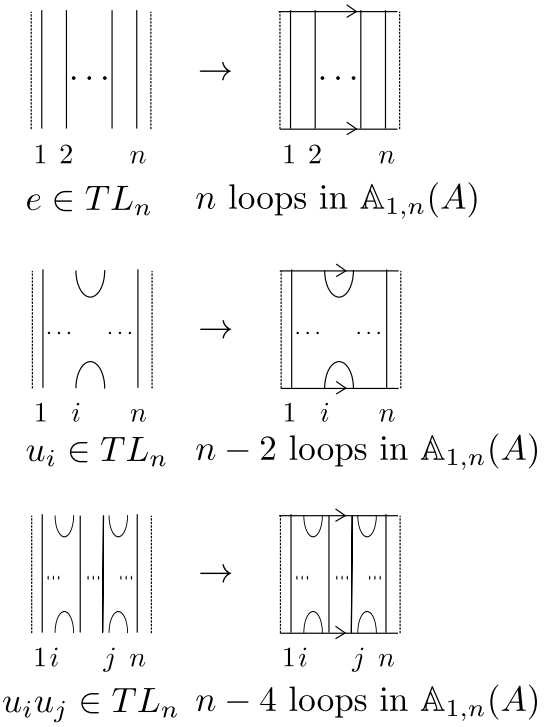

Figure 3.7: These are examples of the elements of TL_n that yield different number of non-trivial loops when embedded in the annulus.

To see that we do not get diagrams with $n-1, n-3, ..., n-(2l+1)$ non-trivial loops, we first look at the through strands before our diagram is embedded in A. The number of these through strands is an upper-bound to the number of resulting non-trivial loops in the diagram once embedded in A and the number of through strands is always $n, n-2, n-4...$ since the caps and cups at the bottom and top of the diagram take up an even number of "spots" from which through strands can no longer emanate.

Moreover, the number of through strands of a diagram D in $I \times I$ is more than the number of non-trivial loops of $\iota_1(D)$, the image of D embedded in A, in only two cases. First, $2j$ of the through strands can be "closed-off" by a top cup and a bottom cap of D and become a trivial loop in $\iota_1(D)$ as in Figure 3.8. This happens when the bottom cap and top cup are exactly $2j$ "spots" away from each other, that is when one comes from u_i and the other from $u_{i\pm 2j}, j > 0$ without any other cups or caps between them. This diminishes the number of through strands becoming non-trivial loops by $2j$, an even number.

Figure 3.8 shows two examples of through strands being closed-off by caps and cups.

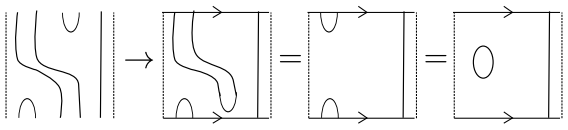

2 strands closed-off

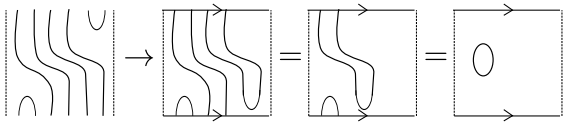

4 strands closed-off

Figure 3.8: This Figure shows how an even number of through strands of an element of TL_n can be "closed-off" when embedded in A.

Second, a top cup and a bottom cap can reduce $2j+1$ strands to one non-trivial loop by creating a zigzag, as in Figure 3.9. This happens when the bottom cap comes from u_i and the top cup from $u_{i\pm(2j+1)}, j > 0$ without other caps and cups between them. This also diminishes the number of through strands in D which become non-trivial loops in $\iota_1(D)$ by $2j$. There is thus no irreducible diagram of $\mathbb{A}_1(A)$ with $n-(2k+1), k \geq 0$ non-trivial loops.

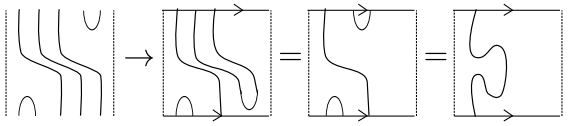

3 through strands reduce to one loop

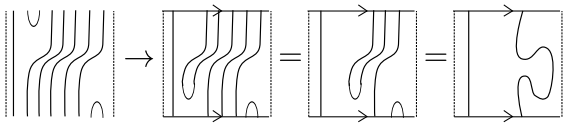

5 through strands reduce to one loop

Figure 3.9: These are examples of through strands of elements of TL_n reduced to one non-trivial loop in the annulus.

We now know that the irreducible elements of $\mathbb{A}_1(A, \emptyset, R)$ are diagrams with non-trivial loops. We also know that these loops all have winding number 1 (they can only go once around the annulus). Looking more specifically at the subspace $\mathbb{A}_{1,n}(A)$ of $\mathbb{A}_1(A, \emptyset, R)$, we can say that the irreducible elements are exactly the diagrams with $n, n-2, n-4, ..., 2, 0$ non-trivial loops. However, we are not yet able to claim that these irreducible elements are linearly independent and thus form a basis of $\mathbb{A}_1(A, \emptyset, R)$. For this, we have to wait until Section 3.3.1.

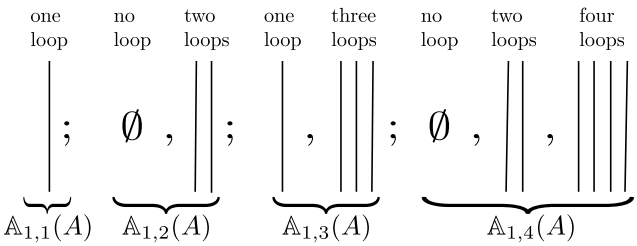

Figure 3.10: These are the irreducible diagrams in $\mathbb{A}_{1,n}(A)$ for various values of n.

A_1-Webs on the Moebius band

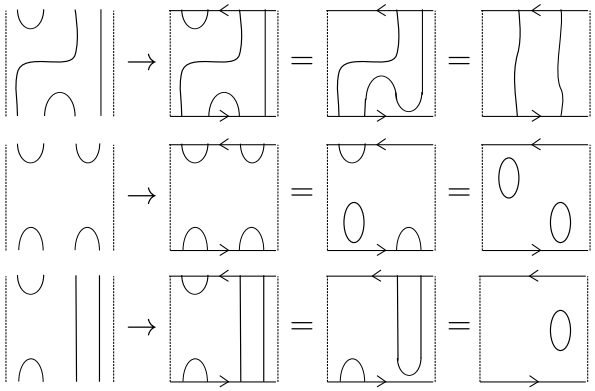

Figure 3.11: These diagrams show how the embedding into the Moebius band works for A_1-webs.

Let M be the Moebius band. Here, we look at the space $\mathbb{A}_1(M, \emptyset, R)$ of $\mathbb{A}_1$-webs without boundaries on the Moebius band. As we did for webs on the annulus, we will sometimes concentrate on the subspace $\mathbb{A}_{1,n} \subset \mathbb{A}_1(M, \emptyset, R)$ of images under the embedding $\iota_2 : D \to M$ of diagrams without trivial loops or crossings, with n bottom boundary points and n top boundary points. ι_2 identifies the first top boundary point with the nth bottom boundary point, the second top point with the $n-1$st bottom point, etc. We want to determine what the irreducible diagrams of $\mathbb{A}_1(M)$ and of $\mathbb{A}_{1,n}(M)$ are, if possible.

Similarly to diagrams on the annulus, the irreducible diagrams on the Moebius band will be non-trivial loops since our reduction rules allow us to reduce all diagrams with crossings and with trivial loops. Because our diagrams cannot contain any crossing, we can have only one non-trivial loop with winding number one in the core of the Moebius band. Any other loop going around the Moebius band only once would have to cross this first one, as can be seen in Figure 3.12, where the first diagram shows that for two loops on the Moebius band to both have winding number 1, they must cross.

In $\mathbb{A}_{1,n}(M)$, we have:

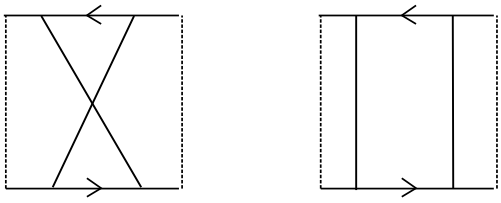

Two loops going around the Moebius band once

One loop going around the Moebius band twice

Figure 3.12: Non-trivial loops going once and twice around the Moebius band, respectively.

Proposition: *The irreducible diagrams are those with* $\lceil \frac{n}{2} \rceil, \lceil \frac{n-2}{2} \rceil, ..., \lceil \frac{n-2j}{2} \rceil$ *non-trivial loops. When n is even, all loops have winding number 2 and when n is odd, exactly one of the loops has winding number 1 and the others have winding number 2.*

The irreducible diagram with $\lceil \frac{n}{2} \rceil$ non-trivial loops is the image $\iota_2(D)$ of $D = e \in TL_n$. The one with $\lceil \frac{n-2}{2} \rceil$ is the image of $u_1u_2...u_{n-1} \in TL_n$ and in general, the one with $\lceil \frac{n-2j}{2} \rceil$ is the image $\iota_2(D)$ of

$$D = u_1u_3u_5...u_{2j-1}u_2u_4...u_{2j}u_3u_5...u_{2j+1}...u_{n-(2j-1)}u_{n-(2j-3)}...u_{n-1}.$$

The argument showing that we only see irreducible webs with $\lceil \frac{n-2j}{2} \rceil$ non-trivial loops on the Moebius band is the same as on the annulus. The number of through strands in $D \in TL_n$ before embedding it into the Moebius band is $n - 2k$, where k is the number of bottom caps or top cups. The number $\lceil \frac{n-2k}{2} \rceil$ is an upper-bound for the number of non-trivial loops in $\iota_2(D)$. As on the annulus, the number of through strands that do not become non-trivial loops is even and thus the number of those loops is always $n - 2j$ for some j. Figure 3.13 shows examples of how to obtain irreducible diagrams with different numbers of non-trivial loops in the Moebius band.

We have therefore determined that the irreducible elements of $\mathbb{A}_1(M)$ correspond to diagrams with non-trivial loops. Furthermore, we know that the irreducibles of $\mathbb{A}_{1,n}(M)$ are exactly the diagrams with $\lceil \frac{n-2j}{2} \rceil, 0 \leq j \leq \lceil \frac{n-1}{2} \rceil$ non-trivial loops. Figure 3.14 shows these irreducible diagrams for different values of n. Note that the number of irreducible webs in $\mathbb{A}_{1,n}(M)$ is the same as the number of irreducible webs in $A_{1,n}(A)$. Once we show that these irreducibles are in fact linearly independent, we will have shown that the dimension of $\mathbb{A}_{1,n}(M)$ is the same as the dimension of $A_{1,n}(A)$.

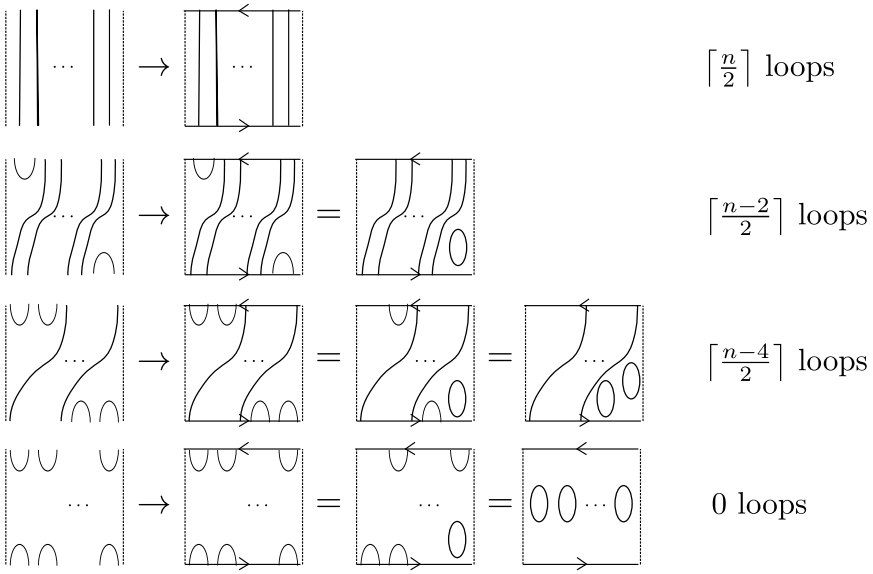

Figure 3.13: The embedding of different A_1-webs into the Moebius band results in different numbers of non-trivial loops in the Moebius band..

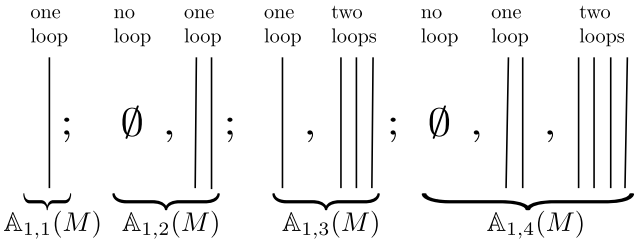

Figure 3.14: These are the irreducible diagrams in $\mathbb{A}_{1,n}(M)$ for various values of n.

3.2.2 A_2-Webs

As before, we let F be a surface and B a distinguished set of base points in the boundary of F that are now marked by $+$ or $-$. An A_2-web in (F, B) is an oriented graph with univalent vertices points of B with the corresponding edge having inward or outward orientation depending on whether the univalent vertex $p \in B$ is marked by $+$ or $-$ and with internal vertices either trivalent of 4-valent. All trivalent vertices are either sources or sinks and all 4-valent vertices are positive or negative crossing as illustrated in Figure 3.15. To remember which crossings are positive and which are negative, we can simply look at the slope of the overstrand; if it is positive, so is the crossing.

Still following the notation in [21], we denote the set of A_2-webs in (F, B) by $\mathcal{W}_{A_2}(F, B)$ and the A_2-webspace by

$$\mathbb{A}_2(F, B, R) = R\mathcal{W}_{A_2}(F, B)/\mathcal{R}(T_1, T_2, T_3, T_4, T_5, T_6),$$

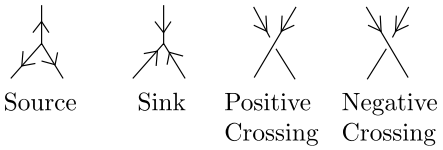

Figure 3.15: In A_2-webs, trivalent vertices can be either sources or sinks and 4-valent vertices are positive or negative crossings

where the T_i's are the elements shown in Figure 3.16 and R is a ring with a distinguished invertible element denoted by $q^{\pm\frac{1}{6}}$. The elements T_i gives us a corresponding reduction rule S_i illustrated in Figure 3.17.

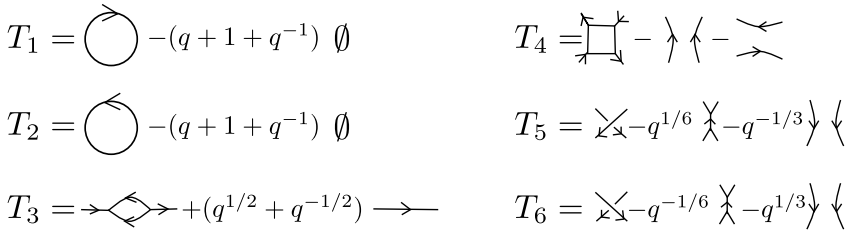

Figure 3.16: These elements generate the quotient ideal used to define $\mathbb{A}_2(F, B, R)$.

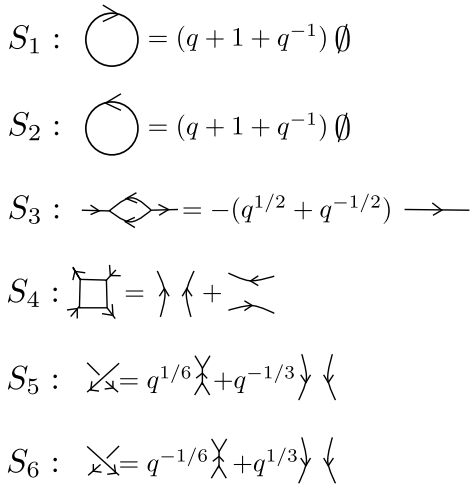

Figure 3.17: The reduction rules for A_2-webs are derived from the elements T_i above.

It is worth noting that the space $\mathbb{A}_2(I \times I, 2m, R)$ can be made an algebra. To do so, as for the case of the Temperley-Lieb albebra, we place m of the boundary points at the bottom of the interval and m at the top. Here, however, we also need to fix their orientation. Since multiplication will be the concatenation (and resizing) of webs above each other, we need the orientation of the m bottom

points to be the opposite of that of the top m points. We will call the sequence of orientations of the m bottom points s and refer to this algebra as $\mathbb{A}_{2,s}(I \times I)$ or simply $\mathbb{A}_{2,s}$. Figure 3.18 gives examples of multiplication in $\mathbb{A}_{2,s}(I \times I)$ for $s = ++-+$. Left multiplication corresponds to top concatenation, as before.

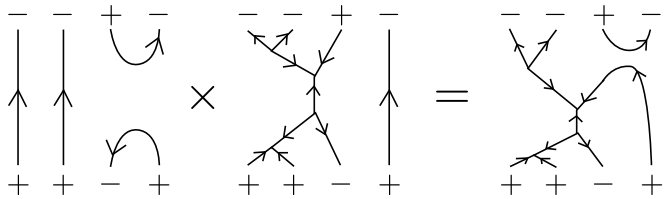

Figure 3.18: An example of the multiplication of A_2-webs by concatenation.

In $\mathbb{A}_{2,s}$, we will draw all edges so that they are either oriented upwards or downwards. We can then talk about an element $b \in \mathbb{A}_{2,s}$ factoring through a certain sequence s' when one can draw a curve accross the interval with the usual restrictions about singularities or monotonicity. For instance, the first diagram in Figure 3.20 factors through the sequences $s' = --$ and $s'' = +$.

We can also consider the algebra consisting of the set of elements of all spaces $\mathbb{A}_{2,s}$ with sequences s of length no greater than n. This algebra is denoted $\mathbb{A}_{2,m\leq n}$. Multiplication in $\mathbb{A}_{2,m\leq n}$ is zero unless the two elements to be multiplied belong to the same $\mathbb{A}_{2,s}$.

We concentrate on irreducible webs and so we can, for now, ignore 4-valent vertices since they can always be reduced using reduction rules S_5 and S_6.

A_2-Webs on the Annulus

We look at elements of $\mathbb{A}_2(A, \emptyset, R)$, the space of A_2-webs without boundaries on the Annulus, and we want to first identify the irreducible elements. Like before, we will often abbreviate this space to $\mathbb{A}_2(A)$. We will sometimes consider specifically the subset of elements of $\mathbb{A}_2(A)$ that are the images of elements of $\mathbb{A}_2(I \times I, ss, R)$ under the usual embedding into the annulus. We denote that subset by $\mathbb{A}_{2,s}(A)$.

Our main claim:

Proposition: *An element b of $\mathbb{A}_{2,s}(A)$ on the annulus reduces to a scalar multiple of the identity of the shortest sequence it contains, plus lower order terms, all themselves scalar multiples of the identity of shorter sequences. Irreducible elements of $\mathbb{A}_2(A)$ are therefore identity elements on certain sequences, represented as non-tivial oriented loops on the annulus.*

To prove this claim, we first show

Lemma: *No connected component of a $\mathbb{A}_2$-web on the annulus can have a trivalent vertex without also*

having a digon or a 4-gon and hence being reducible.

We start by reducing all crossings and, therefore, we can assume that our web has no 4-valent vertices. If e is the number of edges and v the number of vertices in our web, and knowing that we have no boundary point, we have

$$2e = 3v.$$

Now let a_2 be the number of digons in our component, a_4 the number of 4-gons, a_6 the number of 6-gons, etc. We place our component on a sphere as in Figure 3.19 and therefore create two exterior regions. One region will be an a-gon and the other a b-gon. Note that $a, b > 0$.

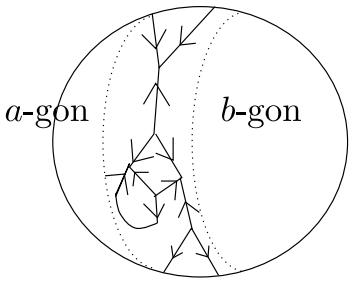

Figure 3.19: We place a A_2-web on the sphere, creating two exterior regions: a a-gon and a b-gon.

Counting each edge twice we have

$$2e = a + b + \sum_{i=1}(2i * a_{2i})$$

and given that we are on a sphere, which has Euler characteristic $\chi = 2$, we have

$$\chi = 2 = v - e + f.$$

The number of faces

$$f = 1 + 1 + a_2 + a_4 + a_6 + a_8 + ... = 2 + \sum_{i=1} a_{2i},$$

the first two summands being the a-gon and the b-gon. Thus,

$$0 = v - e + \sum_{i=1} a_{2i} = 2/3e - e + \sum_{i=1} a_{2i}$$

and

$$2e = 6 \sum_{i=1} a_{2i},$$

so that $a + b + \sum_{i=1} 2ia_{2i} = 6\sum_{i=1} a_{2i}$. Now suppose that $a_2 = a_4 = 0$. This gives us

$$a + b + 6a_6 + 8a_8 + ... = 6a_6 + 6a_8 + ...,$$

which is a contradiction, for the left-hand sum is greater than the right-hand sum given that $a, b > 0$.

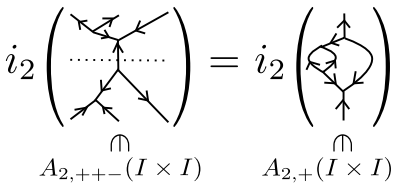

Figure 3.20: By rotating the annulus, the embedding of this non-identity element of $A_{2,++}(I \times I)$ can be seen as the embedding of an element of $A_{2,+}(I \times I)$

We therefore know that the connected component b mapped to A will reduce to a linear combination of identity elements of sequences s_i all no longer than s. But on A, we can see b as being an element of $\mathbb{A}_{2,s''}(I \times I)$ where s'' is any sequence it contains, in particular we can take s'' to be the shortest sequence it contains. Our claim that an element $\mathbb{A}_{2,s}(A)$ on the annulus reduces to a scalar multiple of the identity of the shortest sequence it contains, plus lower order terms all themselves scalar multiples of the identity of shorter sequences, follows.

Remark:
It is possible for an element b of $\mathbb{A}_{2,s}(I \times I)$ to contain different sequences of the shortest length. In that case, b can be reduced to the identity element of any of these sequences, plus lower order terms. However, we will see in Section 3.3.2 that the identity elements of all these sequences are equivalent and we will decide on which one we want as our irreducible by adding a reduction rule on the annulus.

We would like to say more about the number of irreducible elements of $\mathbb{A}_{2,s}(A)$. To do so, we now need to look more closely at the sequences through which elements of $\mathbb{A}_{2,s}(A)$ can be factored. Sequences can be reduced to shorter sequences by sinks ($++ \to -$), sources ($-- \to +$) and caps ($+- \to \emptyset$ or $-+ \to \emptyset$). First, we observe that the sequence s can ultimately reduce to one of three sequences: the empty sequence $\emptyset$, the sequence $+$ or the sequence $-$. If we represent all sequences as a graph with an edge between two sequences if and only if they can be obtained from each other by a web, we will have three connected components corresponding to the three possible resolutions just mentioned.

We must therefore start by deciding to which component of our graph the sequence s belongs. We start by assigning $+ \mapsto j$, $- \mapsto k$ and $\emptyset \mapsto 1$. Notice now that $1, j, k$ form $\mathbb{Z}_3$: $j^2 = k, k^2 = j, jk = kj = 1$.

Determining to which component s belongs is now a simple computation. For instance, the sequence $++-++$ corresponds to $j^2kj^2 = k^3 = 1$ and hence belongs to the component of the empty sequence $\emptyset$ and the sequence $-+++-$ corresponds to $kj^3k = k^2 = j$ and hence belongs to the component of the sequence $+$.

We now need to count the number of sequences of length less than the length of s that belong to the same component as s. For instance, sequences of length five will belong to the $\emptyset$ component if they correspond to jk^4 or kj^4. There are therefore ${}_5C_1 + {}_5C_4$ of them. They will belong to the $+$ component if they correspond to k^5 or j^3k^2 and so there are ${}_5C_0 + {}_5C_3$ of them. Clearly there are as many sequences that belong to the $-$ component since they are isomorphic. If we could ascertain that all sequences belonging to the same component as s were achievable from s via irreducible webs on $I \times I$, these graphs would possibly give us a way to compute the dimension of $\mathbb{A}_{2,s}(A)$. Unfortunately, we could not show that and so it will have to be saved for future work. Using results from section 3.3.2, we will however be able to compute the dimension of $\mathbb{A}_{2,m\leq n}(M) = \bigoplus_{m=0}^{n} \mathbb{A}_{2,m}$.

A_2-Webs on the Moebius band

Here we look at the irreducible elements of $\mathbb{A}_2(M)$: $\mathbb{A}_2$ webs without boundaries on the Moebius band.

Proposition: *Irreducible elements of $\mathbb{A}_2(M)$ are in bijection with sequences s' of $+$'s and $-$'s along with an additional choice of $\emptyset, +, -$ or $\pm$.*

If we think of these webs as elements of the algebra $\mathbb{A}_{2,s}(I \times I)$ embedded into the Moebius band, we must restrict the sequence s to a palindromic sequence; a sequence that is symmetric. For instance, s cannot be $++--$, but it can be $+--+$. All elements of $\mathbb{A}_2(M)$ are images of elements of $\mathbb{A}_{2,s}(I \times I)$ for some palindromic s.

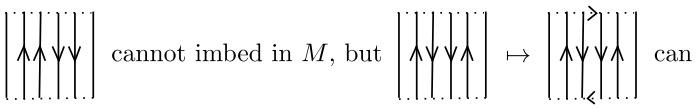

Figure 3.21: Elements of $A_{2,s}(I \times I)$ can be embedded in M when the sequence s is palindromic.

Clearly, the identity on any of these palindromic sequences embeds into an irreducible diagram on the Moebius band. Moreover, since away from the center of the band we simply have an annulus, we know from the argument in the previous section that we can have no vertices in an irreducible diagram. Therefore, for connected components of our web that are away from the center, we can only have embeddings of the identity: non-trivial loops.

The center component of a web on the Moebius band can be more than a loop, as shown in Figure 3.22. However, it is easy to see that this is the only other option, anything else being reducible. We can identify the non-trivial loops with their corresponding sequence indicating their orientation. We will denote by $\pm$ the "sequence" corresponding to the diagram of Figure 3.22.

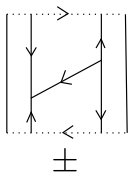

Figure 3.22: On the Moebius band, the irreducible core component can be a non-identity connected component. We denote this component by $\pm$.

The irreducible elements on the Moebius band can therefore be identified with any sequence s' indicating the direction of the loops on the left side of the Moebius band and to be repeated backward on the right side (we will denote the backward sequence $\bar{s'}$) along with four choices for the center of the diagram: $+$, $-$, $\pm$ and $\emptyset$.

For instance, the diagram on M associated with $s' = ++-+$ and center $-$ is the embedding in M of the identity of $\mathbb{A}_{2,s}(I \times I)$ with $s = s' - \bar{s'} = ++-+-+-++$. This diagram on M has four non-trivial loops with winding number two and one with winding number one in the center of the Moebius band. See Figure 3.23 for more examples.

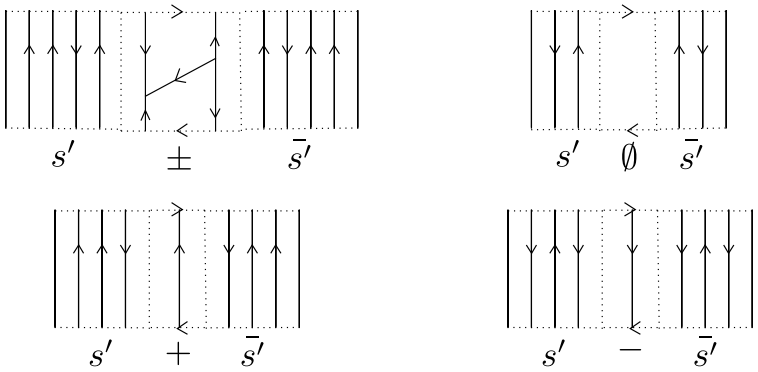

Figure 3.23: Examples of irreducible webs on the Moebius band with different core components.

3.2.3 B_2-Webs

Once again, we let F be a surface with a specific finite set of boundary points B, but this time each point is marked by 1 or 2. Note that we do not here require F to be oriented. A B_2-web is a graph with edges

labelled by 1 or 2; edges labelled by 1 will be depicted as usual and edges labelled by 2 will be depicted as double or thick edges. The labels of edges containing a point of B must coincide with the label of the corresponding point and all internal vertices are trivalent, with exactly one edge being a thick edge as shown in Figure 3.24.

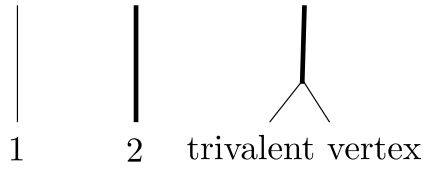

Figure 3.24: B_2-webs have single edges, labelled 1, double or thick edges labelled 2 and trivalent vertices with exactly one thick edge.

The set of all B_2-webs in (F, B) is denoted by $\mathcal{W}_{B_2}(F, B)$ and the B_2-webspace by

$$\mathbb{B}_2(F, B, R) = R\mathcal{W}_{B_2}(F, B)/\mathcal{R}(T_1, T_2, T_3, T_4, T_5, T_6),$$

where the elements T_i are the ones depicted in Figure 3.25.

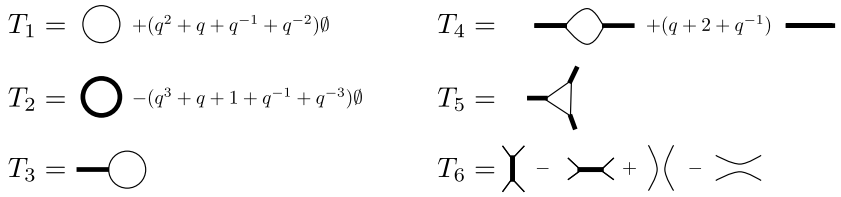

Figure 3.25: These are the elements generating the quotient ideal for the space of B_2-webs.

As noted in [21], while the first five T_i's give us obvious corresponding reduction rules S_i, T_6 is problematic because the corresponding rule would not be terminal since it would not strictly decrease in degree. This problem is traditionally remedied by expanding the B_2-webspace to allow for 4-valent vertices, a new relation $T_6' = 0$ and a new rule S_6. T_6' and S_6 are depicted in Figure 3.26. From now on, when we write $\mathcal{W}_{B_2}(F, B)$, we think of this expanded set of webs where 4-valent vertices are allowed. Note that 4-valent vertices here do not have an overstrand and an understrand, as opposed to 4-valent vertices in $\mathcal{W}_{A_1}(F, B)$ and $\mathcal{W}_{A_2}(F, B)$.

Before we look for irreducible diagrams on the annulus and on the Moebius band, let us remark that, already in D^2, if B does not contain points labelled by 2, any diagram containing an internal double edge is reducible via rule S_6. In this case, double edges can therefore only appear as non-trivial loops in an irreducible diagram, since trivial loops can be reduced using S_2.

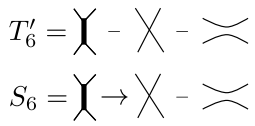

Figure 3.26: We transform the element T_6 into T_6' and introduce 4-valent vertices in order the make the reduction rules be strictly degree decreasing and hence terminal.

B_2-Webs on the Annulus and the Moebius band

Proposition: *The irreducible B_2-webs on the annulus and on the Moebius band without boundaries are simply sequences of single and double non-trivial loops.*

We have just established that the only double edges that can appear in irreducible diagrams must be non-trivial loops, which also means that irreducible diagrams cannot contain trivalent vertices. If we show that they cannot contain 4-valent vertices either, our claim will have been justified. However, we will have to wait for new reduction rules to be introduced in Section 3.3.3 to be able to show this easily.

On the annulus, a diagram composed solely of non-trivial loops is determined by the sequence s of 1's and 2's which mark the single and double loops. Such a diagram is the embedding in A of the identity on s in the algebra $\mathbb{B}_{2,n}(I \times I)$, similarly to the $\mathbb{A}_{2,n}(A)$ case. On the Moebius band, these diagrams are determined by the sequence s of 1 and 2's on the left of the center and by the center component $c \in \{\emptyset, 1, 2\}$ where the labels 1 and 2 here mean that the center loop is a single or double loop, respectively. The irreducible core component of $\mathbb{A}_{2,n}(M)$ which was denoted by $\pm$ in Section 3.2.2 does not exist here since it contains trivalent vertices with only single edges. The sequence to the right of the center is $\bar{s'}$ since the complete sequence $s'c\bar{s'}$ needs to be palindromic to exist on M. Figure 3.27 shows diagrams on the annulus and the Moebius band with their corresponding sequences.

Figure 3.27: Examples of diagrams on the annulus and the Moebius band and their determining sequences.

On the annulus and on the Moebius band, diagrams determined by different sequences of 1 and 2's are not isotopic. We still need to show that they are irreducible and linearly independent to prove that they are the basis elements of the corresponding spaces of diagrams.

3.2.4 G_2-Webs

As in the B_2 case, we let F be a surface with a specific finite set of boundary points B, each point marked by 1 or 2. A G_2-web is a graph with the labels of edges adjacent to points of B coinciding with the labels of those points and with all internal vertices trivalent, either with all single edges or with exactly one double edge as shown in Figure 3.28.

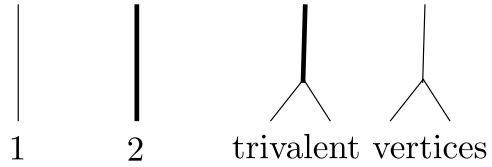

Figure 3.28: G_2-webs have single edges, labelled 1, double or thick edges labelled 2 and trivalent vertices with no or exactly one thick edge.

$\mathcal{W}_{G_2}(F,B)$ is the set of all G_2-webs on F with boundary B. The G_2 webspace is

$$\mathbb{G}_2(F,B,R) = R\mathcal{W}_{G_2}(F,B)/\mathcal{R}(T_1,T_2,T_3,T_4,T_5,T_6,T_7,T_8),$$

where the elements T_i are those shown in Figure 3.29. As usual, the reduction rule S_i corresponds to the element T_i in the obvious way. Here, we also need q^2-1+q^{-2} and $q+1+q^{-1}$ to be invertible for element T_8 to exist.

G_2-Webs on the Annulus and the Moebius band

Reduction rule S_8 guarantees that no irreducible web can have an internal double edge and rule S_2 that it cannot have a trivial double loop. Since we are working with $B=\emptyset$, we know that double edges can thus only appear as non-trivial loops in irreducible diagrams. This also means that irreducible diagrams can only have internal trivalent vertices with all single edges.

Now, an argument using Euler characteristic similar to the one used in Section 3.2.2 shows that irreducible diagrams on the annulus cannnot have any vertices.

Lemma: *Irreducible G_2-webs without boundaries on the annulus do not have any vertices.*

To prove this, we show that no connected component of a $\mathbb{G}_2$-web can have a trivalent vertex consisting of only single edges without also having a digon, a trigon, a 4-gon or a 5-gon consisting of solely single edges, and hence be reducible. Let e be the number of edges and v the number of trivalent vertices in

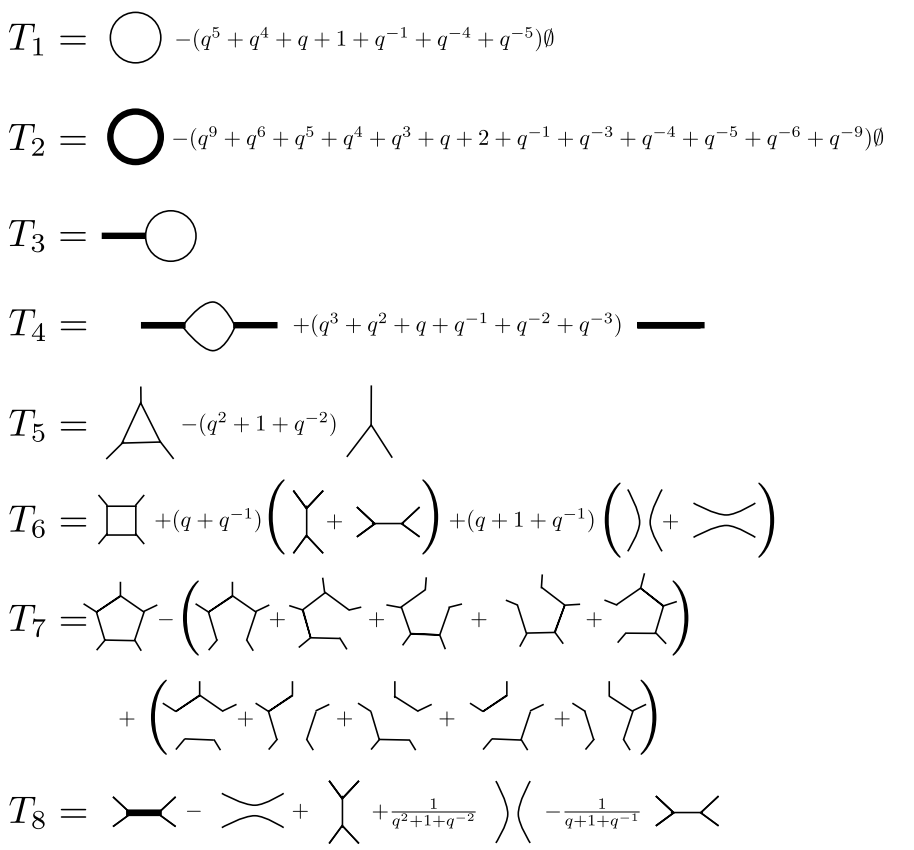

Figure 3.29: These are the elements generating the quotient ideal for the space of G_2-webs.

our web. Then, knowing that we have no boundary point, we have

$$2e = 3v.$$

Next, let a_i be the number of i-gons. We place our component on a sphere like we did for A_2-webs and therefore create two exterior regions. One region will be an a-gon and the other a b-gon. Note that $a, b > 0$.

Counting each edge twice we have

$$2e = a + b + \sum_{i=2} i a_i$$

and given that we are on a sphere we have

$$\chi = 2 = v - e + f,$$

where the number of faces $f = 1 + 1 + \sum_{i=2} a_i$, the first two faces being the a-gon and the b-gon. Thus,

$$2 = v - e + 2 + \sum_{i=2} a_i = 2/3e - e + 2 + \sum_{i=2} a_i$$

and

$$2e = 6 \sum_{i=2} a_i$$

so that $a + b + \sum_{i=2} i a_i = 6 \sum_{i=2} a_i$. Now suppose that $a_2 = a_3 = a_4 = a_5 = 0$. This gives us

$$a + b + 6a_6 + 7a_7 + 8a_8 + \cdots = 6a_6 + 6a_7 + 6a_8 + \ldots,$$

which is a contradiction, for the left-hand sum is strictly greater than the right-hand sum given that $a, b > 0$.

Hence, we have shown the following:

Proposition: *Irreducible G_2-webs without boundaries on the annulus are single and double non-trivial loops, corresponding to sequences s of 1's and 2's.*

On the Moebius band, the case is also very similar to the A_2 case. We have:

Proposition: *Irreducible G_2-webs without boundaries on the Moebius band are single and double non-trivial loops away from the core along with a choice of four components for the core: a single non-trivial loop, a double non-trivial loop, an empty set or the equivalent of the component we previously called $\pm$ but without orientation, which we will now label "3/2". They correspond to a sequence $s = s'c\bar{s}'$ with s' a sequence of 1's and 2's on the left of the core and its reflection $\bar{s}'$ on the right and a choice of $c \in \{1, 2, \emptyset, 3/2\}$.*

Figure 3.30 shows examples of irreducible webs with all these cores.

In conclusion, irreducible G_2-webs on the annulus are classified by a sequence of 1's and 2's and the irreducible webs on the Moebius band are classified by the sequence of 1 and 2's left of the core and by a choice of core component.

3.3 The Independence of Irreducible Graphs

Recall that, to find out more about the zeroth Hochschild homology of certain algebras of interest, we look at graphs or diagrams on the annulus and on the Moebius band. The first step is to find out what diagrams are irreducible on these manifolds, which is what we have been doing in the previous sections.

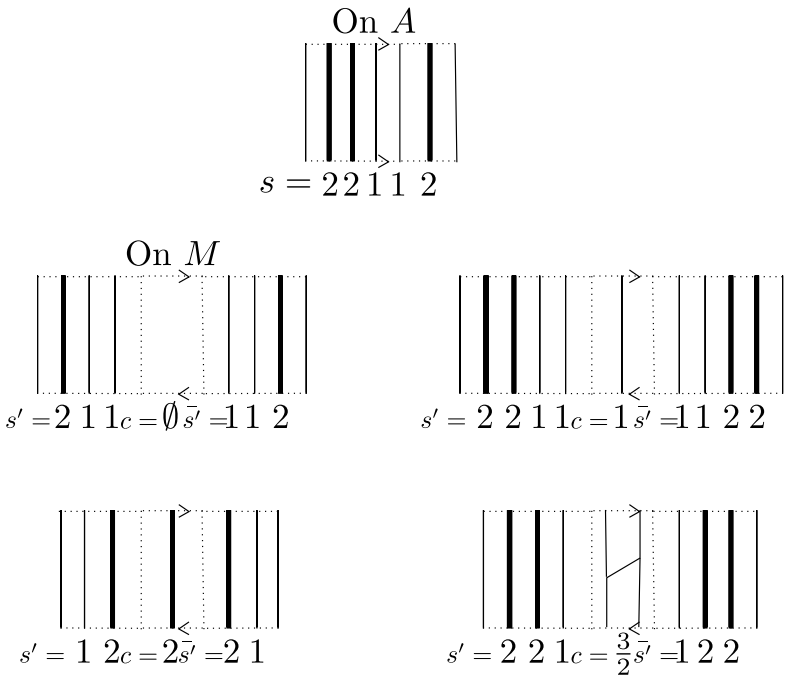

Figure 3.30: Examples of irreducible webs on the annulus and on the Moebius band with the different possible core components.

However, it is not in general obvious whether those diagrams are linearly independent. To prove that they are, we use results from Sikora and Westbury in [21]. Their results are based on the Diamond Lemma [19]. Let us first define certain terms used to state those results.

In general, we start with a directed graph (V, E). The vertices V of the graph will in cases of interest to us be diagrams (or linear combinations of diagrams) and the directed edges E will be reduction rules going from one diagram to another (or one linear combination of diagrams to another). Given a path $v_1 \to v_2 \to ... \to v_n$, we say that v_n is a *descendant* of v_1 for $v_i \in V$. We say that the reduction rules E are *globally confluent* if for all vertices v_1, v_2 connected by a finite path, v_1 and v_2 have a common descendant. We say that the rules E are *locally confluent* if for any v, w_1, w_2 such that $v \to w_1$ and $v \to w_2$, the elements w_1, w_2 have a common descendant. It is clear that global confluence implies local confluence, but the opposite implication is not true in general.

Reduction rules are said to be *terminal* if all descending paths are finite. The Diamond Lemma states that if reduction rules are terminal, then local confluence implies global confluence. Moreover, they show that if the rules are strictly degree reducing for some notion of degree, then the rules are terminal. In the case of diagrams, the degree is often related to the complexity of the diagram, for example to the number of crossings or of components in the diagram.

Sikora and Westbury prove a linear version of the Diamond Lemma that allows us to have reduction rules sending a diagram to a linear combination of diagrams. Given a ring R, let RV be the free R-module over V. For any terminal rules $\{S_i\}_{i\in I}$ for RV, local confluence implies global confluence. They then show that if the reduction rules $\{S_i\}_{i\in I}$ are globally confluent in RV , then the irreducible elements of V are a basis for $RV/\mathcal{R}(S_i, i \in I)$.

To show that our irreducible diagrams are in fact linearly independent, we therefore only need check for local confluence (given that our reduction rules do in fact strictly decrease the complexity of our diagrams and are therefore terminal). This means that, given a diagram which can be resolved using two different rules, we need to show that it ultimately resolves into the same linear combination of diagrams no matter which rule we decide to apply first. Diagrams which can be resolved using different rules are called *overlaps* in [21]. Fortunately, they also show that we only need check confluence of a finite set of overlaps, as long as the diagrams overlapping are simple graphs.

3.3.1 Linear Independence for Irreducible A_1-Webs

We have found the irreducible A_1-webs on the annulus and on the Moebius band in Section 3.2.1 but were then unable to prove their linear independence. Fortunately, thanks to the results of [21], it is now fairly easy to establish.

Lemma: The irreducible A_1-webs without boundaries on the annulus and on the Moebius band are linearly independent and are thus a basis of the corresponding space.

We will follow the notation in [21] and let the number of crossings of a A_1-web Γ be denoted by $v(\Gamma)$ and the number of its connected components by $c(\Gamma)$. We know that the reduction rules for A_1-webs send each diagram Γ to a linear combination of diagrams Γ_i so that $(v(\Gamma_i), c(\Gamma_i)) < (v(\Gamma), c(\Gamma))$ if $\mathbb{Z}_{\geq 0} \times \mathbb{Z}_{\geq 0}$ is given the lexicographical order. The pair $(v(\Gamma), c(\Gamma))$ is set as the degree of the diagram Γ and the results from [21] quoted in Section 3.3 then tell us that since the reduction rules decrease the degree, the rules are terminal.

We now need to check that overlaps can be resolved. This is trivial in this case since the two source diagrams of our reduction rules (the crossing and the trivial loop) have no non-trivial overlaps. Figure 3.31 shows the trivial overlap. Therefore, our rules are locally confluent and thus also globally confluent. Note that this is true on any surface, oriented or not, since all overlaps are trivial no matter the embedding.

Since we have already determined that the irreducible A_1-webs on the annulus and the Moebius band were diagrams with a number of non-trivial loops, we now know that they are a basis for the A_1-web space

Figure 3.31: This trivial overlap is the only overlap for A_1-webs.

over R. Below, we denote

$$\bigoplus_{m \leq n} \mathbb{A}_{1,m}(F,R) = \mathbb{A}_{1,m \leq n}(F,R).$$

We can now compute the dimensions of spaces of diagrams on the annulus and Moebius band:

Theorem:

$$dim(\mathbb{A}_{1,n}(A,R)) = dim(\mathbb{A}_{1,n}(M,R)) = \left\lceil \frac{n+1}{2} \right\rceil$$

and

$$dim(\mathbb{A}_{1,m \leq n}(A,R)) = dim(\mathbb{A}_{1,m \leq n}(M,R)) = n+1.$$

3.3.2 Linear Independence for Irreducible A_2-Webs

To find a set of independent irreducible A_2-webs, we need to find terminal and confluent reduction rules. As we did for A_2-webs, we denote the number of connected components of an A_2-web b by $c(b)$, the number of its trivalent vertices $v_3(b)$, and the number of crossings $v_4(b)$. We can then give $\mathbb{Z}_{\geq 0} \times \mathbb{Z}_{\geq 0} \times \mathbb{Z}_{\geq 0}$ the lexicographical ordering. The reduction rules of Figure 3.17 replace the web b by a linear combination of webs b_i with $(v_4(b_i), v_3(b_i), c(b_i)) < (v_4(b), v_3(b), c(b))$. This means that our reduction rules are terminal. Unfortunately, they are not confluent on any surface containing a non-contractible annulus, that is on any surface other than D^2 and S^2. Indeed, Figure 3.32 shows that there is an overlap on which the two possible applications of S_4 yield two different diagrams on the annulus: the identity on $+-$ and the identity on $-+$.

We therefore add an additional rule S_7 pictured in Figure 3.33 which reduces the identity on $-+$ to the one on $+-$. $S_1, ..., S_7$ are now terminal in the oriented case, but not in the unoriented one since there S_7 is its own inverse. This is because on the Moebius band, the two diagrams of Figure 3.34, the identity on $+-\emptyset-+$ and on $-+\emptyset+-$ are isotropic. Therefore we confine ourselves to the oriented case for now and will come back to the Moebius band after. In the oriented case, all overlaps were checked in [21] and we can conclude that rules $S_1, ..., S_7$ are locally confluent on all overlaps and therefore globally confluent.

Theorem: *The irreducible A_2-webs with respect to rules $S_1, \ldots, S_7$ on an oriented surface (F,B) form a basis of the free R-module $\mathbb{A}_2(F,B,R)$.*

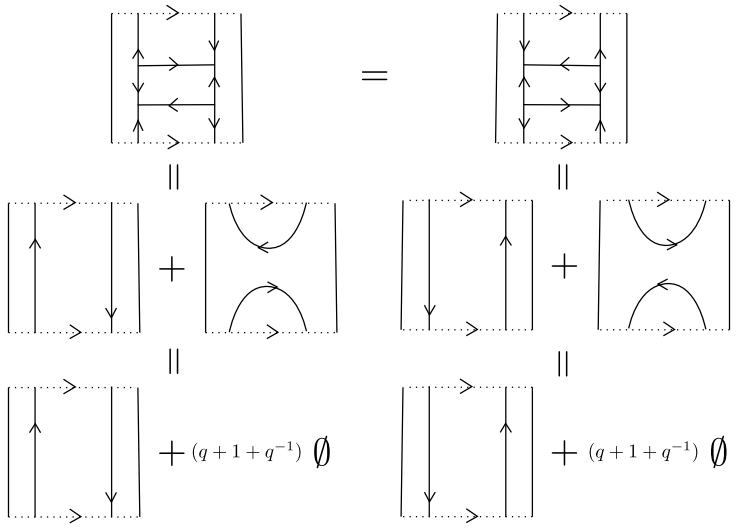

Figure 3.32: This overlap of A_2-webs shows that reduction rules $S_1, \ldots, S_6$ are not terminal on any surface containing an annulus.

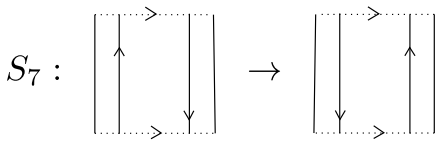

Figure 3.33: Adding reduction rule S_7 to our set of reduction rules makes these rules terminal and confluent on all oriented surfaces.

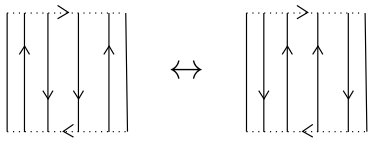

Figure 3.34: These two diagrams are isotropic on the Moebius band.

We did characterize all irreducible webs on the annulus in Section 3.2.2, but we need to revise our conclusions because of the additional rule S_7. With rules $S_1, ..., S_6$ we had an irreducible web corresponding to each sequence s of $+$'s and $-$'s. However, S_7 now reduces such sequences by moving all the loops marked $+$ to the left. We therefore have an irreducible element corresponding to each sequence $+...+-...-$ with only $+$'s on the left and $-$'s on the right. If s has a length of n, we have exactly $n+1$ such sequences and hence $n+1$ corresponding basis elements. From this we can conclude that for s no longer than n, we have

Theorem:

$$dim(\mathbb{A}_{2,m\leq n}(A)) = \sum_{i=0}^{n}(i+1) = \frac{n(n+1)}{2} + n + 1.$$

The new reduction rule S_7 also changes the set of irreducible diagrams on the Moebius band. Instead of these diagrams being determined by any sequence s' along with a choice of core, s' must now be restricted in the same way as the sequences determining the irreducible diagrams on the Annulus: $s' = +...+-...-$.

Now, in order to find the linearly independent diagrams on the Moebius band, we define a procedure for taking diagrams embedded in the Moebius band to the Annulus. This procedure can be thought of as looking at a diagram on the Moebius band, itself in a solid torus and projecting it onto the Annulus also in the solid torus. Diagramatically, this corresponds to cutting the diagram on the Moebius band and adding a half-twist to it.

It is not clear whether this map is well-defined since it could depend on where the Moebius band band is cut to add the half-twist and, in fact, it does. One can show that factors of $q^{-4/3}$ and $-q^{-2/3}$ will be introduced depending on where the cut occurs. However, in the special case where $q = q_0$ such that $q_0^{-4/3} = 1, q_0^{-2/3} = -1$, the result does not depend on where the cut is made and the map is a well-defined map of vector spaces. Up to lower order terms, this procedure maps irreducible diagrams in the Moebius band to irreducible diagrams in the Annulus surjectively. This is seen fairly easily diagramatically. We can think of this map as being upper triangular. Let us look at the image of the map a little bit more closely. Again, we are working up to lower order terms. Given an irreducible diagram D on Moebius band characterized by a left hand sequence s and a core $c \in \{\emptyset, -, +, \pm\}$, it is not difficult to determine exactly which irreducible on the Annulus will be the highest order term D' of its image. Because of the extra reduction rule S_7, s is determined by the number of $+$ and the number of $-$ it contains. Let us denote the former by m_1 and the latter by m_2 and let us denote the sequence determining D' by s', with $m_1'+$ and $m_2'-$. If $c = \emptyset$, D' will be the identity on the sequence s', with $m_1' = 2m_1$ and $m_2' = 2m_2$. If $c = +$, $m_1' = 2m_1 + 1$ and $m_2' = 2m_2$, if $c = -$, $m_1' = 2m_1$ and $m_2' = 2m_2 + 1$ and, finally, if $c = \pm$, $m_1' = 2m_1 + 1$ and $m_2' = 2m_2 + 1$.

Since the number of irreducibles is the same on both surfaces and since we already know that the irreducibles on the Annulus are a basis, this shows that, at least when $q = q_0$, the irreducibles on the Moebius band are also linearly independent.

Assume now that for some other value of $q \neq q_0$ there exists a relation

$$P(D_1, ...D_m);$$

P is a polynomial in the irreducible diagrams on the Moebius band with coefficients in $\mathbb{C}[q^{\pm 1/6}$. We then also get a relation for $q = q_0$, which is a contradiction, unless $P = 0$ when $q = q_0$. However, we can then divide P by $(q - q_0)^i$, for i the largest power of $q - q_0$ by which P is divisible. This yields a new relation P' which is non-zero when $q = q_0$, which is a contradiction. We have therefore shown that the irreducible diagrams on the Moebius band are linearly independent and are therefore a basis of $\mathbb{A}_{2,m\leq n}(M)$.

Remark: Over and under crossings, or 4-valent vertices, are not well-defined on the Moebius band. Hence, we cannot try to map diagrams from the annulus to the Moebius band, since we then would need to define those crossings. By limiting ourselves to irreducible diagrams, which do not have crossings, and by mapping them from the Moebius band to the annulus, we avoid this problem.

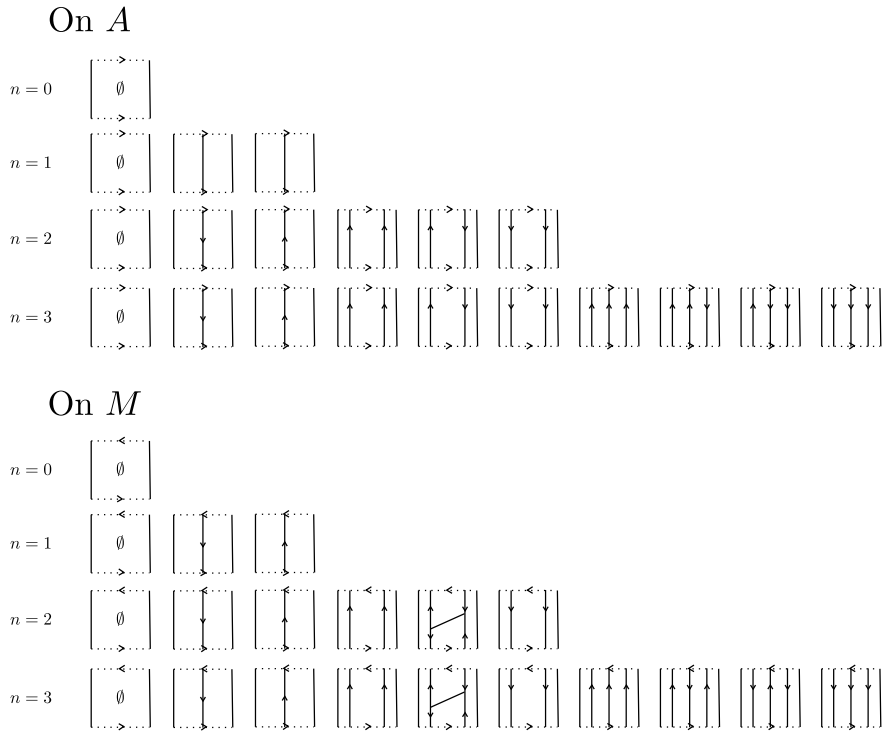

Figure 3.35: Examples of the basis diagrams for $\mathbb{A}_{2,m\leq n}(S)$ for $S = A$ and $S = M$ and small values of n.

To make the reduction rules terminal on the Moebius band, one could also simply orient the core of the Moebius band with an oriented non-trivial loop which is not part of our web, but an additional structure of the Moebius band itself. This loop then orients the annulus which is in the Moebius band away from core and allows us to use rule S_7 on that annulus. See Figure 3.36 for a representation of that rule on the Moebius band.

Theorem: *The irreducible A_2-webs with respect to rules $S_1, \ldots, S_7'$ on the Moebius band form a basis*

of the free R-module $\mathbb{A}_2(M)$ *and*

$$dim(\mathbb{A}_{2,m\leq n}(M)) = \sum_{i=0}^{n}(i+1) = \frac{n(n+1)}{2} + n + 1.$$

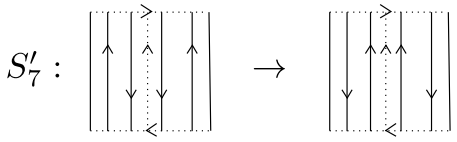

Figure 3.36: By orienting the core of the Moebius band, we can define reduction rule S_7', which makes the new set of rules terminal on the Moebius band.

3.3.3 Linear Independence for Irreducible B_2-Webs

Remember that in the case of B_2-webs, we have not yet characterized the irreducible diagrams, knowing that the reduction rules were going to change. We did, however, see that any diagram on the annulus or on the Moebius band could be expressed as a linear combination of diagrams which are sequences of non-trivial single and double loops.

Now, rules $S_1, \ldots, S_6$ each either decreases the number of vertices or decreases the number of components without increasing the number of vertices. They are therefore terminal. After checking the basis of overlaps, Sikora and Westbury conclude that rules $S_1, \ldots, S_6$ are unfortunately not confluent. However, they are able to find a new set of 18 reduction rules which are terminal and confluent for graphs in $\mathcal{W}_{B_2}(F, B)$. Figure 3.37 depicts the ones which take place in D^2 and the ones in the annulus and the Moebius band that do not have boundary points, and will therefore be of interest to us. Their numbering is taken from that of [21].

Once we show that 4-valent vertices can always be reduced, we will finally see that the diagrams which are simply sequences of non-trivial single and double loops are the irreducible diagrams. Since these new rules are confluent and terminal for $\mathcal{W}_{B_2}(F, B)$, this will also show that those diagrams are a basis of $\mathbb{B}_{2,m\leq n}(A)$.

We have three cases of 4-valent crossings to address: they are shown in Figure 3.38. The first case, a diagram with two strands crossing only once, can be reduced by rules S_{10} on the annulus and S_{11} on the Moebius band. The case with two strands locally crossing more than once can be reduced via S_{14} and the one with one strand via S_7. Thus diagrams with 4-valent vertices are reducible and we are left

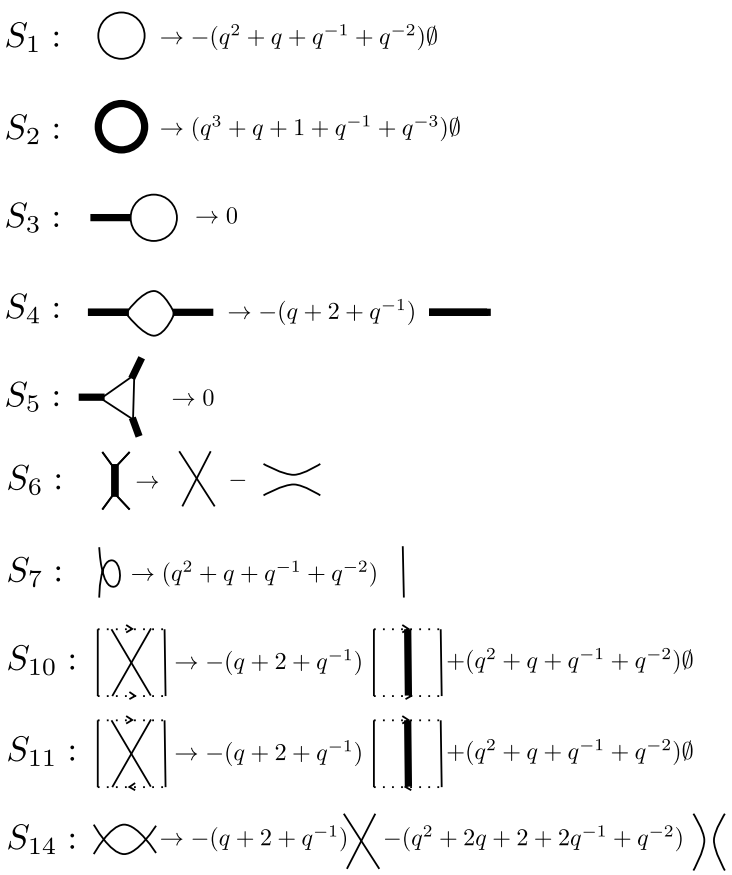

Figure 3.37: These are the reduction rules for B_2-webs without boundaries which are terminal and confluent on D^2, A and M .

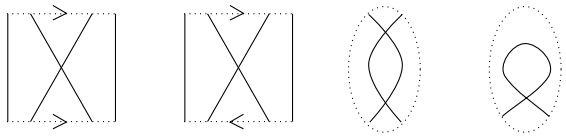

Figure 3.38: These are the three cases of 4-valent vertices in $\mathcal{W}_{B_2}(F,B)$. We need to show that they all can be reduced on the annulus and the Moebius band via the reduction rules of Figure 3.37.

with diagrams containing only non-trivial loops as our irreducibles. Since reduction rules $S_1,\ldots,S_{18}$ are confluent and terminal, these irreducible diagrams are linearly independent and hence a basis for the space of diagrams on A or M.

Therefore,

Theorem: Diagrams that are single and double non-trivial loops and thus correspond to sequences

of 1's and 2's on the annulus and on the Moebius band are a basis of their corresponding spaces and thus

$$dim(\mathbb{B}_{2,m\leq n}(A)) = \sum_{i=0}^{n} 2^i$$

and

$$dim(\mathbb{B}_{2,m\leq n}(M)) = \sum_{i=0}^{\lfloor \frac{n+1}{2} \rfloor} 2^i.$$

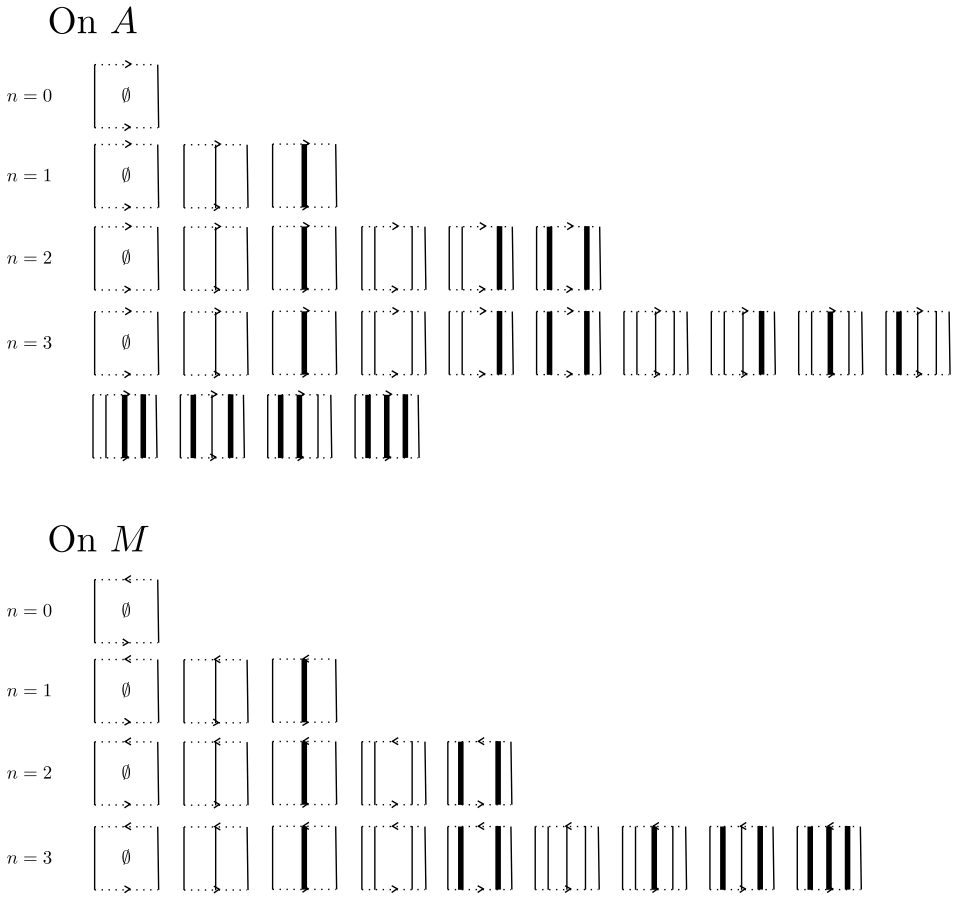

Figure 3.39: Examples of the basis diagrams for $\mathbb{B}_{2,m\leq n}(A)$ and $\mathbb{B}_{2,m\leq n}(M)$ for small values of n.

Figure 3.39 shows the basis diagrams on the annulus and the Moebius band for small values of n.

3.3.4 Linear Independence for Irreducible G_2-webs

Proposition: *The irreducible G_2-webs on the annulus and on the Moebius band are linearly independent and therefore form a basis of the corresponding spaces.*

Sikora and Westbury do verify the confluence and terminality of the reduction rules of G_2-webs in the case of orientable surfaces. They determine that one more rule must be added on the annulus, but since the webs involved in that rule all have boundaries, we do not need it here. This result tells us that the irreducible G_2 diagrams on the annulus that we found in Section 3.2.4 are linearly independent.

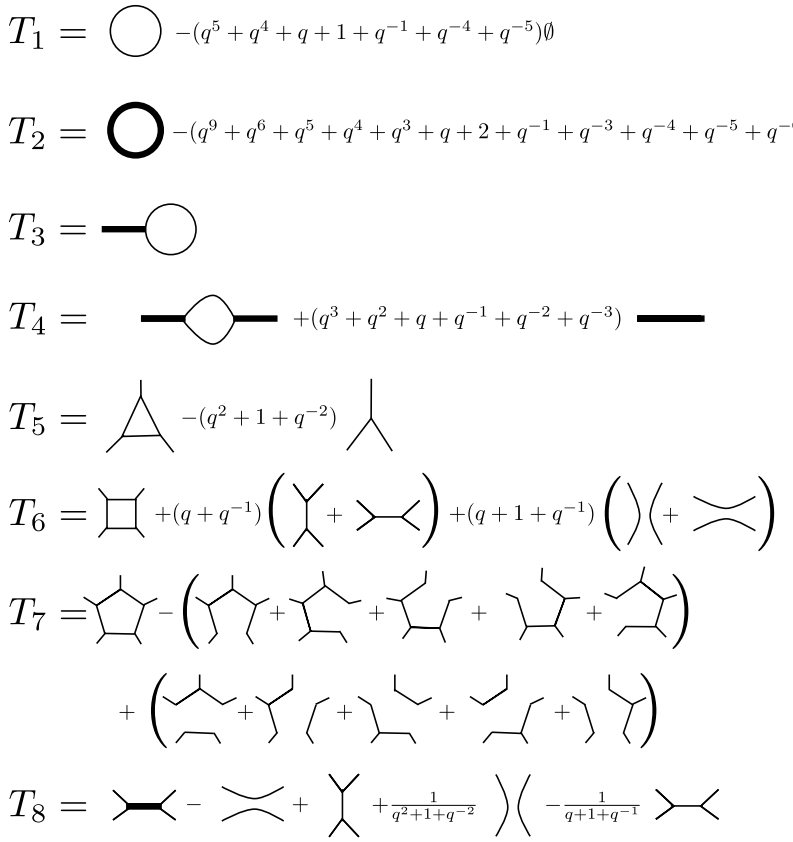

Figure 3.40: These are the elements generating the quotient ideal for the space of G_2-webs.

Though Sikora and Westbury do not verify the confluence of the rules on non-orientable surfaces, it is not hard to see that overlaps on the Moebius band and without boundaries resolve on the Moebius band just as they do on the annulus. We only need consider overlaps that cannot be contained in D^2 since those were clearly verified by Sikora and Westbury in their analysis of the confluence on orientable surfaces, which already eliminates all overlaps involving rules S_1, S_2 and S_3. Moreover, irreducible overlaps involve only two reduction rules per overlap. We can now see that in our case, since we have no boundaries, the overlaps we need to check are all embeddings in the Moebius band of diagrams of the form $D_1 D_2$, where D_1 and D_2 are diagrams from the left hand side of one of the reduction rules $S_4, \ldots, S_8$. Since these overlap in D^2 have been checked, our only concern is that the reduction of $D_1 D_2$ be equal to that of $D_2 \bar{D}_1$,

where $\bar{D_1}$ is the reflection of D_1 about the axis of the core of the Moebius band, since $D_1D_2 = D_2\bar{D_1}$ on the Moebius band. Remark that on the annulus, one would have to check that the reduction of D_1D_2 is the same as that of D_2D_1. Once we notice that all of the diagrams on both the left and right hand sides of rules $S_4, \ldots, S_8$ are symmetric so that $D = \bar{D}$ for these diagrams, we can conclude that, in fact, all of the overlaps of concern to us have been checked already when confluence was checked on the annulus. Figure 3.41 shows two examples of overlaps that would need to be checked on the Moebius band, but have in fact already been verified because they are the same on the annulus.

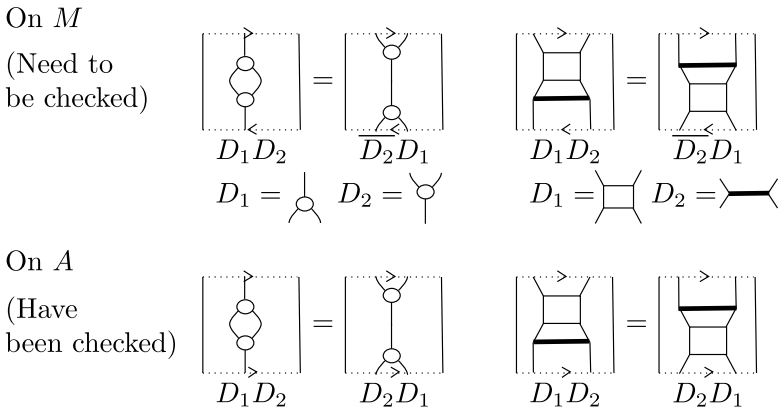

Figure 3.41: Two examples of overlaps which should be checked on M, but have already been checked on A.

The irreducible G_2-webs are therefore linearly independent. We can now see that

Theorem:

$$dim(\mathbb{G}_{2,m\leq n}(A)) = \sum_{i=0}^{n} 2^i$$

and

$$dim(\mathbb{G}_{2,m\leq n}(M)) = \sum_{i=0}^{\lceil \frac{n}{2} \rceil} 2^i + \sum_{i=0}^{\lfloor \frac{n}{2} \rfloor} 2^i + 2^{i-1}.$$

Figure 3.42 shows the basis diagrams on A and M for small values of n.

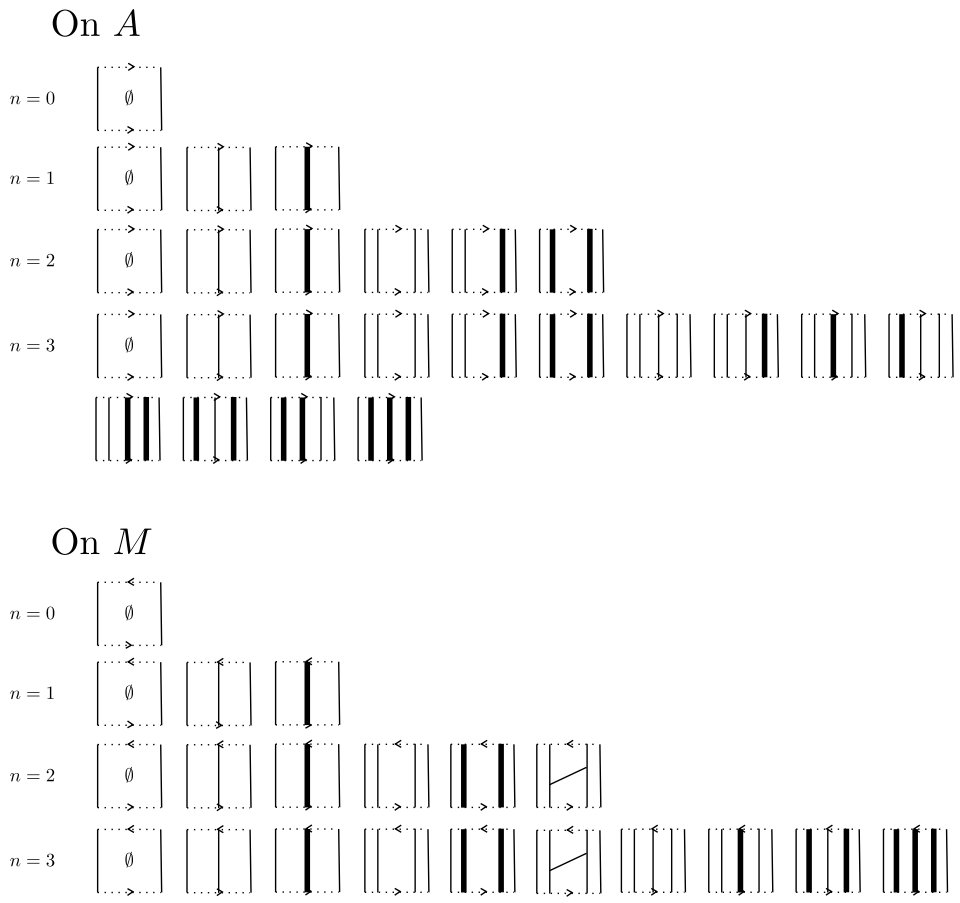

Figure 3.42: Examples of the basis diagrams for $\mathbb{G}_{2,m\leq n}(S)$ for $S = A$ and $S = M$ and small values of n.

Chapter 4

The Natural Transformations Between Compositions of the Induction and Restriction Functors in the Cyclotomic Quotients of the NilHecke Algebra

4.1 The Categorification Work of Lauda

In [17], Lauda categorifies the algebra $\mathbf{U}_q(\mathfrak{sl}_2)$ by constructing a 2-category $\dot{\mathcal{U}}$ whose Grothendieck group $K_0(\dot{\mathcal{U}})$ is isomorphic to Lusztig's $\dot{\mathbf{U}}$. Recall that this categorification of the algebra $\dot{\mathbf{U}}$ is a 2-category rather than simply a category. This is natural in the following way. The algebra $\dot{\mathbf{U}}$ is obtained from the integral version of $\mathbf{U}_q(\mathfrak{sl}_2)$ by adjoining an idempotent 1_n for $n \in \mathbb{Z}$. These idempotents are orthogonal and are indexed by the weight lattice of $\mathbf{U}_q(\mathfrak{sl}_2)$. We can use them to decompose $\dot{\mathbf{U}}$ into a direct sum $\bigoplus_{n,m\in\mathbb{Z}} 1_m\dot{\mathbf{U}}1_n$. We can now describe $\dot{\mathbf{U}}$ as a category with objects the collection of $n \in \mathbb{Z}$ and $\hom(n,m) = 1_m\dot{\mathbf{U}}1_n$. The identity morphisms are the idempotents 1_n and composition is given by multiplication. Thus, a categorification of $\dot{\mathbf{U}}$ will naturally be a 2-category denoted by $\dot{\mathcal{U}}$. The 2-morphisms are graded and we will follow Lauda's notation by denoting the set of grading preserving

2-morphisms by $\dot{\mathcal{U}}(x,y)$ for x,y 1-morphisms in $\dot{\mathcal{U}}$. One can then use the grading shift operation on 1-morphisms to denote 2-morphisms of degree s by $\dot{\mathcal{U}}(x,y\{s\})$.

The 2-category $\dot{\mathcal{U}}$ is the Karoubian envelope of another 2-category $\mathcal{U}$, itself obtained from restricting a graded additive 2-category $\mathcal{U}^*$ the its degree preserving 2-morphisms. We will therefore briefly restate the definition of $\mathcal{U}^*$ here and refer the reader to [16]for more details on its construction.

The objects of the 2-category $\mathcal{U}^*$ are simply n for $n \in \mathbb{Z}$. They are depicted as regions in the plane labelled by the appropriate integer n.

The 1-morphisms from n to m of $\mathcal{U}^*$ are formal direct sums of composites of

$$\mathbb{1}_m \mathcal{E}^{\alpha_1}\mathcal{F}^{\beta_1}...\mathcal{E}^{\alpha_k}\mathcal{F}^{\beta_k}\mathbb{1}_n\{s\},$$

where $m = n + 2(\sum \alpha_i - \sum \beta_i)$ and $s \in \mathbb{Z}$. They are depicted as formal sums of sequences of signed points.

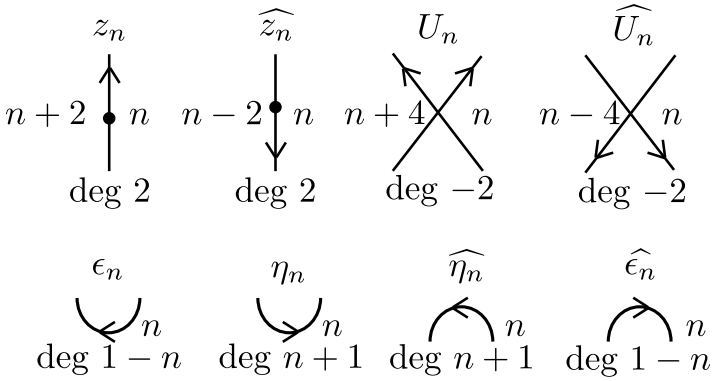

Figure 4.1: These are the basic 2-morphisms of $\mathcal{U}^*$, graphically depicted

Finally, the generating 2-morphisms of $\mathcal{U}^*$ are the diagrams depicted in Figure 4.1, together with the identity 2-morphisms and grading shifts isomorphisms $x \simeq x\{s\}$, subject to the following relations:

- $\mathbb{1}_{n+2}\mathcal{E}\mathbb{1}_n$ and $\mathbb{1}_n\mathcal{F}\mathbb{1}_{n+2}$ are biadjoints with units and counits given by the pairs (η_n, ϵ_{n+2}) and $(\widehat{\epsilon_n}, \widehat{\eta_{n-2}})$. This relation is expressed by the diagram of Figure 4.2.

- All 2-morphisms are cyclic with respect to the biadjoint structure mentioned above. The diagram of Figure 4.3 shows the relations that ensure this cyclic property.

- The cyclic conditions on 2-morphisms imply that 2-morphisms are preserved under boundary preserving planar isotopies, as in Figure 4.4.

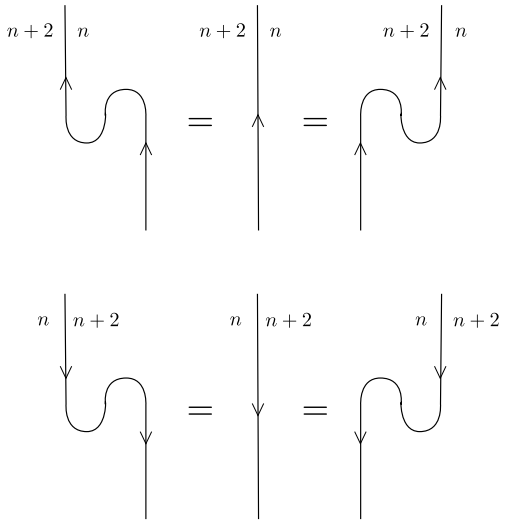

Figure 4.2: This diagram expresses the biadjoint relation between $\mathbb{1}_{n+2}\mathcal{E}\mathbb{1}_n$ and $\mathbb{1}_n\mathcal{F}\mathbb{1}_{n+2}$.

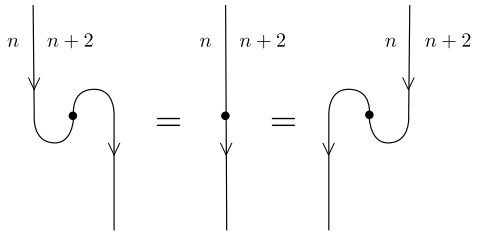

Figure 4.3: This diagram expresses the cyclical nature of 2-morphisms with respect to the biadjoint structure given by Figure 4.2

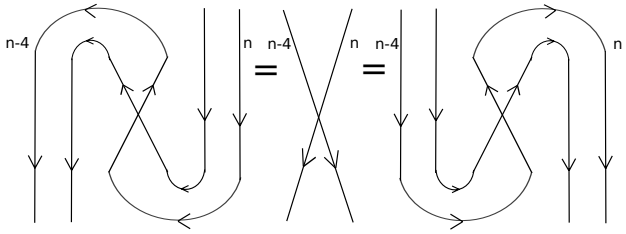

Figure 4.4: 2-morphisms are preserved under boundary preserving planar isotopies of diagrams.

- All dotted bubbles of negative degree are zero, as expressed in Figure 4.5

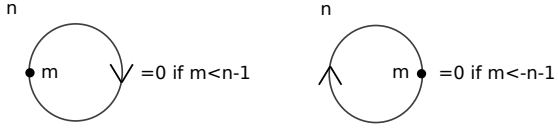

Figure 4.5: Dotted bubbles of negative degrees are zero.

- The nilHecke algebra $\mathcal{NH}_a$ acts on $\mathcal{U}^*(\mathcal{E}^a\mathbb{1}_n, \mathcal{E}^a\mathbb{1}_n)$ and $\mathcal{U}^*(\mathcal{F}^a\mathbb{1}_n, \mathcal{F}^a\mathbb{1}_n)$ for all $n \in \mathbb{Z}$, which implies the graphical relations of Figure 4.6.

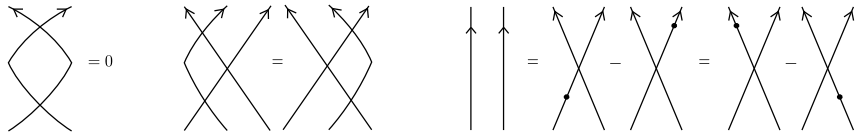

Figure 4.6: The action of the nilHecke algebra implies the depicted relations.

Moreover, we want the 1-morphisms $\mathcal{E}$ and $\mathcal{F}$ to lift the relations of E and F in $\mathbf{U}_q(\mathfrak{sl}_2)$. The equalities of Figure 4.7 and 4.8 will ensure that this in fact happens. Note that all summations are increasing sums or taken to be zero.

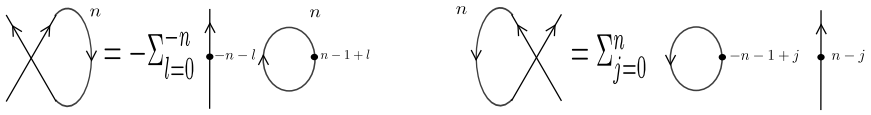

Figure 4.7: These two equalities reducing crossing and cycles and bubbles, along with the ones of Figure 4.8 ensure that $\mathcal{E}$ and $\mathcal{F}$ lift the relations of E and F in $\mathbf{U}_q(\mathfrak{sl}_2)$.

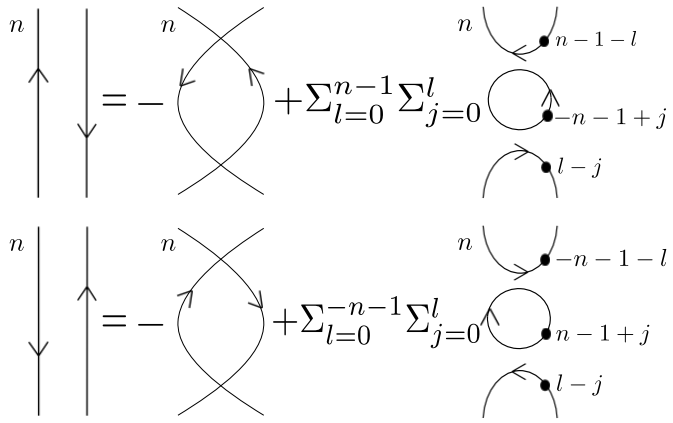

Figure 4.8: These equalities, which decompose the identity on $\mathcal{EF}$ and $\mathcal{FE}$, along with the ones of Figure 4.7 ensure that $\mathcal{E}$ and $\mathcal{F}$ lift the relations of E and F in $\mathbf{U}_q(\mathfrak{sl}_2)$.

In the previous figures, for some values of n, the dots on the bubbles have negative labels. Of course, a composite of z or $\widehat{z}$ with itself a negative number of times does not make sense. Bubbles with negative labels are called *fake bubbles* and are formal symbols defined by the equations in Figure 4.9. Note that the degree of all the fake bubbles in Figures 4.8 and 4.9 remains positive hence fake bubbles do not violate the positivity of the dotted bubble axiom illustrated in Figure 4.5.

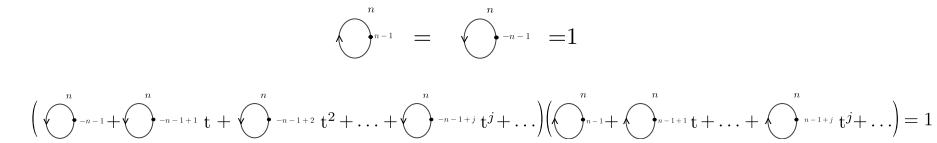

Figure 4.9: These two equations define fake bubbles; formal symbols looking like bubbles with negative labels.

4.2 The Diagramatic Calculus for Quotients of the NilHecke Algebra

We now want to look at so-called cyclotomic quotients of the NilHecke Algebra. Remember first the ring R of $\mathbb{Z}$-linear combinations of diagrams for a Kac-Moody algebra $\mathfrak{g}$ associated to an arbitrary Cartan Datum, which was shown by Khovanov and Lauda to categorify $U_q^-(\mathfrak{g})$ ([10], [11]). R decomposes

$$R = \bigoplus_{\nu \in \mathbb{N}[I]} R(\nu),$$

where $R(\nu)$ is the subring generated by diagrams with ν_i strands of color i for each $i \in \mathrm{Supp}(\nu) = \{i | \nu_i \neq 0\}$. For a more complete but still concise explanation, see [6]. We are here only concerned with these rings when the algebra $\mathfrak{g}$ is simply $\mathfrak{sl}_2$, which means that all strands have the same color and $\nu = m$, the number of strands. We will therefore omit this color, usually denoted i, from our notation.

In order to algebraically describe diagrams, we write x_j for the diagrams with all vertical lines and a dot on the jth strand and δ_j for a diagram with all vertical lines except for a crossing between the jth and $j+1st$ strands.

In type A, the rings $R(m)$ are just the NilHecke algebras defined by the relations of Figure 4.10.

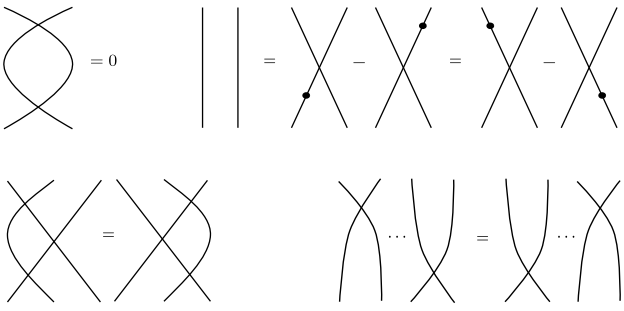

Figure 4.10: These are the relations of the NilHecke algebra.

We now define the cyclotomic quotients $R^N(m)$ of $R(m)$ for $\mathfrak{g} = \mathfrak{sl}_2$ as the quotient of $R(m)$ by the

2-sided ideal generated by the element x_1^N. The relation defining this quotient is pictured in Figue 4.11. The integer N is referred to as the level of the quotient.

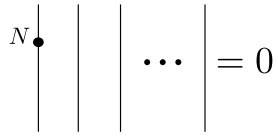

Figure 4.11: This is the relation defining the cyclotomic quotient $R^N(m)$ of $R(m)$ in type A.

This relation has interesting consequences, such as the relation

$$\sum_{l_1+\ldots+l_m=N-(m-1)} x_1^{l_1} x_2^{l_2} \ldots x_m^{l_m} = 0$$

of Figure 4.12.

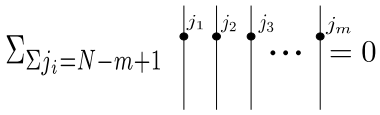

Figure 4.12: This relation is a consequence of the relation $x_1^N = 0$ imposed in the quotient $R^N(m)$ of $R(m)$.

This last relation was used by Lauda in [6] to construct an upper bound for the nilpotency degree of elements in these cyclotomic quotients for type A_∞. It will also give us a spanning set of diagrams for $R^N(m)$, but there will be more details on that in Section 4.4. Figure 4.13 shows some examples of this important relation for different values of N. Since $R(m)$ is simply the NilHecke algebra when $\mathfrak{g} = \mathfrak{sl}_2$, we refer to its quotient $R^N(m)$ as H_N or $H_{N,m}$ with m the number of strands in the diagrams with which we are specifically concerned at the moment.

4.3 The Diagramatics of Natural Transformations Between Compositions of the Induction and Restriction Functors in the Cyclotomic Quotients of the NilHecke Algebra

The graphical calculus for $\dot{\mathcal{U}}$, its induction and restriction functors and their natural transformations was already introduced in Section 4.1 and will be used here to describe the natural transformations between compositions of the functors $\mathcal{E}$ and $\mathcal{F}$, the functors that lift the actions of E and F. Remember that we

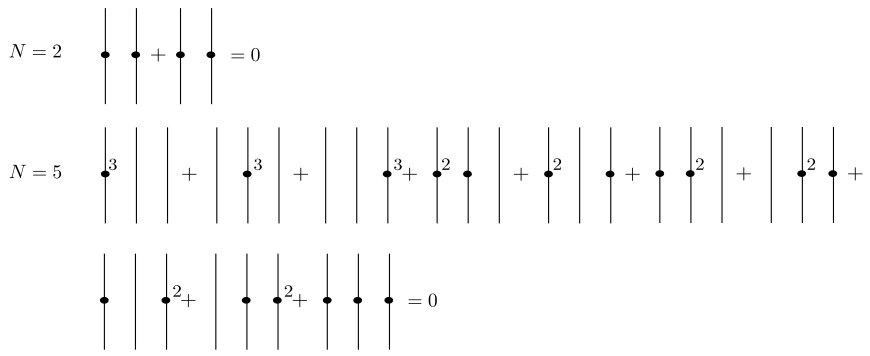

Figure 4.13: Some examples of the relation of Figure 4.12 for specific values of N.

use as indices on the cyclotomic quotient of the NilHecke algebra $H_{N,m}$ the level N of the quotient and the number of strands $m = (N + n)/2$, where n is the weight of the corresponding representation of $\mathfrak{sl}_2$. When the level is clear from context or when it is not specified, we omit it in the index and simply write H_m.

Now, let us review in detail the diagramatics that we will be using to represent these natural transformations. The induction and restriction functors are represented by signed points. We identify the induction functor $E\mathbb{1}_m : H_m \to H_{m+1}$ with a positive point and $F\mathbb{1}_m : H_m \to H_{m-1}$ with a negative point on the unit interval. For instance, the sequence $++-+$ corresponds to $\mathcal{EEFE} : H_m \to H_{m+2}$. For another example, see Figure 4.14.

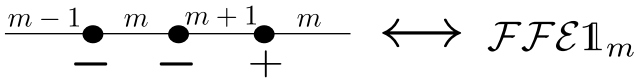

Figure 4.14: This sequence of signed points correspond to the composition $\mathcal{FFE}\mathbb{1}_m$.

Next, to represent the natural transformation between compositions of these functors, we place two unit intervals with signed points one above the other. The natural transformations are now represented as the oriented paths from the bottom unit interval to the top unit interval, as in Figure 4.15.

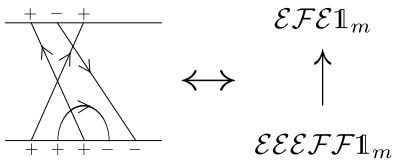

Figure 4.15: These paths between the two sequences of signed points represents a natural transformation from $\mathcal{EEEFF}\mathbb{1}_m$ to $\mathcal{EFE}\mathbb{1}_m$.

Using the $\dot{\mathcal{U}}$ calculus, we can reduce all possible paths to straight paths, clockwise and counter clockwise caps and cups, dots and crossings. We therefore only need to characterize these transformations and then use the pre-established relations in $\dot{\mathcal{U}}$ to find all others. The paths we need to characterize are given in Figure 4.16.

Figure 4.16: Using the relations of the $\dot{\mathcal{U}}$ calculus, we reduce all possible paths to the above six irreducible paths. These are the ones we need to characterize.

The approach here taken consists in representing compositions of the induction and restriction functors as H_m bimodules and their natural transformations as bimodule homomorphisms. The induction and restriction functors themselves will be the bimodules $E\mathbb{1}_m = {}_{m+1}(H_{m+1})_m$ and $F\mathbb{1}_m = {}_{m-1}(H_m)_m$. We use a short-hand notation: ${}_{m+1}(H_{m+1})_m$ is the bimodule H_{m+1} with an action by H_{m+1} on the left and an action of H_m on the right. The actions are straightforward; a left action of $H_{l\leq m}$ on H_m is simply the top concatenation of diagrams in H_l with diagrams in H_m. The action happens on the l leftmost strands of the diagrams in H_m. Algebraically, it is left multiplication. Similarly, the right action of $H_{l\leq m}$ on H_m is the bottom concatenation of diagrams in H_l with diagrams in H_m. Algebraically, it simply is right multiplication.

Composition is then a tensor product. For instance, $EF\mathbb{1}_m : H_m \to H_m$ is ${}_m(H_m)_{m-1} \bigotimes_{m-1} (H_m)_m = {}_m(H_m \bigotimes_{m-1} H_m)_m$ and $FE\mathbb{1}_m : H_m \to H_m$ is ${}_m(H_{m+1})_{m+1} \bigotimes_{m+1} (H_{m+1})_m \cong {}_m(H_{m+1})_m$. Figure 4.17 shows the correspondance between a path and a bimodule homomorphism.

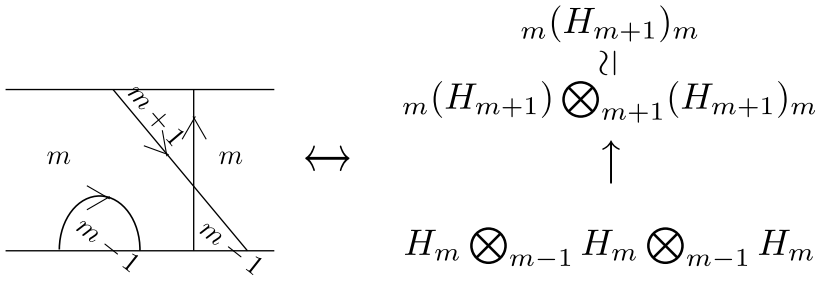

Figure 4.17: This Figure shows a path and the corresponding bimodule homomorphism.

4.4 A Basis for the Cyclotomic Quotients of the NilHecke Algebra

In order to determine what these bimodule homomorphisms are, we need to have a basis for the cyclotomic quotients of the NilHecke algebra $H_{N,m}$. Using bead and runner diagrams introduced in [2], Brundan and Kleshchev were able to find a formula for the graded dimension of these cyclotomic quotients. This formula is in fact much more general as it applies to all of type A.

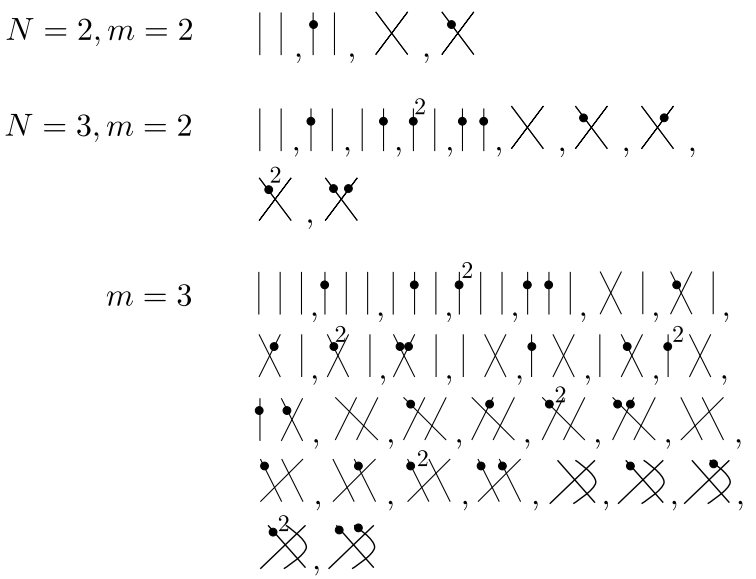

Figure 4.18: These are the basis diagrams for level $N = 2$ and $m = 2$ and for level $N = 3$ and $m = 2, 3$.

For the NilHecke algebra, it is fairly easy to see that the number of diagrams without crossings counted by Brundan and Kleshchev is $N!/(N-m)!$. On the other hand, work by Lauda in [6] on the nilpotency of elements in these quotients using antigravity showed that the elements $x_1^{i_1} x_2^{i_2} ... x_m^{i_m} \times D$, with $i_j \leq N - j - 1$ and where D is a diagram without dots, form a spanning set for $H_{N,m}$. These number $N * (N-1) * ... * (N-m+1) = N!/(N-m)!$ per diagram D, which corresponds to the result of Brundan and Kleshchev and are therefore a basis. It is the basis we will use. Figure 4.18 shows an example of this basis for level $N = 2$ and diagrams of two strands ($m = 2$) and level $N = 3$ and diagrams with two and three strands respectively ($m = 2$ and $m = 3$). One can see that the size of the basis increases fairly fast and that, more importantly, it is not easy to write down a basis for general level N and number of strands m. This is especially hard for general m and it is in part why we were not yet able to generalize completely the natural transformations which we wanted. In Section 4.5.2, the algorithm

used to generate this basis will be explained in more details. Thus, while we can automatically generate such basis elements for any N and m, it remains very difficult to work with such a general basis.

Remark:
As far as we know, no bijection between the Brundan-Kleshchev diagrams and a diagramatical basis has been found for all of type A. We were able to find such a bijection for the NilHecke case but unable to extend it further.

General diagrams are easily reduced to linear combinations of basis diagrams. One first needs to move all dots to the top of the diagram (an example is shown in Figure 4.19) and then use the nilpotency relation of Figure 4.12 to move the dots toward the left as much as possible, as in Figure 4.20. The specific algorithm that was used to reduce a general monomial to a linear combination of basis diagrams is explained in Section 4.5.3.

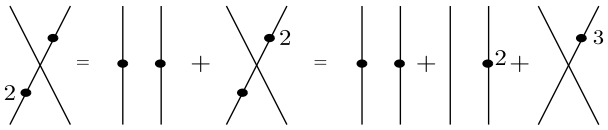

Figure 4.19: This Figure shows how dots can be moved to the top of diagrams.

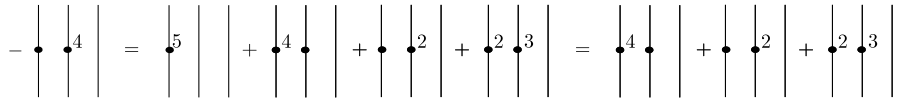

Figure 4.20: This Figure shows how dots are moved towards the left, using the nilpotency relation.

4.5 Computer Program

4.5.1 The Data Structure

To be able to use a computer program to compute and test these maps, we must first establish an appropriate data structure that will allow us to represent the different kinds of elements with which we are dealing.

First are the dots and crossings. In algebraic notation, n dots on the ith string of a diagram is denoted x_i^n. A crossing between the ith and $i+1st$ strands is denoted δ_i. Note that $\delta_i^n = 0$ whenever $n > 1$.

In our data structure, both dots and crossings will be represented by an ordered triplet (type, strand, power). For instance, $x_i^n \leftrightarrow (dot, i, n)$ and $\delta_j^m \leftrightarrow (crossing, j, m)$.

A simple diagram, or element of $R(\nu)$, is algebraically represented as $D = \prod_{l=1}^{N} \prod_{k} x_{i_l}^{n_l} \delta_{j_k}$. In the data structure, a diagram D is simply an ordered list of triplets.

Now, we must be able to build linear combinations of diagrams. Not only must we be able to add diagrams and allow for coefficients in $\mathbb{C}$, but we must be able to encode undetermined coefficients c_i as well to later express the constraints of our maps in terms of equations in the unknown c_i's. Every term in a linear combination of diagrams is encoded as an ordered pair (coefficient, diagram). However, every diagram in a linear combination can have as a coefficient a linear combination of c_i. That linear combination is itself encoded as a sorted list of ordered pairs $(z,\ i)$, where $z \in \mathbb{C}$. For instance, $(3c_2 - 4c_5)D \leftrightarrow (((3,2),(-4,5)),D)$. The list of pairs representing the coefficient of the diagram is ordered based on the second element, the one corresponding to i in c_i.

A linear combination of diagrams is then simply a sorted list of terms (coefficient, diagram). This list is sorted by diagrams, where diagrams are themselves sorted using the lexicographical order on $(n_1, n_2, ..., \delta_1, \delta_2)$, where n_i is the number of dots on the ith strand. Note that since every diagram is reduced upon entering the list, this is a well-ordering. The list also combines coefficients after sorting, so that $3c_2D + 4c_2D = 7c_2D$.

We must also be able to have linear combinations of tensor products of diagrams. The above structure is easily extended to allow for this: $T = D_1 \otimes D_2 \leftrightarrow (D_1, d_2)$ and$(3c_2 - 4c_5)T \leftrightarrow (((3,2),(-4,5)),T)$ and linear combinations are then represented by the same sorted list of tensor products with linear combinations of unknown c_i's as their coefficients. The list is sorted as above using the left diagram D_1 first, then the right one D_2.

This data structure is summarized in Figure 4.21.

4.5.2 Generation of a Graded Basis for a Particular Cyclotomic Quotient

We will use this computer program to generate the constraints needed for the clockwise cup $H_m \rightarrow H_m \bigotimes_{m-1} H_m$ to be a bimodule homomorphism. Since this map is generated by the image of $e \in H_m$, and since we know that this image has degree $2(1-2m+N)$, we first want to generate all basis elements of $H_m \bigotimes_{m-1} H_m$ of that degree.

As we will see more in details in section 4.6.4, we can choose a basis of monomials, each a tensor product of a basis element of H_m with one other basis element of H_m chosen from a rather reduced set. The right element of this product can only have dots on its last strand since all others can be moved to the left element via the tensor product. Its crossings must also follow a specific sequence: $\delta_{m-1}\delta_{m-2}\ldots\delta_{m-i}$

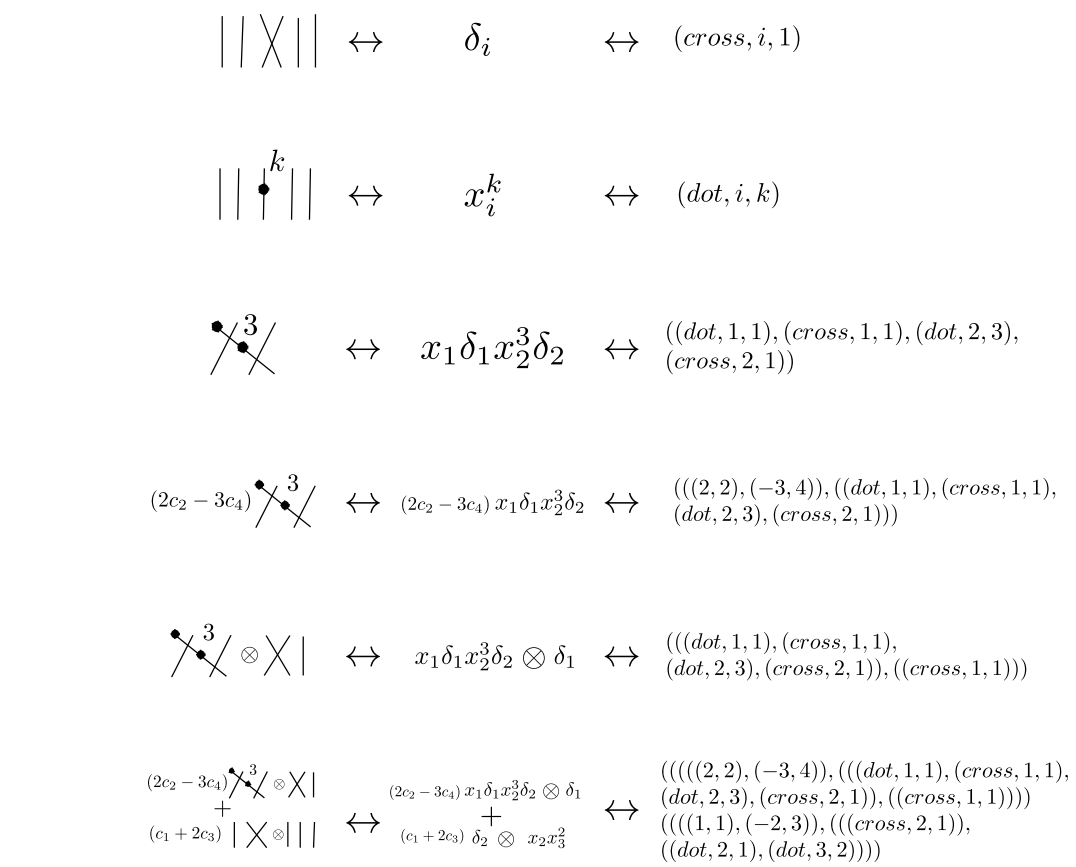

Figure 4.21: This Figure illustrates the data structure used in this computer program.

since crossings $\delta_k, k < m-1$ which are not blocked by other crossings can also be moved to the left side.

We will therefore start by generating all of those elements $x_m^j\delta_{m-1}\dots\delta_{m-i}$ for $0 \le j \le (N-m)$, where $j = 0$ means that the diagram has no dots and $N - m$ is the maximum number of dots which can exist on the mth strand of a basis element of $H_{N,m}$, a quotient of level N, and for $0 \le i \le m-1$, where $i = 0$ means that the diagram has no crossings. These elements are stored along with their degree.

We now want to generate the left elements of the monomials; all the basis elements of $H_{N,m}$. We start by generating all crossings configurations. These correspond to permutations of the m strands. Clearly, many crossing configurations can represent a single permutation, but recall that in H_n diagrams representing a certain permutation with a non-minimal number of crossings are zero. The minimal crossing configuration for a given permutation is still not unique, for instance $\delta_1\delta_2\delta_1$ and $\delta_2\delta_1\delta_2$ represent the same permutation. However, all these configurations are equal. The reduction algorithm explained in the next section will choose a unique diagram as a basis element. For now, we simply generate any minimal representation for each permutation and then use the reduction algorithm to get basis elements.

What we need to do to find a minimal crossing representation of a permutation is to decompose this permutation into a product of transpositions. We use the bubble sort algorithm to do that. More specifically, we look at the permutation as an unordered list needing ordering. For instance, the permutation (135) of 5 elements would correspond to the list $[5, 2, 1, 4, 3]$. As we use bubble sort to sort this list, we keep track of every swap, or every transposition. As an example, if we were to sort the list $[5, 2, 1, 4, 3]$ and convert it to crossings we would get:

$[5, 2, 1, 4, 3] \to [2, 5, 1, 4, 3] \Rightarrow \delta_1$

$[2, 5, 1, 4, 3] \to [2, 1, 5, 4, 3] \Rightarrow \delta_2$

$[2, 1, 5, 4, 3] \to [2, 1, 4, 5, 3] \Rightarrow \delta_3$

$[2, 1, 4, 5, 3] \to [2, 1, 4, 3, 5] \Rightarrow \delta_4$

$[2, 1, 4, 3, 5] \to [1, 2, 4, 3, 5] \Rightarrow \delta_1$

$[1, 2, 4, 3, 5] \to [1, 2, 3, 4, 5] \Rightarrow \delta_3$.

And so our element would be $D = \delta_1\delta_2\delta_3\delta_4\delta_1\delta_3$.

It is well-known that the bubble sort algorithm generates the minimum number of swaps so that our diagram will have the minimal number of crossings as well. We store all of those elements along with their degree.

Now we must generate all configurations of dots appearing in basis elements. Remember that if we are working in level N, we can use the nilpotency relation to move dots to the left when the jth strand of a diagram has more than $N - j$ dots. We simply need to generate diagrams with m strands with $x_{i_1}x_{i_2}\dots x_{i_m}$ with $0 \leq i_j \leq N - j$.

We then create all left elements by combining dot configurations with crossing configurations, computing their degree and then matching these elements with the already generated right elements and retaining the matches that have the desired degree of $2(1 - 2m + N)$. We then store them in a sorted list and assign them each an undetermined coefficient c_i. This linear combination is the image of e. Our goal will be to derive the constraints on these c_i that make our map a bimodule homomorphism.

4.5.3 Reduction of a General Monomial to a Linear Combination of Basis Elements

We also need an algorithm that will reduce a monomial (a single diagram or a tensor of two diagrams) to a linear combination of basis elements. We start with the case of a sinle diagram and will address tensor products after. Let us first define what a basis diagram looks like.

First, we know that all the dots need to be on top of all the crossings, that is x_i is left of δ_j for all i, j. A basis element is therefore of the form

$$D = x_{i_1}^{k_1} x_{i_2}^{k_2} \dots x_{i_l}^{k_l} \delta_{j_1} \delta_{j_2} \dots \delta_{j_m}.$$

Because of the nilpotency relation, dots can be pushed to the left until either the element is seen to be zero or until it is a linear combination of elements each with all $x_i^k, k \leq N - i$. Our basis elements are those whose dots satisfy this condition that $x_i^k, k \leq N - i,\ \forall i$.

In a basis diagram, if we have $\delta_{j_n} \delta_{j_{n+1}}$, then either $j_{n+1} = j_n - 1$ or $j_{n+1} > j_l,\ \forall\, l < n$. For instance, the diagram corresponding to $\delta_3\delta_2\delta_1\delta_3$ is not a basis diagram, but $\delta_2\delta_3\delta_2\delta_1$ is one. To these descriptions of basis elements, we add the zero diagram. A diagram is recognized as being zero if we either have a triplet (dot, i, k) with $k > N$ corresponding to x_i^k with $k > N$ or if we have $(crossing, j, m)$ with $m > 1$, corresponding to a double crossing. The program uses these parameters to determine whether a diagram is already a basis element or whether it needs to be reduced to a linear combination of basis elements.

The algorithm contains several functions, which simplify or reduce elements in different ways. The simplest of these is to recognize the zero diagram and remove it, which is done using the constraints just discussed. Then we have a simplification function which converts adjacent $(gen, i, j), (gen, i, k)$ into $(gen, i, j+k)$, where "gen" can be either a dot or a crossing. This corresponds to computing $x_i^j x_i^k = x_i^{j+k}$ or $\delta_i^j \delta_i^k = \delta_i^{j+k}$.

We also need to sort dots. This simply means that, since $x_i x_j$ commute, we order them so that $i < j$. We then use the previous function to combine them when the indices i match.

Now, we want to move all dots up, or all x_i in front of all δ_j. We start by finding a pair of misordered generators $\delta_j x_i$. If $i \neq j$ and $i \neq j+1$ then we just swap the crossing and the dot and replace $\delta_j x_i \to x_i \delta_j$. We then sort dots and simplify. We test the resulting diagram to see if it is zero and continue if it is not. If $j = i$, we replace

$$\delta_i x_i \to x_{i+1} \delta_i + e$$

and if $i = j + 1$,

$$\delta_{i-1} x_i \to x_{i-1} \delta_{i-1} - e,$$

where e is the identity element, the diagram without crossing or dots. If the disordered pair was in a diagram $D = D' \delta_j x_i D''$, it is replaced by a list of two diagrams $(D_1, D_2) = (D' x_{i+1} \delta_i D'', D' D''$ each

with the same coefficient as the original diagram D when $i = j$ and with

$$(D_1, D_2) = (D' x_{i-1} \delta_{i-1} D'', -D' D''),$$

with the coefficient of D_2 being the negation of the coefficient of D. In both cases, we then sort dots, simplify the diagrams and then eliminate all zero diagrams.

Next, we want to move dots to the left, that is we want to reduce the diagrams that have x_i^k with $k > N - i$. Say $D = D' x_i^k D''$ with $k > N - i$ and i is the smallest index at which this occurs in this diagram. The algorithm first computes all ways to distribute k dots on $N - k + 1$ strands, the $N - k + 1$ strands preceding strand i on which these k dots presently are. Our present diagram is in the configuration $[00...00k]$, which we do not want. We replace our diagram by a list of new diagrams $(D''' D'')$, where D''' has the same crossing configuration as D' but with the new configuration of dots. We assign as their coefficient the negative of the original coefficient of D. For instance, let $N = 3$ and $D = x_1 x_3$. $1 > 3 - 3$ and therefore this diagram needs to be reduced. Recall that for $N = 3$, we have the nilpotency relation $x^1 + x^2 + x^3 = 0$. We compute all ways of distributing 1 dot on 3 strands: $[100], [010], [001]$. The last one is the one we have now, so we replace $D = x_1 x_3$ by $-x_1^2 - x_1 x_2$.

To be in our chosen basis form, all braided crossings $\delta_{i+1} \delta_i \delta_{i+1}$ must be converted to $\delta_i \delta_{i+1} \delta_i$. We do this iteratively until no braidings of the first type are left. This function afterwards simplifies the resulting diagrams using the other functions and eliminates it if it is zero.

Finally, a crossing sorting function finds the first crossing δ_{i_l} with i_l less than or equal to the previous highest i_k and for which the previous entry is not δ_{i_l+1}. It then swaps δ_{i_l} with the previous $\delta_{i_{l-1}}$ if either $i_{l-1} - i_l > 1$ or if both $i_{l-1} - i_l < -1$ and $i_{l+1} < i_l$ or δ_{i_l} is the last crossing in our diagram. Here is a first simple example:

$$D = \delta_{i_1} \delta_{i_2} \delta_{i_3} \delta_{i_4} = \delta_3 \delta_2 \delta_1 \delta_3.$$

The i_l that needs to be moved is $i_4 = 3$ since it is equal to the previous greatest i_k: $i_1 = 3$ and $i_{l-1} = i_3 \neq i_l - 1 = 2$. Here, we have $i_{l-1} - i - l = 1 - 3 = -2 < -1$ and δ_3 is the last crossing in our diagram so we swap it with the preceding δ_1 to get

$$D = \delta_3 \delta_2 \delta_3 \delta_1.$$

The braiding function would then take care of the braiding to obtain the basis element $D = \delta_2 \delta_3 \delta_2 \delta_1$.

Here is a longer example:

$$D = \delta_{i_1}\delta_{i_2}\delta_{i_3}\delta_{i_4} = \delta_4\delta_6\delta_2\delta_1.$$

The first crossing for which the index is less than or equal to the previous maximal index without the preceding crossing having an index one higher is $\delta_{i_3} = \delta_2$. $i_3 \leq max = i_2 = 6$ and $i_2 - i_3 = 6 - 2 = 4 > 1$ so we swap δ_{i_2} and δ_{i_3} to obtain

$$D = \delta_{i_1}\delta_{i_2}\delta_{i_3}\delta_{i_4} = \delta_4\delta_2\delta_6\delta_1.$$

Then $i_2 \leq max = i_1 = 4$ and $i_1 - i_2 = 4 - 2 = 2 > 1$ so we swap δ_{i_1} and δ_{i_2} to obtain

$$D = \delta_{i_1}\delta_{i_2}\delta_{i_3}\delta_{i_4} = \delta_2\delta_4\delta_6\delta_1.$$

Now $i_4 \leq max = i_3 = 6$ and $i_3 - i_4 = 6 - 1 = 5 > 1$ so we swap δ_{i_3} and δ_{i_4} to obtain

$$D = \delta_{i_1}\delta_{i_2}\delta_{i_3}\delta_{i_4} = \delta_2\delta_4\delta_1\delta_6.$$

Finally, $i_3 \leq max = i_2 = 4$ and $i_2 - i_3 = 4 - 1 = 3 > 1$ so we swap δ_{i_2} and δ_{i_3} to obtain a basis element

$$D = \delta_{i_1}\delta_{i_2}\delta_{i_3}\delta_{i_4} = \delta_2\delta_1\delta_4\delta_6.$$

As usual, the function then simplifies and removes zero diagrams.

The complete reduce function combines all the above subfunctions as follows: we keep a list of diagrams that need processing and of diagrams that have been reduced to a linear combination of basis diagrams. We iteratively choose a diagram from the first list and attempt one of these operations on it:
-Remove zero diagrams
-Move dots up
-Move dots left
-Braid crossings
-Sort crossings.

If all operations are trivial on the chosen diagram (the returned diagram is equal to the input diagram for all operations), the diagrams should be a basis. If the function testing diagrams agrees, the diagram is added to the second list, but, as a safety measure, if all operations were trivial and yet the diagram not in basis form, the function would return an error. No errors were returned while running the program!

If one of the operations is non-trivial, we test the returned diagram to see if it is now in basis form and add it to the list corresponding to the result of that test.

Extending this algorithm to tensor product monomials in $H_m \bigotimes_{m-1} H_m$ is straight forward. We first reduce the righthand side diagrams to (linear combinations of) basis diagrams. If this generates a linear combination of monomials, we treat each one separately.

Recall that the right diagram can be put in the form $D = x_m^k \delta_{m-1}\delta_{m-2}\dots\delta_{m-i}$ by sliding all other dots to the bottom of the left diagrams, as well as all other crossings. For instance, in $H_5 \bigotimes_4 H_5$:

$$\delta_3 \otimes x_2 x_3^2 x_5 \delta_1 \delta_4 \delta_3 \delta_2 =$$

$$\delta_3 x_2 x_3^2 \delta 1 \otimes \delta_4 \delta_3 \delta_2.$$

After putting the right diagram in this form, we need to reduce the left hand diagram, which gives us a new linear combination of monomials. Then, for each of these monomials, we reduce the left hand side diagram, this itself giving us new linear combinations, but where this time all the left hand side diagrams are basis elements and the right hand side diagrams are in the correct form.

4.5.4 Generation of the Constraints for a Graded Bimodule Homomorphism

This is the simplest part of the program. Remember that we look at the image of $e \in H_m$ under the clockwise cup map ϕ. This image $\phi(e)$ is a linear combination of the basis elements of $H_m \bigotimes_{m-1} H_m$ and generates the map. Since we want this map to be a bimodule homomorphism, we need $\phi(x_i e) = \phi(e x_i) = x_i\phi(e) = \phi(e)x_i$ and $\phi(\delta_i e) = \phi(e\delta_i) = \delta_i\phi(e) = \phi(e)\delta_i$, for all i. We therefore write $\phi(e)$ as a linear combination of basis elements of $H_m \bigotimes_{m-1} H_m$ with undetermined coefficients c_i and impose these conditions on $\phi(e)$, which gives us constraints, or equations, in terms of the coefficients c_i.

The program computes $x_i\phi(e) - \phi(e)x_i$ for $1 \le i \le m$ and $\delta_i\phi(e) - \phi(e)\delta_i$ for $1 \le i \le m-1$ and puts the resulting linear equations in the c_i's on a per-term basis into a matrix, which we put into reduced row echelon form using matlab. The resulting matrix was seen to have a one dimensional solution space in all computed cases. By hand, we solved for all the other coefficients in terms of c_1. For bigger example, the solution could be found using Mathematica, for instance.

4.6 Partial Results: $m \leq 3$

4.6.1 Dots

The dots in $\dot{\mathcal{U}}$ correspond to natural transformations $E\mathbb{1}_m \to E\mathbb{1}_m$ and $F\mathbb{1}_m \to F\mathbb{1}_m$ for a dot put on an upward and downward arrow respectively. In bimodule notation, the maps are ${}_{m+1}(H_{m+1})_m \to {}_{m+1}(H_{m+1})_m$ and ${}_m(H_{m+1})_{m+1} \to {}_m(H_{m+1})_{m+1}$. We want this map to have degree two, since a dot has degree two in $\dot{\mathcal{U}}$. Two obvious options come to mind: $a \mapsto \alpha a x_{m+1}$ or $a \mapsto \alpha' x_{m+1} a$ for $a \in H_{m+1}$. These correspond graphically, up to the constant α, to adding a dot on top or at the bottom of the right-most strand. We will see that the map $E\mathbb{1}_m \to E\mathbb{1}_m$ corresponding to a dot on an upward arrow is the first homomorphism $a \mapsto \alpha a x_{m+1}$ and that the map $F\mathbb{1}_m \to F\mathbb{1}_m$ corresponding to a dot on a downward arrow is $a \mapsto \alpha' x_{m+1} a$ for $a \in H_{m+1}$. Moreover, the relations will tell us that both α and α' equal 1. Figure 4.22 explicitely shows the maps corresponding to adding a dot to an upward or downward strand, both algebraically and graphically.

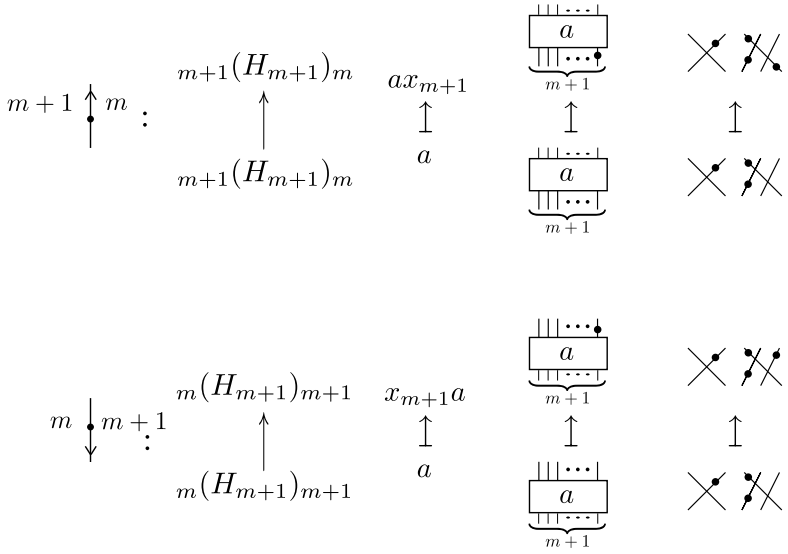

Figure 4.22: This Figure shows the bimodule homomorphisms corresponding to adding a dot to an upward or downward strand both algebraically and graphically.

4.6.2 Two Easy Maps: Counter Clockwise Cup and Clockwise Cap

We will now look at two adjoint transformations: the counter clockwise cup and the clockwise cap. The counter clockwise cup is a natural transformation $\mathbb{1}_m \to FE\mathbb{1}_m$, which corresponds to a bimodule homomorphism $H_m \to {}_m(H_{m+1} \bigotimes_{m+1} H_{m+1})_m \simeq {}_m(H_{m+1})_m$. The natural choice for this map is the

inclusion map $i : H_m \hookrightarrow H_{m+1}$: $a \mapsto i(a)$. Graphically, this map corresponds to adding an $m+1$st strand to the right of a. Figure 4.23 shows the details of the map.

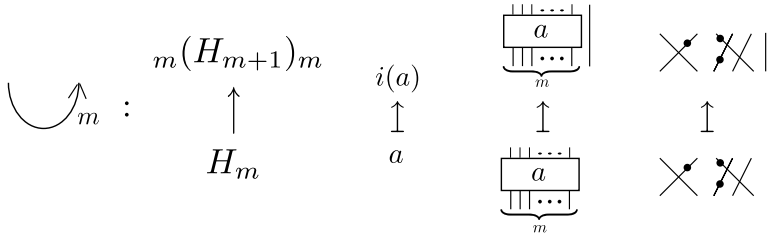

Figure 4.23: The counter clockwise cup map as a bimodule homomorphism is a simple inclusion. Graphically, it adds a strand to the right of the figure.

The clockwise cap corresponds to a natural transformation $EF\mathbb{1}_m \to Id$, which corresponds to a bimodule homomorphism $H_m \bigotimes_{m-1} H_m \to H_m$. Once again, there is a natural qualifying map : $a \otimes b \mapsto ab$. Graphically, this map stacks a on top of b, as seen in Figure 4.24.

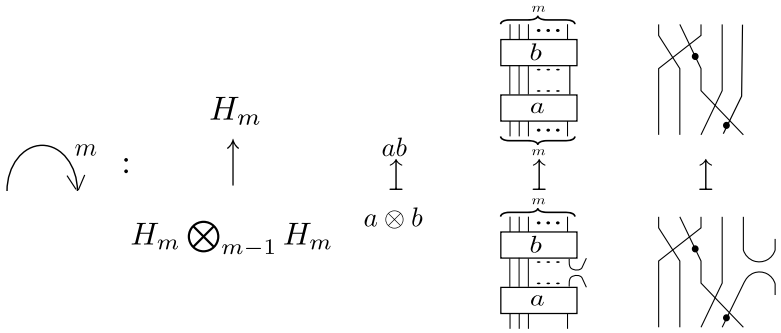

Figure 4.24: The clockwise cap map as a bimodule homomorphism is multiplication. Graphically, it stacks the first element a on top of b, the second element.

We are assuming that these two natural maps are the right ones and will try to find the other cap and cup starting with that assumption.

4.6.3 Crossings

There are two natural transformations corresponding to crossings, one $EE\mathbb{1}_m \to EE\mathbb{1}_m$ represented by a crossing on two upward strands and one $FF\mathbb{1}_m \to FF\mathbb{1}_m$ corresponding to a crossing on two downward strands. Crossings on strands going in different directions can be optained by composing one of these two crossing with caps and cups as shown in the $\dot{\mathcal{U}}$ relations. The two maps are shown in Figures 4.25 and 4.26.

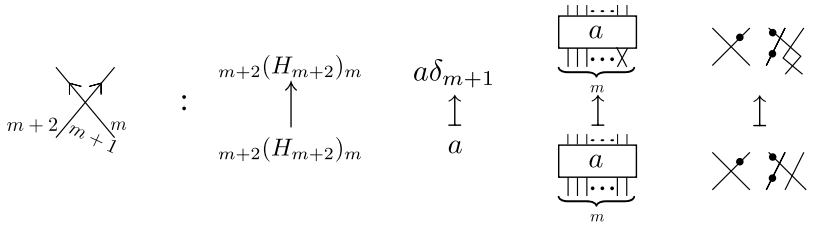

Figure 4.25: The upward crossing map corresponds to right multiplication by δ_{m+1}. Graphically, it adds a crossing of the right-most two strands to the bottom of the figure.

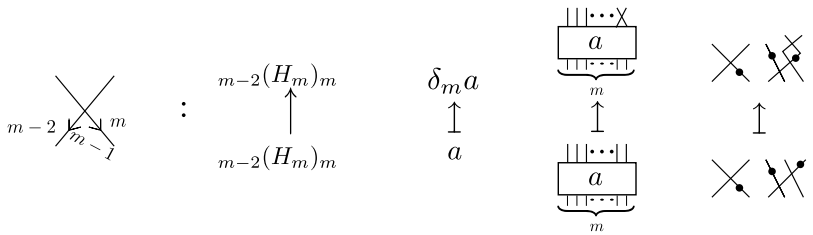

Figure 4.26: The downward crossing map corresponds to left multiplication by δ_m. Graphically, it adds a crossing of the right-most two strands to the top of the figure.

4.6.4 Clockwise Cup

We are now looking for the natural transformation $Id\mathbb{1}_m \to EF\mathbb{1}_m$ corresponding to the clockwise cup. As a bimodule homomorphism, this map is $H_m \to H_m \bigotimes_{m-1} H_m$, as in Figure 4.27. Since H_m, as a bimodule

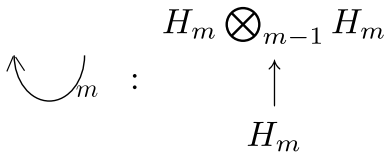

Figure 4.27: The clockwise cup as a bimodule homomorphism will be much more complicated than the other maps we have encountered so far.

over itself, is generated by the identity e, we need only find the image of e to find the homomorphism we need. First, note that the degree of the map corresponding to the clockwise cap is always zero. Now, remember that if N is the level of the representation and n its weight as used in $\dot{\mathcal{U}}$, and m is the number of strands in the corresponding grahical calculus for $H_{N,m}$ we have $n = 2m - N$. From $\dot{\mathcal{U}}$, we also know that a clockwise bubble with $n-1$ dots in a region of weight n is 1 and thus has degree zero. Therefore, the degree of the cap, the degree of $n-1$ dots and the degree of the cup must add to zero. This means that the degree of the cup is $-2(n-1) = 2(1-2m+N)$. Unfortunately, there is no obvious bimodule homomorphism of that degree. The computer program introduced in the previous subsection **??** tested the

homomorphism relations on a basis of $H_m \bigotimes_{m-1} H_m$ to determine the relations on the coefficients of these basis elements in the image of e. In all tested cases, $dim(Hom_{deg=2(1-2m+N)}(H_m, H_m \bigotimes_{m-1} H_m)) = 1$. The program yielded results for $m = 2, N = 2, 3, 4$ and $m = 3, N = 3, 4, 5$. These results allowed us to extrapolate a possible map for $m = 2$ and $m = 3$ and general level $N \geq m$.

In $H_m \bigotimes_{m-1} H_m$, there is a right action of H_{m-1} on the left H_m factor, which we represent graphically as the action on the bottom of the left $m-1$ strands, see Figure 4.28. Correspondingly, the left action of H_{m-1} on the right H_m factor is represented graphically as an action on the top of the first $m-1$ strands of H_m. To create a basis of $H_m \bigotimes_{m-1} H_m$, we move all possible dots and crossings to the left diagram. Therefore, all dots on the first $n-1$ strands of the right diagram in a tensor monomial can

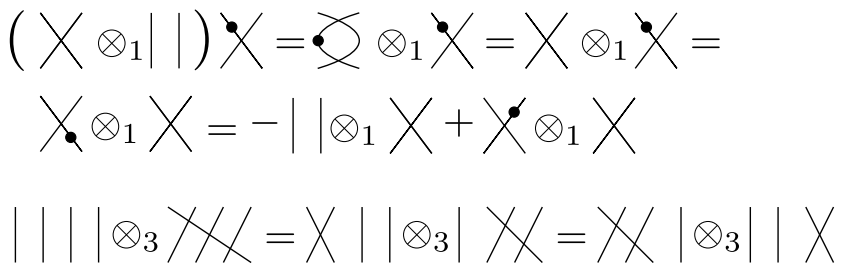

Figure 4.28: An example of how the tensor actions translate graphically.

be moved to the bottom of the left diagram. From there, they can be moved to the top of the diagram using the usual relations on H_m. Hence, a basis monomial of $H_m \bigotimes_{m-1} H_m$ will have no dots on the first $m-1$ strands of the right diagram. Similarly, only a crossing of the last two strands δ_{m-1} of the right diagram can block other crossings from being moved to the left diagram. It is easy to see that the only possible sequence of crossings which cannot be moved to the left diagram is $\delta_{m-1}\delta_{m-2}\delta_{m-3}...\delta_{m-i}$. Our basis of $H_m \bigotimes_{m-1} H_m$ is therefore all monomials with a basis diagram of H_m on the left and a diagram $x_m^i \delta_{m-1}\delta_{m-2}\delta_{m-3}...\delta_{m-j}$ on the right.

Let us fix some notation we will need in this section. Remember that x_j^i corresponds to i dots on the j-th strand, counting the left-most strand as the first one. Let $\varphi_{d,m}^{(N)} = \sum_{\sum i_j = d} x_1^{i_1} x_2^{i_2} ... x_m^{i_m}$ be the symmetric sum of crossingless diagrams with m strands of degree $2d$. When the level N or the number of strands m is obvious from context or irrelevant, we might omit it. In some cases, instead of distributing the dots symmetrically on all m strands, we will want to distribute them on a subset S of those strands and will then use the notation $\varphi_{d,S}^{(N)}$ to denote the corresponding sum. Two examples are shown in Figure 4.29

We give the image of e for $m = 2$ and $m = 3$ as a table where each row is a linear combination of

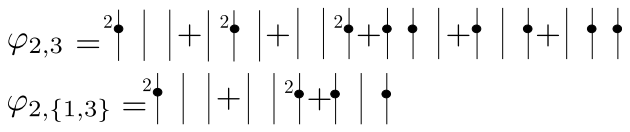

Figure 4.29: Examples of the φ symmetric sums notation. This notation is particularly useful in giving the image of e under the clockwise cup map.

tensors of diagrams with the same right side diagram. This right side diagram $x_m^i\delta_{m-1}\delta_{m-2}\delta_{m-3}...\delta_{m-j}$, is denoted simply as (i,j), where, by convention, $j=0$ means that there are no crossings in the right diagram.

$$m=2, 0\leq i\leq N-2$$

$$(i,0):\ \varphi_{N-(2+i)}\delta_1$$
$$(i,1):\ x_1^{N-(1+i)}\delta_1 - x_2^{N-(1+i)}\delta_1 - \varphi_{N-(2+i)}$$

$$m=3, 0\leq i\leq N-3$$

$$(i,0):\ \varphi_{N-(3+i),3}(\delta_2\delta_1-\delta_1\delta_2)+(-\varphi_{N-(3+i),\{1,3\}}(x_1)+\varphi_{N-(3+i),\{2,3\}}(x_2))(\delta_1\delta_2\delta_1)$$
$$(i,1):\ \varphi_{N-(3+i),3}(\delta_1+\delta_2)+(-\varphi_{N-(3+i),\{1,2\}}(x_1)+\varphi_{N-(3+i),\{2,3\}}(x_3))(\delta_1\delta_2)$$
$$(i,2):\ \varphi_{N-(3+i)}+(\varphi_{N-(3+i),\{1,3\}}(x_1)-\varphi_{N-(3+i),\{2,3\}}(x_2))(\delta_1)+(\varphi_{N-(3+i),\{1,2\}}(x_1)+$$
$$+\varphi_{N-(3+i),\{2,3\}}(x_3))(\delta_2)+\varphi_{N-(2+i),\{2,3\}}(x_1\delta_1\delta_2)+$$
$$+(-x_1^{N-(1+i)}+x_2^{N-(1+i)}+x_3^{N-(1+i)})(\delta_1\delta_2)$$

These maps are the basis for the one dimensional space

$$Hom(H_m 2(1-2m+N), H_m \bigotimes_{m-1} H_m)$$

of bimodule maps of degree $2(1-2m+N)$. They are therefore the maps we want, up to a constant.

4.6.5 Counter Clockwise Cap

The last natural transformation we need to find is $FE\mathbb{1}_m \to Id\mathbb{1}_m$ which corresponds to a bimodule homomorphism ${}_m(H_{m+1} \bigotimes_{m+1} H_{m+1})_m \simeq {}_m(H_{m+1})_m \to H_m$. As before, the action of H_m on H_{m+1} on the left is graphically represented by an action on the top of the m left-most strands, and the action of H_m on the right is an action at the bottom of the m left-most strands. Therefore, a basis for the bimodule ${}_m(H_{m+1})_m$ will contain all elements with dots only on the last strand, and at most $N-2$ dots on that last strand, and δ_m, the crossing of the last two strands, as the only crossing. We need to determine the images of each of these elements under the cap map. We will call the image of x_{m+1}^i, γ_i and the image of $x_{m+1}^i\delta_m$, η_i, as shown in Figure 4.30.

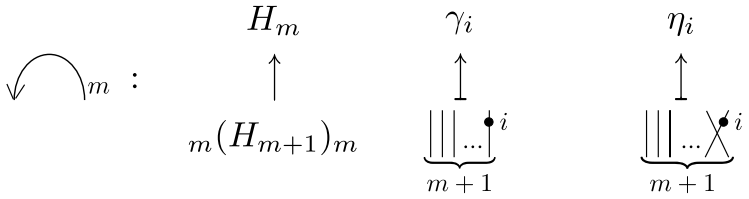

Figure 4.30: To define the counter clockwise cap map, we need to find the image of all elements with dots on the last strand only and of those with a crossing of the right-most two strands along with dots on the last strand, above the crossing. We call these images γ_i and η_i respectively, with i being the number of dots.

We again use the bubble in $\dot{\mathcal{U}}$ to determine the degree of this map. A counter clockwise bubble in a region of weight n has degree zero when it has $-1-n$ dots. Since the degree of the counter clockwise cup has already been determined to be zero, the degree of the cap has to be $2(1+n) = 2(1+2m-N)$.

We will first look at the case $m=1$. The degree of the cap map is then $2(3-N)$. since the element of lowest degree in H_1 has degree zero, $\gamma_i = \eta_{i+1} = 0$ for $i < N-3$. Using the NilHecke relation $x_2^{N-(i+1)}\delta_1 x_1 - x_2^{N-i} = x_2^{N-(i+1)}$, which implies that $x_1\eta_{N-(i+1)} - \eta_{N-i} = \gamma_{N-(i+1)}$ and the quotient relation $\varphi_{N-1,2} = 0$, which implies that $-\eta_{N-1} = x_1\eta_{N-2}$ we find that the images of the basis elements under the counter clockwise cap must be, up to a scalar,

$$\gamma_{N-2} = 2x;\ \gamma_{N-3} = -e;\ \eta_{N-2} = e,$$

where x is represented as a dot on the only strand of H_1 and e is the strand itself.

Let us now consider the case $m=2$, for which the map has degree $2(5-N)$. A priori, the element of lowest degree in H_2 is δ, which has degree -2. However, this element does not commute with x_1 and x_2 and therefore cannot be γ_{N-6} or η_{N-5}. These two images are therefore zero. We therefore need only

to determine $\gamma_{N-3}, \gamma_{N-4}, \gamma_{N-5}$ and η_{N-3}, η_{N-4}. To simplify the computations, we notice that none of the images can have a crossing. Moreover, the γ_i's must be central and hence have to be a multiple of $\varphi_{i-N-5,2}$. We then use the same NilHecke relations as well as the quotient relation $\varphi_{N-2,3} = 0$ to find that these elements are:

$$\gamma_{N-6} = \eta_{N-5} = 0;$$

$$\gamma_{N-3} = -5\varphi_{2,2};\ \gamma_{N-4} = 2\varphi_{1,2};\ \gamma_{N-5} = 3e;$$

$$\eta_{N-3} = -2x_1 + 3x_2;\ \eta_{N-4} = -3e.$$

4.7 Future Work

4.7.1 Generalization to all m

Our next goal should, of course, be to generalize the partial results here obtained to all weights and quotient levels or, equivalently, to all values of m and N. We were unable to form a conjecture as to the generalization of the two "hard maps", the clockwise cup and the counter clockwise cap, based on the current results and those generated by our computer program. It is possible that generating more data would help hint at the general result. However, we suspect that the basis of diagrams we are using is not the one in which these maps are natural. We would therefore first endeavor to find a different basis in which the maps we already have might be more easily generalized.

4.7.2 Generalization to type A and Beyond

Once our results have been generalized to all weights and quotient levels, we will want to generalize them to all of type A first, and then, possibly, to all types. The major obstacle to this generalization is the lack of a good diagramatical basis for the quotients of rings $R(\nu)$. We hope that the discovery of a good basis for type A will easily lead to one for the other types. Looking at the results of Brundan and Kleshchev in [2], one could possibly find a bijection between their bead and runner diagrams and a diagramatical basis for quotients of type A. However, we suspect that such a bijection is not obvious and will probably not lead to a basis of monomials.

Bibliography

[1] J.N. Bernstein, I.M. Gelfand, and S.I. Gelfand. Schubert cells and cohomology of the spaces G/P. *Russian Math. Surveys*, 28:1–26, 1973.

[2] J. Brundan and A. Kleshchev. Blocks of cyclotomic Hecke algebras and Khovanov-Lauda algebras. *Inventiones Mathematicae*, 178:451–484, June 2009.

[3] R.W. Carter. Representation theory of the 0-Hecke algebra. *J. Algebra*, 104:89–103, 1986.

[4] G. Duchamp, F. Hivert, and J.-Y. Thibon. Noncommutative symmetric functions VI: Free quasi-symmetric functions and related algebras, 2001.

[5] S. Fomin and R.P. Stanley. Schubert polynomials and the nilCoxeter algebra. *Advances in Math.*, 103:196–207, 1994.

[6] A. E. Hoffnung and A. D. Lauda. Nilpotency in type A cyclotomic quotients. *ArXiv e-prints*, March 2009.

[7] James E. Humphrey. *Reflection Groups and Coxeter Groups*, volume 29 of *Cambridge studies in advanced mathematics*. Cambridge University Press, Cambridge,UK, 1990.

[8] D. Kazhdan and G. Lusztig. Representations of Coxeter groups and Hecke algebras. *Invent. Math.*, 53:165–184, 1979.

[9] M. Khovanov. Nilcoxeter algebras categorify the Weyl algebra. *COMM.ALGEBRA 29*, 11:5033, 2001.

[10] M. Khovanov and A. D. Lauda. A diagrammatic approach to categorification of quantum groups I. *ArXiv e-prints*, March 2008.

[11] M. Khovanov and A. D. Lauda. A diagrammatic approach to categorification of quantum groups II. *ArXiv e-prints*, April 2008.

[12] M. Khovanov and A. D. Lauda. A diagrammatic approach to categorification of quantum groups i, 2008.

[13] D. Krob and J.-Y. Thibon. Noncommutative symmetric functions IV. quantum linear groups and hecke algebras at $q = 0$. *J. Algebraic Combin.*, 6:339–376, 1997.

[14] G. Kuperberg. Spiders for rank 2 Lie algebras. In *eprint arXiv:q-alg/9712003*, pages 12003–+, November 1997.

[15] A. Lascoux and M.-P. Schützenberger. Fonctorialit'e des polynômes de Schubert˙ In *Proceedings of the AMS Special Session on Invariant Theory, Vol. 88 (Denton,Texas, 1986)*, pages 585–595, Providence, RI, 1987. Amer. Math. Soc.

[16] A. D. Lauda. A categorification of quantum sl(2). *ArXiv e-prints*, March 2008.

[17] A. D. Lauda. Categorified quantum sl(2) and equivariant cohomology of iterated flag varieties. *ArXiv e-prints*, March 2008.

[18] I.G. Macdonald. *Notes on Schubert polynomials*. Université du Québec à Montréal, Montréal,QC, Canada, 1991.

[19] M.H. A. Neuman. On theories with a combinatorial definition of "equivalence". *Ann. of Math.*, 43(2):223–243, 1942.

[20] P.N. Norton. 0-Hecke algebras. *J. Austral. Math. Soc.*, A27:337–357, 1979.

[21] A. S. Sikora and B. W. Westbury. Confluence Theory for Graphs. *ArXiv Mathematics e-prints*, September 2006.